# Resource Management and Optimization for Cognitive Radio Networks

Jie Xiang

Doctoral Dissertation



Submitted to
the Faculty of Mathematics and Natural Sciences
at the University of Oslo
in partial fulfillment of the requirements for
the degree of Philosophiae Doctor

September 2011

This thesis work was carried out at Simula Research Laboratory under the supervision of Dr. Yan Zhang, Prof. Olav Lysne and Prof. Tor Skeie. Financial support is from the Resilient Wireless Networks project at Simula (2007.9-2010.9).

To my family

## Abstract

Wireless technologies have been greatly developed and used in the last decade, such as Wi-Fi, Zigbee, Bluetooth, 3G, and 4G networks. The appearance of new technologies leads to an increased request of the wireless spectrum. However, the frequency bands for wireless communications are limited and in danger of being exhausted owing to the fixed allocation regulation. Fortunately, recent measurement campaign on spectrum usage showed that spectrum is not efficiently used by the licensed systems. For example, the recent results released by FCC in US show that on average only 5% of the spectrum from 30MHz to 30GHz is used. Cognitive radio, which can sense spectrum usage, identify and intelligently access spectrum bands licensed to primary systems, is thus a good candidate to improve spectrum utilization and system performance.

In this thesis, we explore the resource management and optimization problems for cognitive radio wireless networks including both one-hop and multi-hop cases. In the one-hop case, we studied the cognitive radio cellular networks (CogCell) and femtocell networks (CogFem), while in multi-hop case, we studied the cognitive radio mesh networks (CogMesh).

Firstly, we studied CogCell, where the cognitive radio enabled base station is operated to provide service to secondary users (SUs) with the coexistence of primary users (PUs). We investigated the uplink admission and power control problem aiming to maximize the revenue received by operators while guaranteeing interference constraints on PUs and Signal-to-Interference-and-Noise-Ratio (SINR) requirements for SUs. We formulated it as an instance of multidimensional knapsack problem in the one-channel case, and as an instance of multidimensional multiple knapsack problem in the multiple-channel case, respectively. Furthermore, we proposed low-complexity heuristic algorithms which can achieve much more revenue than the existing schemes, and are close to the optimal results obtained by MOSEK optimization software.

Secondly, we proposed a radically new communication paradigm by incorporating cognitive radio in femtocell networks, where the cognitive radio enabled femtocell base station (FBS) can opportunistically use the spectrum from licensed systems, support all kinds of indoor communications, and improve the quality of service for macrocell networks. We investigated the downlink spectrum sharing and power allocation problem for CogFem aiming to maximize the downlink capacity of each FBS while considering the constraints on SINR measured by SUs and transmission power of FBS. We employed a mixed primal and dual decomposition method, and proposed a joint channel allocation and fast power control scheme to solve the problem. Simulation results showed that CogFem with more spectrum opportunity could achieve much higher capacity than normal femtocells. The proposed channel allocation and power control scheme can converge very fast, achieve much higher average capacity and lower user blocking rate than the traditional coloring method. We also found that even use the fixed power control scheme together with our proposed channel allocation scheme, the capacity is sacrificed only 2% comparing with dedicated power control schemes.

Finally, we studied CogMesh, where the cognitive radio enabled secondary mesh routers (SMRs) can opportunistically utilize the primary licensed spectrum to deliver data from secondary mesh users. We investigated the route and channel selection problem in CogMesh aiming to maximize the route availability, while guaranteeing the end-to-end delay from SMRs to the gateway. We formulated it as a non-liner integer programming problem, and transformed to a linear integer programming problem, which is further modeled as a variant of multiple-choice knapsack problem. Then, we proposed a low-complexity heuristic algorithm to solve it. Simulation results showed that our proposed scheme achieve quite close successful solution ratio and route availability to the results from MOSEK, and outperforms the channel selection schemes based on best SINR and best channel availability schemes.

As a conclusion, we believe that our proposed resource management and optimization schemes lay down a solid foundation for building cognitive radio networks in future to efficiently use the invaluable spectrum resource.

# Acknowledgments

This dissertation could never have been written without help and support from many people around me.

First of all, I would like to thank my supervisors Dr. Yan Zhang, Prof. Tor Skeie and Prof. Olav Lysne for hiring me as a PhD student in Simula Research Laboratory. I would also like to thank my master supervisor Dr. Jianhua He for his continuous advising on my PhD research. I am greatly indebted to Dr. Yan Zhang, whose guidance and stimulating suggestions helped me a lot in all the time of my research. I am genuinely thankful to Prof. Tor Skeie, who not only constantly fueled me with strength, hope, and support to take on challenges and go through frustrations, but also hired me as a research engineer after my PhD funding ended. Specially, I would like to thank Dr. Frank Olaf Sem-Jacobsen and Dr. Amund Kvalbein for assigning me not so heavy tasks in NaNoC and eValg projects that I could finish my thesis writing.

I would like to thank Simula for providing me such a good working environment, where I have got a lot of help from IT support and administration group, and learnt a lot from many smart researchers and students in different research groups.

I would also like to thank my collaborators during my PhD research. They are Lang Xie, Dr. Qin Xin, Hai Ngoc Pham and Sabita Maharjan. We had a lot of valuable discussions and glad cooperations. I would like to thank Prof. Stein Gjessing and Prof. Paal E. Engelstad for their valuable suggestions during cross project meetings. I am also grateful to Ralph Lorentzen for his valuable suggestions on my optimization problems.

Special thank goes to Ernst Gunnar, my former officemate, whose special humor made our office joyful. He was always helpful, and taught me the Norwegian culture and working methods at the beginning of my life in Norway. I also would like to thank my current officemate Ahmed Elmokashfi, who helped me a lot during my thesis writing. I would like to thank Åshild Grønstad Solheim and Halvard Moe for our perfect cooperation in eValg project. I would like to thank many people in the former ND department. They are

Audun Fosselie Hansen, Knut-Helge Vik, Ole Kristoffer Apeland, Sven-Arne Reinemo, and Thomas Sødring. Special thank goes to Prof. Carsten Griwodz who provided enough financial support for ND cakes when I was serving as the "cake man".

During my PhD study, I visited Hong Kong University of Science and Technology and Princeton University, where I made many good friends. Thanks Prof. Qian Zhang and Prof. Mung Chiang for enrolling me in their project meetings and discussions. Special thank goes to Prof. Mung Chiang for his instruction on optimization theory for wireless communications.

Finally, I owe an enormous debt of gratitude to my wife, my brother, and my parents. Their unconditional love, understanding, and support are the origin of the power for me to keep on moving in my research.

# Contents

Li	st of	Figure	es	XV
Li	st of	Table	s X	VII
Li	List of Algorithms XIX			
1	Intr	oducti	ion	1
	1.1	Motiv	ations	3
		1.1.1	Cognitive radio cellular networks	3
		1.1.2	Cognitive radio femtocell networks	5
		1.1.3	Cognitive radio mesh networks	7
	1.2	Resear	rch methods	8
		1.2.1	Research methods for computer science	8
		1.2.2	Research methods in this thesis	9
	1.3	Contr	ibutions	10
		1.3.1	Admission and power control for one-channel cognitive	
			radio cellular networks	10
		1.3.2	Channel allocation with admission and power control	
			for multi-channel cognitive radio cellular networks	11
		1.3.3	Channel allocation and power control for cognitive ra-	
			dio femtocell networks	11
		1.3.4	Channel selection for cognitive radio mesh networks	12
	1.4	Thesis	s organization	12
2	Bac	kgroui	nd and Related Work	<b>15</b>
	2.1	Backg	round of cognitive radio networks	15
		2.1.1	Definition of cognitive radio	15
		2.1.2	Cognitive cycle and key technologies	16
		2.1.3	Deployment challenges	18
	2.2	Resear	rch problems in our work	21
		$2\ 2\ 1$	Power control	21

	2.3		Admission control	
		2.3.1	Resource management in cognitive radio cellular net-	23
		2.3.2 2.3.3	works	24 24 25
3	Pov	ver and	d Admission Control for One-channel Cognitive Ra-	
U			ar Networks	27
	3.1		m model and problem formulation	28
		3.1.1	System model	28
		3.1.2	Interference power	29
		3.1.3	QoS definition and requirement	30
		3.1.4	The operator problem	31
	3.2	Joint	admission and power control schemes	32
		3.2.1	JAPC-MRER	32
		3.2.2	JAPC-MSRA	34
		3.2.3	JAPC-Rand	35
		3.2.4	Simulation results and analysis	36
	3.3	Discus	ssions on power control and pre-admission schemes	40
	3.4	Furth	er improvements	45
		3.4.1	Lower and upper bounds	47
		3.4.2	Multidimensional knapsack problem modeling and so-	
			lutions	50
		3.4.3	Proposed efficiency based heuristics method	53
	3.5		ation results	54
		3.5.1	Effect of the number of primary users	55
		3.5.2	Effect of the number of secondary users	57
		3.5.3	Effect of the interference threshold on primary users	58
		3.5.4		59
	3.6	Concl	usion	60
4	Res	ource	Optimization for Multi-channel Cognitive Radio	
	Cel		Networks	61
	4.1		m model and problem formulations	61
		4.1.1	System model	62
		4.1.2	Interference from SUs to PUs	63
		4.1.3	Uplink capacity of SUs	64
		4.1.4	The operator problem	64
	4.2	MMK	P modeling	65

## CONTENTS

	4.3	MKP	modeling by matrix transformation	. (	67
	4.4	Propo	sed heuristic algorithm to MKP		70
	4.5	Best S	SINR channel selection scheme		75
	4.6		ation results and analysis		75
	4.7	Conclu	usions and discussions		84
		4.7.1	Conclusions		84
		4.7.2	Discussions	. 8	85
5	Spe	$\operatorname{ctrum}$	Sharing in Cognitive Radio Femtocell Networks	. 8	87
	5.1	System	n model and assumptions		88
		5.1.1	System initialization		88
		5.1.2	Number of transceivers		88
		5.1.3	Spectrum sensing and primary system protection		89
		5.1.4	Control channel		90
		5.1.5	Handover between macrocell and femtocell		90
		5.1.6	Deployment example	. !	91
	5.2	Proble	em formulations		92
		5.2.1	Channel model		92
		5.2.2	Downlink capacity		92
		5.2.3	Downlink spectrum sharing problem	. 9	93
	5.3	Proble	em decompositions and solutions		94
		5.3.1	The master problem	. !	94
		5.3.2	Subproblems		95
	5.4	Simula	ation results and discussion		01
		5.4.1	Existing schemes	. 10	02
		5.4.2	Average capacity with different density of apartments		
		5.4.3	System performance with different number of available		
			channels		05
		5.4.4	The convergence	. 10	06
	5.5	Conclu	usion		
6	QoS	S-aware	e Spectrum Access for Cognitive Radio Mesh Ne	et	
Ū	wor		o spectrum recess for cognitive reads with re-	1(	9
	6.1	System	m model and assumptions		
		6.1.1	System model	. 1	10
		6.1.2	Channel model and adaptive modulation coding $\dots$ .	. 1	11
		6.1.3	Interference-avoid channel selection for adjacent links	. 1	13
		6.1.4	End to end delay	. 1	13
		6.1.5	Route availability	. 1	15
	6.2	Proble	em formulation	. 1	16
			Formulation of route and channel selection		

## CONTENTS

		6.2.2 Problem transformation	7
	6.3	Solutions from Lagrangian relaxations	
	6.4	Low-complexity heuristic channel selection schemes 12	
		6.4.1 Proposed channel selection scheme	
		6.4.2 Alternative channel selection schemes	
	6.5	Matrix transformation for problem solving by optimization	
		software	4
	6.6	Simulation results and analysis	
		6.6.1 Successful solution ratio	
		6.6.2 Route availability	
	6.7	Conclusion	
7	Con	nclusion and Future Work 13	1
	7.1	Conclusion	1
		7.1.1 On research scenarios	1
		7.1.2 Comparison	3
		7.1.3 On research methods	3
	7.2	Future work	4
Bi	bliog	graphy 13	6
Ap	pen	dix A Publication list	9
Ar	pen	dix B Acronym List	3

# List of Figures

1.1	The spectrum allocation table from USA $[1]$	2
1.2	An illustration of the coexistence between cognitive radio users	
	and and primary systems in cognitive radio cellular networks .	4
1.3	An illustration of the coexistence between cognitive radio fem-	
	tocells and primary systems such as macrocells and TV systems	6
1.4	An example of cognitive radio mesh network	7
2.1	Cognitive radio operation cycle [2]	16
3.1	System model of one-channel cognitive radio cellular networks	28
3.2	The secondary revenue in terms of the number of PUs	38
3.3	The secondary revenue in terms of the number of SUs	39
3.4	The secondary revenue in terms of the interference threshold .	40
3.5	The flow chart of joint admission and power control schemes	
	for one-channel CogCell	43
3.6	Secondary Revenue in terms of number of PUs $(n_s = 50, \Gamma =$	
	$-100dBW$ , and $I_p = -110dBW$ )	56
3.7	Secondary revenue in terms of number of SUs $(n_p = 50, \Gamma = 100 \text{ JPHz})$	- <del>-</del>
0.0	$-100dBW$ , and $I_p = -110dBW$ )	57
3.8	Secondary Revenue in terms of $\Gamma$ ( $n_s = 50$ , $n_p = 50$ , and	<b>F</b> 0
0.0	$I_p = -110dBW$ )	58
3.9	Secondary Revenue in terms of $I_p$ ( $n_s = 50$ , $n_p = 50$ , and	50
	$\Gamma = -100dBW) \dots \dots$	59
4.1	System model of multi-channel cognitive radio cellular networks	62
4.2	Heuristic Algorithm to MKP	74
4.3	Revenue in terms of number of channels $(n_{pc}^{max} = 10, \Gamma =$	
	$-70dBm, I_p = -80dBm, \text{ and } n_s = 100) \dots$	77
4.4	Percentage of optimal solution from MOSEK in terms of num-	
	ber of channels $(n_{pc}^{max} = 10, \Gamma = -70dBm, I_p = -80dBm, \text{ and})$	
	$n_s = 100$ )	78

4.5	Revenue in terms of number of SUs $(n_{pc}^{max} = 10, \Gamma = -70dBm,$
	$I_p = -80dBm$ , and $n_c = 10$ )
4.6	Percentage of optimal solution from MOSEK in terms of num-
	ber of SUs $(n_{pc}^{max} = 10, \Gamma = -70dBm, I_p = -80dBm, \text{ and}$
	$n_c = 10$ )
4.7	Revenue in terms of different number of PUs per channel ( $\Gamma$ =
	$-70dBm$ , $I_p = -80dBm$ , $n_{SU} = 100$ , and $n_c = 10$ ) 80
4.8	Percentage of optimal solution from MOSEK in terms of num-
	ber of maximum PUs per channel $(n_{pc}^{max} = 10, \Gamma = -70dBm,$
	$I_p = -80dBm$ , and $n_c = 10$ )
4.9	Revenue in terms of different interference to BS from each
	PU transmitter $(n_{pc}^{max} = 10, \Gamma = -70dBm, n_{SU} = 100, \text{ and})$
	$n_c = 10$ )
4.10	Percentage of optimal solution from MOSEK in terms of differ-
	ent interference to BS from each PU transmitter $(n_{pc}^{max} = 10,$
	$\Gamma = -70dBm, n_{SU} = 100, \text{ and } n_c = 10)$
4.11	Revenue in terms of different interference level per PU $(n_{pc}^{max} =$
	10, $I_p = -80dBm$ , $n_{SU} = 100$ , and $n_c = 10$ ) 83
4.12	Percentage of optimal solution from MOSEK in terms of dif-
	ferent interference level per PU $(n_{pc}^{max} = 10, I_p = -80dBm,$
	$n_{SU} = 100$ , and $n_c = 10$ )
5.1	An example of deploying CogFem networks with FBS controller 91
5.2	The decomposition of spectrum sharing problems in CogFem . 99
5.3	An illustration of the simulation scenario 102
5.4	Average capacity per femtocell in terms of number of floors in
	each building. (3 rows, and 5 buildings per row) 103
5.5	Average capacity per femtocell in terms of number of buildings
	in each row. (3 rows, and 5 floors per building) 104
5.6	Average capacity per femtocell in terms of number of rows of
	buildings. (5 floors per building, and 5 buildings per row) 104
5.7	Average capacity per femtocell in terms of number of channels.
	(5 rows, 5 buildings per row, 10 floors per building) 105
5.8	Average blocking rate in terms of number of channels. (5 rows,
	5 buildings per row, 10 floors per building)
5.9	Average capacity per femtocell in terms of number of Itera-
	tions. (10 available channels, 10 floors per building, 5 build-
	ings per row, and 5 rows)
5.10	,
	(10 available channels, 10 floors per building, 5 buildings per
	row, and 5 rows)

### LIST OF FIGURES

6.1	System model for route and channel selection in cognitive radio
	mesh networks
6.2	An illustration of interfered links
6.3	Successful solution ratio from different channel selection schemes
	(3D visualization)
6.4	Successful solution ratio from different channel selection schemes 128
6.5	Route availability from different channel selection schemes (3D
	visualization)
6.6	Route availability from different channel selection schemes 130

# List of Tables

1.1	Scenarios addressed in each chapter	13
2.1	Related works in cognitive radio cellular networks	24
3.1 3.2 3.3 3.4	Table of notations for one-channel CogCell	29 37 37 44
4.1 4.2 4.3	Table of notations for multi-channel CogCell Simulation parameters for Multi-channel CogCell Revenue allocation table for Multi-channel CogCell	76
5.1	Table of notations for cognitive radio femtocell networks $$	89
6.1 6.2 6.3	Table of notations for cognitive radio mesh networks	126
7.1	Summary of different scenarios	134

# List of Algorithms

1	JAPC-MRER
2	JAPC-MSRA
3	JAPC-MKP
4	Proposed MKP Heuristic Algorithm for MMKP: Part 1 72
5	Proposed MKP Heuristic Algorithm for MMKP: Part 2 73
6	Channel allocation algorithm for the master problem 95
7	Power control algorithms for any FBS $i \dots 98$
8	Proposed joint channel allocation and fast power control algo-
	rithm for FBS $i$
9	Channel selection scheme for route $r$ with Lagrangian Methods 121
10	Proposed heuristic channel selection algorithm for a given route
	r in CogMesh

# Chapter 1

## Introduction

Simplicity is the ultimate sophistication
— Leonardo da Vinci (1452- 1519)

During the last decade, wireless communication and networks have been greatly developed including third generation (3G), fourth generation (4G) cellular networks, IEEE 802.11 Wireless Local Area Networks (WLANs), IEEE 802.15.4/ZigBee Wireless Personal Area Networks (WPANs), Bluetooth, etc. The radio spectrum ranging from 3KHz to 300GHz is the basic resource to carry data in wireless networks. In each country, spectrum is regulated by its radio regulatory agency, such as Federal Communications Commission (FCC) in USA [3], Electronic Communications Committee (ECC) in Europe [4], The Norwegian Post and Telecommunications Authority (NPT) in Norway [5], and Ofcom in UK [6]. Spectrum is traditionally assigned via a fixed frequency allocation policy. For example, the spectrum allocation table by FCC is shown in Fig. 1.1, where each portion of spectrum is exclusively allocated to a specific wireless system, and all subscribers to a wireless system should be granted to access the exclusive spectrum. Following this approach, the spectrum resource is in danger of being exhausted. To get a license on a spectrum band is being more and more difficult and expensive. For example, to deploy 4G cellular networks, TeliaSonera pays SEK 563 million for the 15-year's license in Sweden on four frequency blocks totaling  $2 \times 20$  MHz in the 2.6 GHz band [7], DKK 336.3 million for the 20-year's license in Denmark on  $2 \times 20$  MHz paired spectrum and 10 MHz unpaired spectrum in the 2.5 GHz frequency band [8], EUR 819,000 for the 20-year's license in Finland on five  $2 \times 5$  MHz frequency band pairs in the 2.6 GHz band [9].

The Industrial, Scientific and Medical (ISM) spectrum band which is mostly located around 2.4 and 5 GHz is the only spectrum that can be shared by different networks. WLANs, WPANs, cordless phones, and even

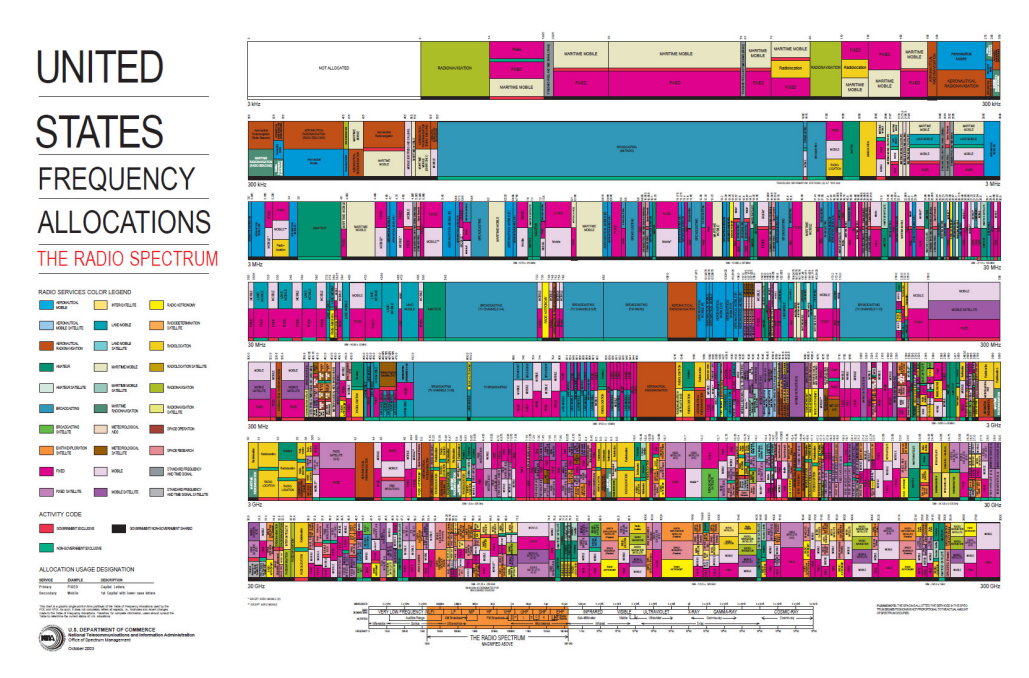


Figure 1.1: The spectrum allocation table from USA [1]

microwave ovens are working in the ISM spectrum band, and suffering the interference with each other. Thus, the performance of wireless networks working in ISM spectrum band is highly limited by the coexistence of other nearby wireless networks.

On the other hand, the licensed spectrum utilization is highly dependent on the location and time. For instance, during some time periods in a certain geographic area, the allocated spectrum bands may be seldom used. In November 2002, FCC published a report to indicate that for 90% of the time many licensed frequency bands remain unused [10]. Furthermore, Shared Spectrum Company (SCC) has published a bunch of spectrum measurement results of US and some Europe Countries since 2004 [11]. From their spectrum reports in [12] [13] [14], we can see the utilization of many licensed frequency band in many cities is less than 25%. This means that it is not an actual spectrum scarcity that is worrisome, but rather the inefficient spectrum usage.

As a result, since 2004, FCC has recommended to consider authorizing new devices in the TV broadcast spectrum at locations where TV channels are not being used for authorized services, including broadcast television, broadcast auxiliary services such as wireless microphones, and private land mobile radio [15] [16]. The IEEE 802.22 Working Group on Wireless Regional Area Networks (WRANs) was formed in October 2004, and has been working

on the standardization for the rural broadband wireless access using the TV broadcast spectrum by Cognitive Radio (CR) technologies [17].

The basic idea behind IEEE 802.22 is to exploit the unused or not fully utilized licensed spectrum, which is called *spectrum hole*. Actually, this idea was proposed in the concept of CR by Joseph Mitola III at Royal Institute of Technology (KTH), Sweden, in 1999 [18]. With CR technologies, secondary users (SUs) can work with primary users (PUs) in two different modes [19]. One is called *underlay* mode, where SUs can work on all of the channels if the interference to the PUs is less than a predefined threshold. The other one is called *overlay* mode, where SUs can only work on the channels which are not occupied by the PUs. Both way can improve the spectrum utilization significantly and solve the problem of spectrum shortage.

Resource management and optimization is one of the most important issues in CR networks for both underlay and overlay spectrum sharing modes, where the resource includes the spectrum bands (channels) and transmission power. How to manage the resource and optimally allocate channels and control the transmission power for the secondary systems is the main problem we investigate in this study. In this thesis, we apply CR technologies in three major types of wireless networks including cellular networks, femtocell networks, and mesh networks, and formulate the resource optimization problems accordingly.

## 1.1 Motivations

Although spectrum sharing brings opportunities for SUs to access the licensed channels, many new challenges come up when deploying CR in practice. For the application of CR technology, we investigate applications for both underlay and overlay spectrum sharing modes from one-hop to multihop topologies. In the case of one-hop scenarios, we study the problem of spectrum sharing in cellular networks and femtocell networks. Regarding the multi-hop application scenarios, we focus on cognitive radio mesh networks.

## 1.1.1 Cognitive radio cellular networks

Wireless cellular networks (also known as macrocell networks) have evolved from 1st generation (1G) to 4G in the last three decades. The 1G mobile communication system was introduced in the 1980s. It is analog and supports the analog cell phones with the speeds up to 2.4kbps. The second generation (2G) system was employed in 1992. It is the first digital communication system with the speeds up to 64kbps. The 3G wireless communication systems

was employed from 2002 with the speeds up to 2Mbps. The first commercial 4G/LTE (Long Term Evolution) networks have been served by TeliaSonera at Oslo and Stockholm since the end of 2009, which can achieve the speed up to 1 Gbps in theory with normal speed of 100 Mbps [20]. However, operators should pay an expensive license fee for the exclusively usage of the spectrum.

With CR, it is not only possible for operators to deploy cellular networks without paying such an expensive license fee, but also can improve the system performance. We call this kind of network Cognitive Radio Cellular Networks (CogCell), where the CR-enabled SUs are able to sense the available spectrum holes, self-configure themselves to best fit with the specific frequency, control the interference to PUs, and share the spectrum with the licensed PUs efficiently.

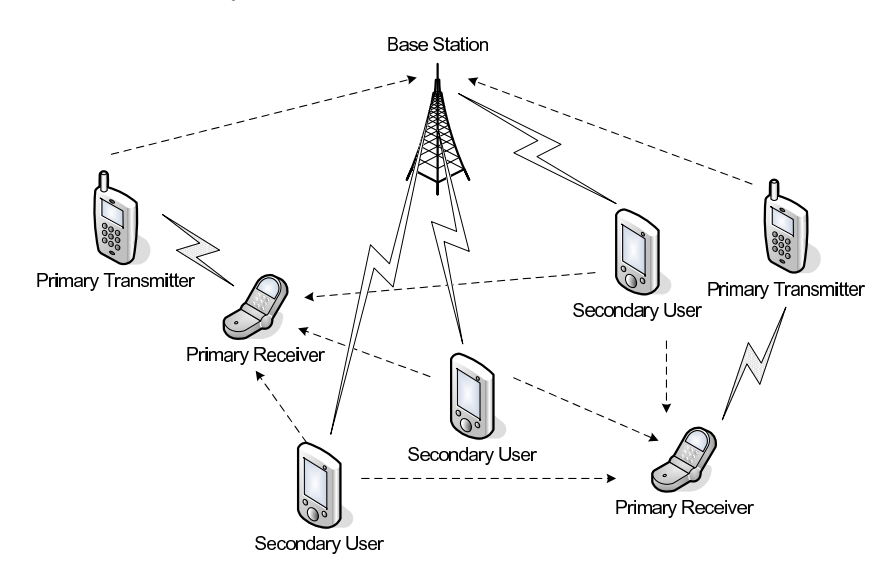


**Figure 1.2:** An illustration of the coexistence between cognitive radio users and and primary systems in cognitive radio cellular networks

Figure 1.2 shows a typical example of CogCell. Spectrum sharing brings us into a great challenge that the SUs activity may cause severe interference with the PUs specially for primary receivers (PRs). Admitting more SUs will increase the interference power received by PRs. To obey the coexisting rule, the interference with PUs from SUs should be not harmful and less than a predefined threshold. Thus, admission control scheme at the BS plays an indispensable role in CogCell. Although, the issue of admission control has been extensively investigated in conventional cellular systems [21], admission control in a power-controlled network is still an open issue [22]. Moreover, conventional cellular networks are considerable different from CogCell. In CogCell, more constraints have to be considered with respect to the admission

control problem due to the presence of PUs. This makes our problem much more complex than the open problem mentioned in [22].

The above problem is not the end of the story, even more challenging problem follows when we consider multi-channel scenarios, where multiple channels are available to allocate to the SUs. On each channel, there are different PUs transmitting and receiving data. SUs which are transmitting data on a channel will cause interference to the PRs on that channel. How to allocate channels to SUs and control the transmission power to guarantee the interference is an essential issue to deploy such a kind of CogCell in practice.

#### 1.1.2 Cognitive radio femtocell networks

In mobile wireless networks, the demand for higher data rates and lower power consumptions is continuously increasing, while the capacity provided by the existing macrocell cellular networks is limited. Studies on wireless usage have shown that more than 50% voice calls and 70% data traffic originate indoors [23]. Specificially, in healthcare environments, a recent study found that 40% of all cellular minutes used by staff were between care providers within the same building [24]. This phenomenon motivates the research and development for femtocell networks, which require that each customer installs a short-range low-cost low-power home base station. These femtocell base stations (FBSs) can communicate with macrocell networks by a broadband connection such as Digital Subscriber Line (DSL), cable modem, or a separate wireless backhaul channel [25]. Femtocells can provide high data rates and Quality of Service (QoS) with low transmission power for consumers. For example, the study in [25] demonstrates that the transmission power can be saved about 34dB and 77dB in different fading environments. As a result, network operators may experience less traffic on their expensive macrocell networks, and can focus their resources on the truly mobile users [25][26].

The spectrum allocated to femtocells is traditionally from the same licensed spectrum bands of macrocells, normally operated by the same mobile network operator. In this case, the capacity of femtocell networks may be highly limited due to the finite number of licensed spectrum bands and also the interference with macrocells and other femtocells. It then inspires us to incorporate the CR technology into femtocell networks, where the CR-enabled femtocell users (FUs) and FBS can identify and utilize the spectrum opportunities from the licensed systems such as macrocell networks and TV broadcast systems as shown in Fig.1.3. In the following, we call this kind of networks Cognitive Radio Femtocell Networks (CogFem). Besides the spectrum agility ability, CogFem has the following features: (a), the number of users in each femtocell is small, e.g., 2, 4 [25]. (b), the size of the cell coverage

is about the house or apartment range, e.g.,  $100 \ m^2$ . (c), the availability of licensed channels is similar in neighboring cells, this is the major difference with CR macrocell networks, where the channel availability may vary a lot between neighboring cells.

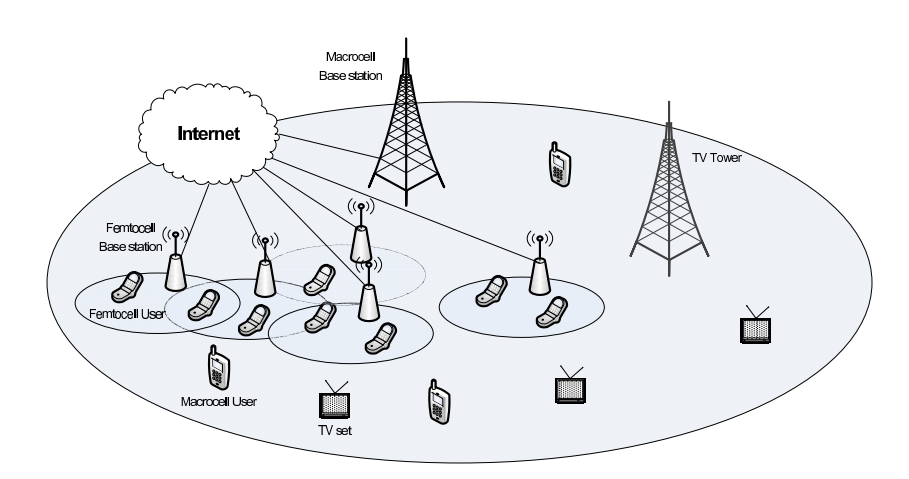


**Figure 1.3:** An illustration of the coexistence between cognitive radio femtocells and primary systems such as macrocells and TV systems

Figure 1.3 shows an illustration of the coexistence between CogFem and primary systems such as macrocells and TV systems. The problem of spectrum sharing emerges when deploying femtocell networks. Spectrum sharing is not the unique problem for CogFem networks, but also an important problem for WLAN and macrocell networks. For the spectrum sharing problem in WLAN, for example in industry such as Cisco, an AP placement strategy is applied to reduce the interference between adjacent floors in a building [24]. In their AP placement strategy, they try to not "stack" APs in adjacent floors. For example, in floor A, APs are placed in the living room, while in floor B, APs are placed in the bedroom. This can increase the distance between APs in adjacent floors, and reduce the interference, but still can not avoid the interference. For macrocell networks, traditional spectrum allocation methods are based on coloring methods that no neighboring cells can use the same spectrum at the same time [27]. Since the number of femtocells could be much higher than the number of macrocells in a certain area, this kind of spectrum allocation requires more spectrum bands and will lead to inefficient and unfair spectrum utilization. This motivates our study to further improve the spectrum utilization and cell capacity in CogFem.

#### 1.1.3 Cognitive radio mesh networks

Wireless mesh networks is believed to be a highly promising technology to extend the network access area in a cheap and convenient way [28] [29]. In this context, there is a strong motivation to utilize the unused spectrum to deliver the mesh network traffic [30]. Thus, Cognitive Radio Mesh Networks (CogMesh), which combines CR and mesh technologies, is proposed with the aim to improve the spectrum utilization and extend the network access area simultaneously [30] [31] [32]. The CogMesh scenario we study is illustrated by a typical example in Fig. 1.4. There are several secondary mesh routers (SMRs) and a Secondary Mesh Gateway (SMG) which connects to the Internet. EachSMR and the SMG are equipped with one CR transceiver and a normal radio transceiver with a dedicated control channel. The CR transceiver in SMRs can sense and utilize the available spectrum holes unused by the PUs [33]. Once PUs in this area return to that channel, the SMRs should release these spectrum, and switch to another spectrum hole. Several secondary mesh users (SMUs) can access their nearby SMRs to communicate with the users not only in the CogMesh but also in the Internet through the SMG.

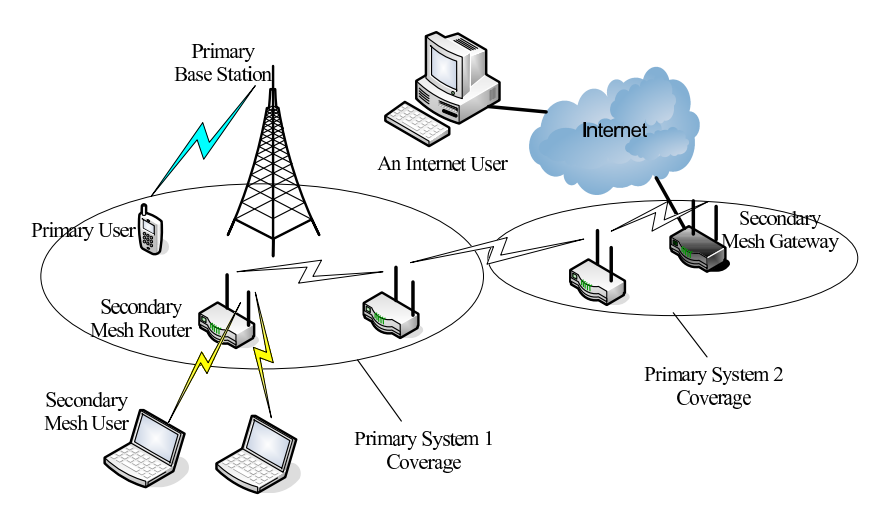


Figure 1.4: An example of cognitive radio mesh network

A significant challenge in CogMesh is the real-time service provision, which has strict constraints on end-to-end delay, jitters, and packet loss rate. We focus on the delay and packet loss caused by the bottleneck of the CogMesh. In CogMesh, the end-to-end delay includes the channel contention delay on each link, channel switching delay on each SMR, queueing delay on each SMR, and the transmission delay from the SMU to the SMG. The quality of a wireless channel varies because of spatial, time, bandwidth, and

central frequency fluctuations [34]. The modulation scheme can be adjusted according to the channel quality to assure that the data can be transmitted successfully, with the help of Adaptive Modulation Coding (AMC) technique. High data rate modulation scheme is used when the channel quality is good, while lower data rate modulation scheme is employed when the channel quality becomes bad. Therefore, the data rate of the channel can vary. Hence the transmission delay will be different if we use different channel selection strategies. On the other hand, channel stability (availability) also varies for different channels due to PUs' activities. During the data transmission, if some PUs return, SUs should stop the transmission and vacate the channel. Thus, packet collisions may happen, and the data transmitted by SMUs could be lost.

All the above challenges motivate us in this work to develop an efficient and reliable channel selection scheme for CogMesh to fulfill the real-time applications.

#### 1.2 Research methods

In this section, we introduce the research methods for general computer science and specify the method used in this thesis work.

## 1.2.1 Research methods for computer science

The author in [35] indicates the research methods for computer science according to the following three categories.

#### • Theoretical computer science [35]

In theoretical computer science, it follows the very classical methodology of building theories as logical systems with stringent definitions of objects and operations for deriving and proving theorems. Theories do not compete with each other but explain the fundamental nature of information. There is no history of critical experiments that decide between the validity of various theories as in physical sciences.

The central topic in theoretical computer science is the design and analysis of algorithms. The results are judged by the insights they reveal about the mathematical nature of various models of computing and/or by their utility to the practice of computing and their ease of application, for example the upper- and lower- resource bounds for the solutions of various problems.

#### • Experimental computer science [35]

In experimental computer science, experiments are used for both theory testing and exploration. The computer scientists must observe phenomena, formulate explanations and theories, and test them, to understand the nature of information processes. Besides, experiments can also be used in areas where theory and deductive analysis are difficult to apply, and can help scientists derive theories from observation. Examples in experimental computer science are automatic theorem proving, planning, NP-complete problems, natural language, vision, games, neural nets/connections, machine learning, and analyzing performance behavior on networked environments in the presence of resource contention from many users.

#### • Computer simulation [35]

Computer simulation comprises computer-based modeling and simulation. It can efficiently handle large data sets, can access a variety of distributed resources and collaborate with other experts over the Internet, etc. It is very efficient to tackle problems of great complexity. It can also provide good visualization.

In addition, modeling is a common way for all these three areas. Modeling is the first step of abstraction, it is used to simplify the phenomenon of interest [35].

#### 1.2.2 Research methods in this thesis

In this thesis, we combine the methods of both theoretical computer science and computer simulation.

Firstly, we model the problem into a mathematical optimization form. Then we use the theory of optimization to analyze and solve this problem. Specifically, we formulate the resource optimization problem in one-channel CogCell as an instance of multidimensional knapsack problem, the resource optimization problem in multi-channel CogCell as an instance of multidimensional multiple knapsack problem, the downlink spectrum sharing problem in CogFem as a mixed integer non-linear programming problem, and the channel and route selection problem in CogMesh as a multiple choice knapsack problem.

Finally, we write simulation codes for computer simulation to evaluate our proposed algorithms. In this study, we build simulation scenarios and implement our algorithms and schemes on Matlab [36]. Other simulation platforms and programming languages can also be used to verify our proposed

algorithms. The results are also compared with a well known optimization software called MOSEK [37].

#### 1.3 Contributions

In this work, we have explored the resource management and optimization problem in one/multiple channel cognitive radio cellular networks, femtocell networks, and mesh networks. Our contributions are as follows.

## 1.3.1 Admission and power control for one-channel cognitive radio cellular networks

In this study, we address the joint admission and power control in CogCell from the perspective of the network operator. We formulate this problem as an optimization problem where the objective is to maximize the secondary revenue achieved by the BS, while satisfying the QoS requirements on SUs and interference constraints on PRs.

In our study in [38], we propose Joint Admission and Power Control scheme using a Minimal Revenue Efficiency Removal algorithm (JAPC-MRER) to address the operator problem. In order to compare the performance of different schemes, we also introduce Joint Admission and Power Control scheme using a Minimal SINR Removal Algorithm (JAPC-MSRA) and Joint Admission and Power Control scheme using a Random removal algorithm (JAPC-Rand), wherein JAPC-MSRA uses an algorithm proposed in [39] to remove the SUs with minimal Signal to Interference and Noise Ratio (SINR), while JAPC-Rand remove SUs randomly when the constraints are not satisfied. The comparison indicates that our proposed JAPC-MRER can achieve much higher secondary revenue for the operator than the other two schemes, while it has the similar time complexity with the other two schemes.

In our study in [40], we further improve JAPC-MRER. Firstly, we find a way to determine the value of the power scale factor in JAPC-MRER and introduce two pre-admission control schemes. Secondly, we reformulate the admission and power control problem as a Multidimentional Knapsack Problem (MKP). Then, we propose a novel admission and power control scheme called JAPC-MKP which is heuristic with low complexity. Finally, simulation results show that our proposed JAPC-MKP can approach the optimal results from the optimization software MOSEK [37], and greatly outperform the previous fixed power scale JAPC-MRER schemes.

# 1.3.2 Channel allocation with admission and power control for multi-channel cognitive radio cellular networks

In multi-channel CogCell, we further extend our study in one-channel CogCell for the operator problem to maximize the revenue while admitting and allocating channels to SUs and control the power for the admitted SUs. Our contributions are threefold.

- We formulate the joint channel allocation, admission and power control problem as a mixed-integer non-linear programming problem which is NP-hard in general. Then, we transfer it to a 0-1 integer linear programming, and can be analogous to a Multidimentional Multiple Knapsack Problem (MMKP).
- Based on the MMKP modeling, we propose a heuristic algorithm to get an approximate solution for the operator problem.
- Simulation results show that our proposed algorithm can achieve quite close revenue to optimal solution by MOSEK [37], and achieve much better revenue than other schemes.

# 1.3.3 Channel allocation and power control for cognitive radio femtocell networks

In this study, we address the spectrum sharing problem in CogFem to maximize the capacity of femtocell networks. In particular, our contributions are fourfold.

- To our best knowledge in the literature, our study is the first to incorporate the concept of CR into femtocells, and formulate the downlink spectrum sharing problems in overlay mode as a mixed integer non-linear programming problem.
- We employ mixed primal and dual decomposition methods to solve the spectrum sharing problem. We also study the robust optimization considering the worst case due the random movements of FUs. According to the solution of the decomposed problem, we proposed a joint channel allocation and fast power control scheme.
- Simulation results show that CogFem could achieve much higher capacity than normal femtocells. The proposed scheme achieved much

higher average capacity and lower user blocking rate than the coloring method.

• Simulation results also show that the proposed joint channel allocation and power control scheme can converge very fast. In addition, the expense for fixed power control scheme with our channel allocation strategies is only 2% less average capacity comparing to the dynamic power control scheme.

# 1.3.4 Channel selection for cognitive radio mesh networks

In the study of cognitive radio mesh networks, our contributions are threefold.

- We jointly consider two major factors, channel availability and channel quality, for CogMesh in a heterogeneous primary system environment.
   We formulate the problem of maximizing the route availability, while guarantee that the end-to-end packet delay is less than a predefined requirement.
- We transform the original non-linear programming problem to a 0-1 integer linear programming, and model it as a variant of Multiple-Choice Knapsack Problem (MCKP). Based on the MCKP modeling, we propose a heuristic method to solve this problem.
- Simulation results show that our proposed heuristic method can achieve close route availability and solution rate to the optimal result from MOSEK. It outperforms the best SINR scheme and best channel availability scheme.

## 1.4 Thesis organization

This thesis is organized as follows. Chapter 2 introduces the background of cognitive radio networks, and summaries the related works in resource management and optimization in cognitive radio networks. Chapter 3 describes our proposed admission and power control schemes for cognitive radio cellular networks sharing one channel with primary users. Chapter 4 describes our proposed channel allocation with admission and power control schemes for cognitive radio cellular networks sharing multiple channels with primary users. Chapter 5 describes our proposed spectrum allocation with power control schemes for cognitive radio femtocell networks. Chapter 6 describes our

#### 1.4 Thesis organization

proposed route and channel selection scheme for cognitive radio mesh networks. Chapter 7 concludes our study in this thesis and points out several future directions in the research on cognitive radio networks.

Table 1.1: Scenarios addressed in each chapter

Chapter	Spectrum Sharing Mode	Hops	Channels
Chapter 3	Underlay	one	one
Chapter 4	Underlay	one	multiple
Chapter 5	Overlay	one	multiple
Chapter 6	Overlay	multiple	multiple

The relationship between the major chapters from Chapter 3 to Chapter 6 can be seen from Table 1.1, where we summarize the scenarios addressed in different chapters. We study the underlay spectrum sharing problem for one-hop scenarios in one and multiple channel cases in Chapter 3 and Chapter 4 respectively. While we study the overlay spectrum sharing problem for multiple channels in both one-hop and multiple-hop cases in Chapter 5 and Chapter 6 respectively.

# Chapter 2

# Background and Related Work

In this chapter, we introduce the background of cognitive radio technologies and present the related work. The background of cognitive radio technologies includes the definition, key technologies, and deployment challenges. We organize the related work around three main themes of our research on cognitive radio networks: (i.) admission and power control with channel allocation in cognitive radio cellular networks, (ii.) channel allocation and power control in cognitive radio femtocell networks, (iii.) channel selection in cognitive radio mesh networks followed by a discussion of previous research related to our own.

## 2.1 Background of cognitive radio networks

## 2.1.1 Definition of cognitive radio

The term "cognitive radio" was firstly introduced by Joseph Mitola in his paper in 1999, where he defined cognitive radio as: " A radio that employs model based reasoning to achieve a specified level of competence in radio related domains." [18].

In 2005, Professor Simon Haykin defined cognitive radio as: "An intelligent wireless communication system that is aware of its surrounding environment (i.e., outside world), and uses the methodology of understanding-by-building to learn from the environment and adapt its internal states to statistical variations in the incoming RF stimuli by making corresponding changes in certain operating parameters (e.g., transmit-power, carrier frequency, and modulation strategy) in real-time, with two primary objectives in mind: (i.) highly reliable communications whenever and wherever needed; (ii.) efficient utilization of the radio spectrum." [2].

On the other hand, the regulator FCC defined cognitive radio as: "A radio that can change its transmitter parameters based on interaction with the environment in which it operates." [41].

There will be a lot of benefits from the new radio regulations, such as getting more capacity, decreasing the cost of communications, improving reliability, and reaching longer distances with wireless equipments.

#### 2.1.2 Cognitive cycle and key technologies

The basic cognitive cycle for a cognitive radio is shown in Fig. 2.1, wherein the receiver is required to do spectrum sensing, analysis, and estimation before transmission in order to protect PUs. The transmitter will then select an appropriate spectrum band (channel) and control the transmit-power to guarantee the interference to PUs are not harmful.

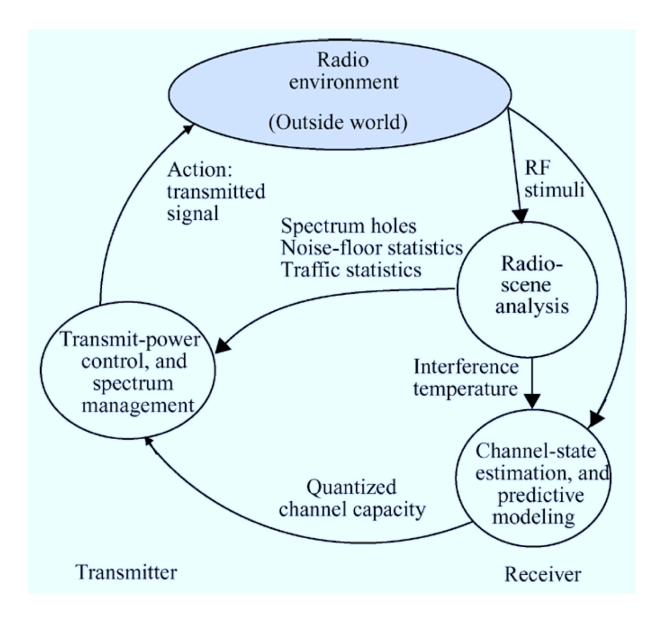


Figure 2.1: Cognitive radio operation cycle [2]

#### Spectrum sensing

In the overlay spectrum sharing mode, SUs detect the activities of PUs in real time, and use the spectrum bands which are not occupied by any PU. Spectrum sensing is one of the most important procedures in CR networks. In literature, there are four major methods for spectrum sensing, i.e., Matched filter, Energy detection[42], Cyclostationary detection[43], and

Wavelet detection [44]. Each method has its own advantages and disadvantages in different scenarios. Detecting the event of PU transmission by a single node is not effective when the SU is shadowed from the PU, or when the SU is out of the PU 's transmission range but it can still interfere with the primary receiver inside the PU 's transmission range [19]. Therefore, cooperative sensing [45] [46], which allows several nodes sense the spectrum environment and make the decision in a cooperative manner, is thought to be an efficient way to solve such problems.

#### Spectrum decision

SUs make decision on which spectrum to use based on the spectrum sensing results. It is one of the most important procedures. A good spectrum decision mechanism should gain as much as possible benefit for transmission, provided the interference to PUs is not harmful or SUs work in a different channel from the channel used by PUs.

Several dynamic spectrum access schemes such as [47], [48], [49], [50], and [51] are proposed using the sensing-based opportunistic spectrum access approaches. For instance, in [47], SUs utilize the past observations to build predictive models for spectrum availability, and choose the channels with the most availability metric. In [48], the authors consider that SUs can only sense some of the available channels because of hardware and energy constraints, and derive the spectrum access strategies under the formulation of finite-horizon Partially observable Markov Decision Processes (POMDPs). In [51], the authors extend the work in [48]. They model the channel occupancy by PUs with a continuous-time Markov chain, and propose an opportunistic spectrum access scheme via periodic channel sensing, while reducing the complexity of the optimal solution in [48].

#### Transmission power control

After spectrum decision, SUs should decide the transmission power on the transmitter.

In the underlay spectrum sharing mode, each SU needs to control its transmission power in order to guarantee the interference to PU is not harmful. The key issue for the underlay approach is how to measure the interference on PUs in an efficient way[52]. Several works have considered the interference constraints for SUs e.g., [53] [54].

On the other hand, in case of the overlay spectrum sharing mode, transmission power control is mainly to achieve the required QoS level in terms of data rate, etc.

#### 2.1.3 Deployment challenges

There are many challenges in deploying cognitive radio into reality, including channel definition, channel availability and heterogeneity, channel quality, and the common control channel.

#### Channel definition

In the literature, a channel in CR networks is always assumed as a spectrum unit. However, there has been no definition about the bandwidth of a channel yet. This issue was firstly addressed by Ian F. Akyildiz et al. in [19]. Later D. Xu et al. studied the optimal channel bandwidth problem in [55] to maximize the SUs' throughput. Generally, a channel can get more capacity when the bandwidth increases, but the channel switching probability may increase because the probability for PUs returning to a wider range of spectrum could be higher than that in a smaller one. The increased channel switching operations will then cause additional overheads like switching delay which would reduce the SUs' throughput.

Another uncertainty in defining a channel is overlapping or not. When the available spectrum is divided into several channels, these channels could be non-overlapping or partially overlapping. Two channels are said to be non-overlapping when they are separated by at least 25 MHz [56]. Using non-overlapping channels can eliminate the interference between different channels, but may be a waste of spectrum. On the contrary, using partially overlapped channels can improve the spectrum utilization, which is not always harmful [57]. Although channel overlapping can increase the number of available channels and improve spectrum utilization, the adjacent SUs that are using the partially overlapped channels may cause interference to each other. Moreover, in this case, the interference to any PU on a certain channel should include the effort of all the SUs' transmissions on the partially overlapped channels, which results in more complexity to model and estimate the interference on PUs.

The aforementioned issues mainly focus on channels divided by continuous spectrum. However, it is possible to construct a channel with discrete subcarriers, as done by Orthogonal Frequency-Division Multiplexing (OFDM) modulation scheme in physical layer, which has been widely used in the IEEE 802.11a/g and the IEEE 802.16 standards [58].

#### Channel availability and heterogeneity

A channel is said to be available for SUs when it is not occupied by any PUs (in the overlay spectrum sharing mode) or the interference from SUs to PUs is under a tolerable threshold (in the underlay spectrum sharing mode). PUs' arbitrary activities result in a dynamic nature of channel availability. In the literature, most work assumes the channel usage pattern of PUs follows an independent and identically distributed ON/OFF random process, such as [59][60][61][62][63]. Where the ON-period represents the channel is occupied by PUs while the OFF-period represents the channel is available for SUs.

The channel availability of SUs on different locations may be distinct from each other because of different PU activities. Even in the same geolocation, SUs may have different available channels because of hardware limitations such as sensing constraints (different SUs may be capable of sensing different range of spectrum) and transmission constraints (SUs may be capable of transmitting on different range of spectrum). This phenomenon would result in the problem of channel heterogeneity where SUs have different available channels at a certain time [64]. In this heterogeneous situation, neighboring SUs should negotiate a common channel to communicate with each other before data transmission.

#### Channel quality

The quality of wireless channels varies over time, space, and frequency. Some important parameters were addressed in [19] as follows.

- Interference: Since channels are shared by different SUs, some channels may be more crowded compared to others. Therefore, an SU using the same transmission power on different channels may result in different SINR on its intent SU receiver. Higher SINR would bring higher throughput to the SU. Moreover, consider the protection of PUs in the underlay spectrum sharing mode, the allowed interference on different channels may be different. Therefore, the allowed transmission power of an SU should be controlled and may be different on different channels.
- Path Loss: The path loss is related to the distance between the SU transmitter and receiver, as well as the channel central frequency. The path loss increases when the distance and frequency increase. Therefore, an SU transmitter may increase its transmission power to compensate for the increased path loss to its intent SU receiver. However, this may cause higher interference to other SUs and PUs.
- Wireless link errors: The errors of links using different channels depend on the modulation scheme as well as the interference at the SU receiver.

• Holding time: The holding time of a channel refers to the expected time duration that SUs can work on this channel. Because the activities of PUs may be different on each channel, the holding time may change accordingly.

The channel quality can be characterized by the above parameters jointly.

#### Common control channel problem

Neighboring SUs in a CR network can communicate with each other directly only if they work on a common channel. But before the communication, they do not know which channel can be used on each other. So, they need to exchange messages to know the available channels on each other. Thus a common channel can be chosen based on their agreement. But the exchanged messages require a Common Control Channel (CCC). This is called the CCC problem as addressed in [65]: "a channel is required to choose a channel".

In [66], the authors analyzed the design requirement of CR networks, and suggested to distinguish control channel and data traffic channels. A simple solution is to have a dedicated CCC. This channel is a dedicated licensed spectrum band to SUs for the exchange of control messages, thus it will not be interrupted by any PUs. In the literature, many contributions are based on this assumption such as [67] [68] [59] [69] [70] [71]. However, this assumption has several following drawbacks.

- License fee: A license fee may be required to get the licensed spectrum band. Therefore, it would be expensive to build and deploy such a CR network.
- Saturation: This dedicated channel can be saturated easily if many SUs contend the control channel for their own traffic. Therefore, it would be the bottleneck of the network throughput.
- Security: It is possible for adversaries to attack SUs by forging control messages to the control channel. It may cause saturation of the control channel that results in Denial-of-Service (DoS). These forged control messages can also cause communication disruptions and gain unfair advantages in resource allocation [72].

Another solution is to choose a control channel among the available channels such as in [65] [73]. There are several challenges related to this case. Firstly, SUs should vacate the channels (in the overlay mode) or reduce the transmission power (in the underlay mode) when PUs are detected. Therefore, the control channel should be the most reliable channel that can not

be interrupted frequently. Secondly, it is sometimes not feasible to select a CCC for the whole network due to the channel heterogeneity problem we have mentioned in 2.1.3.

#### Spectrum sensing problems

Spectrum sensing is not always perfect, thus it gives rise to false alarm and miss detection.

False alarm happens when the spectrum sensing results report the return of PUs which are actually not exist. But following the sensing result, SUs may stop the current transmission and decide to switch to another channel. It then causes additional channel access delay and reduction of throughput.

In contrast to false alarm, miss detection happens when SUs fail to detect the active PUs, and continue working on that channel. Thus, it can cause uncontrolled interference to PUs. It is not only harmful to PUs but also harmful to SUs.

### 2.2 Research problems in our work

We study the following three major problems: power control, admission control, channel allocation. These problems are always considered together.

#### 2.2.1 Power control

Power control in cognitive radio networks is much more complex than in traditional wireless networks.

In cognitive radio networks, SUs control transmission power not only to achieve required QoS level while saving power, but also to protect primary systems. The interference generated by SUs to any PU should be carefully considered, and should not exceed the tolerable threshold.

In our study, we consider the power control problem in cognitive radio cellular networks and femtocell networks. In cognitive radio cellular networks, we focus on the uplink transmission power control for all SUs. SUs, which are allowed to access the Base Station (BS), are required to control transmission power to achieve their QoS level while the interference to PUs is not harmful. In the scenario of CogFem, we focus on the downlink transmission power control for all secondary femtocell base stations. Secondary femtocell base stations control transmission power to achieve the downlink QoS level to secondary femtocell users, while the interference to neighbouring femtocell base stations are minimized.

#### 2.2.2 Admission control

When users' requirement exceeds network's capacity, admission control is usually used besides power control to guarantee the service for dedicated users by rejecting service requests from other users.

In CogCell, a BS is deployed to serve SUs in its coverage area and utilize spectrum from primary systems, when some PUs are in the interference range of the CogCell. SUs are not allowed to transmit any data to the BS if the interference caused by SUs to the PUs is higher than the pre-defined threshold. In addition, different SUs may require different levels of QoS and hence make different payment based on the provided QoS level. From the perspective of operators, the admission problem is to maximize the secondary revenue while the interference from admitted SUs to PUs is less than the tolerated interference threshold, and the QoS level of admitted SUs can be satisfied.

#### 2.2.3 Channel allocation

Channel allocation is an important problem for coexistence between SUs and PUs in cognitive radio networks. It is highly related to spectrum decisions.

In CogCell, we consider the uplink channel allocation from SUs to secondary BS. The channel allocation strategy is designed to not only control the interference between SUs working in the same channel, but also control the interference to PUs working in that channel. In addition, with the constraint of limited transmission power and required QoS level, the channel allocation problem becomes more challenging.

In CogFem, we consider the intra-femtocell channel allocation and down-link channel allocation for femtocell users in each femtocell. Where the intra-femtocell channel allocation handles the interference between neighbouring femtocells, while the downlink channel allocation for femtocell users tries to save power providing the required QoS level is satisfied.

In CogMesh, channel allocation problem is the fundamental problem for each link to select a channel to transmit and receive. However, channels have different characteristics in terms of different channel availability and quality. It is a fundamental requirement to provide a reliable route in CogMesh. In addition, we also consider the real-time applications, where end-to-end delay is required to be less than a threshold. To this end, we need to design a metric for each link to select an appropriate channel so that the end-to-end delay requirements are guaranteed and the route availability is maximized.

#### 2.3 Related work

# 2.3.1 Resource management in cognitive radio cellular networks

Resource management in cognitive radio cellular networks is related to channel allocation, admission control, and power control schemes.

In literature, a few attempts have been made on the resource allocation and power control problems for CogCell in the underlay spectrum sharing mode. They can be classified according to different number of PUs per channel, different number of channels, and different spectrum access schemes as shown in Table 2.1. In the following, we will discuss the previous works according to different number of PUs and different channels.

Related work according to different number of PUs are shown as follows.

- In the case of one PU system model, there are related works such as [74] and [75]. In [74], Y. Xing et al. considered the scenario with one PU, several SUs and separative receivers. The study proposed a distributed constrained power control algorithm and found the optimal link subset to achieve the maximum revenue with the help of a potential game. In [75], L. Zhang et al. modeled a smooth optimization problem, and proposed a minimal SINR removal algorithm (MSRA) to search the optimal set of SUs.
- In the case of multiple PUs system model, there are related works such as [76], [77], [78] and [79]. Specially, in [77], the authors studied the problem of power allocation in a Single Input Multiple Output Multiple Access Channel (SIMO-MAC) based CR network. Where channel is divided into subchannels as the same number of the antennas of the BS. They proposed a multi cap water-filling algorithms to allocate the power for each SU.

Related work according to different number of channels are shown as follows.

• Some efforts have been made in one-channel Code Division Multiple Access (CDMA) CR networks. For example, in [80], the authors studied the problem of power and rate allocation for a set of links sharing only one channel in a CR network. The power allocation is either 0 or maximum power, where if an SU is in a bad channel it stops transmission, otherwise it transmits with the maximum power. In [81], the authors studied the rate and power allocation problem in a CDMA cognitive radio networks sharing one channel.

• For multiple channel scenarios, several efforts have been made in Orthogonal Frequency-Division Multiple Access (OFDMA) CR networks, Where each subchannel can be allocated to only one SU. For example, in [82], the authors studied the problem of frequency, rate and power allocation in OFDMA CR networks. They decomposed the original problem into subproblems to maximize the utility of every subchannel. In [83], the authors studied the subcarrier allocation and power control for OFDMA CR networks.

Table 2.1: Related works in cognitive radio cellular networks

Related Work	Number of PUs	Number of Channels	Medium Access
[74], [75]	one	one	CDMA
[77]	multiple	one	SIMO- MAC
[79], [81], [84] and [80]	multiple	one	CDMA
[82], [83]	one	multiple	OFDMA

# 2.3.2 Spectrum sharing in cognitive radio femtocell networks

Since our work on cognitive radio femtocell networks is the first as far as we know. In literature, there is no study on spectrum sharing in cognitive radio femtocell networks. However, there are few attempts on normal femtocell networks. In [85], the authors studied a downlink case for WiMAX femtocell networks. In [86], the authors applied a finite-difference time-domain (FDTD) method to predict the coverage of WiMAX femtocells. In [87], the authors used a centralized method of dynamic frequency planning (DFP) to minimize the overall femtocell network interference to allocate the spectrum to femtocells. In [88], the authors studied the resource management problem in Orthogonal Frequency-Division Multiple Access (OFMDA) femtocells and proposed a location-based allocation scheme between macrocells and femtocells to adapt the varying user population.

# 2.3.3 Channel selection in cognitive radio mesh networks

In literature, there are some related work on channel assignment considering end-to-end delay requirements in wireless mesh networks. For example, in [89], the authors proposed an interference avoidance channel assignment scheme for different links based on graph coloring. In [90], the authors proposed a channel selection scheme for 802.11 based wireless mesh networks. In [91], the authors designed a routing protocol based on the (weighted) end-to-end delay metric in order to minimize the end-to-end delay in wireless mesh networks. However, in CogMesh, we should take into account channel availability due to the activities of primary systems, thus the channel assignment problem is more challenging.

There are also some related work about channel selection and dynamic spectrum access in CR networks. In [92], a two-person cooperative game theoretical approach is applied in the channel selection between two secondary nodes. However, this work considers only a one-hop scenario with two secondary users. In [93], the authors proposed a channel selection scheme to select the channel with the highest channel weight which is defined as  $e^{-p}(1-p)$ , where p is the occupancy rate of PUs. In [94], the authors studied the channel selection and routing problems in multi hop CR networks, with the objective of minimizing the total bandwidth used in the network. However, they did not consider the end-to-end delay requirement for each flow. In [95], a stochastic channel selection algorithm based on learning automate techniques is proposed. Each secondary node selects one of the channels in a probability which is defined in a probability list. This probability list will be updated according to the result of each selection. The packet will be sent once the channel selected is available to use. However, the end-to-end service requirement is not considered in this work. In [96], three channel selection strategies are proposed for SUs to access heterogeneous channels. The first two are based on the detection of PUs' activities. The third one is based on the monitoring of the throughput of secondary nodes. Thus, in their work, channel selection strategy is made according to either the channel availability (PU's activity) or the channel quality (throughput can be achieved). These two factors are not considered simultaneously. Moreover, only one-hop secondary systems are considered. In a multi-hop network, such as CogMesh, the channel selection problem will be more complex.

## Chapter 3

## Power and Admission Control for One-channel Cognitive Radio Cellular Networks

We start with the resource management and optimization problem in one-channel CogCell, where joint power and admission control is one of the most important issues. In such a CogCell, a BS is deployed to serve SUs in its coverage area and utilize spectrum from primary systems, when some PUs are in the interference range of the CogCell. In the uplink, SUs can be admitted to the BS provided that the interference caused by SUs to the PUs is no higher than the pre-defined threshold. In addition, different SUs may require different levels of QoS and hence make different payment based on the provided QoS level.

In this chapter, we address the joint admission and power control problem in CogCell from the perspective of the network operator to maximize the revenue obtained from SUs subjected to the interference constraints on PUs and QoS requirements of SUs.

The rest of this chapter is organized as follows. We introduce the CogCell model and formulate the optimization problem in Section 3.1. In Section 3.2, we describe and evaluate the performance of our proposed JAPC-MRER and two other schemes, i.e. JAPC-MSRA, and JAPC-Rand. We then discuss the power control schemes and propose three pre-admission control schemes in Section 3.3. We further improve our results by reformulation the problem and propose the Joint Admission and Power Control with Multidimensional Knapsack Problem modeling (JAPC-MKP) scheme in Section 3.4. Then we evaluate the performance of all the proposed schemes in Section 3.5. Finally, Section 3.6 concludes this chapter.

### 3.1 System model and problem formulation

In this section, we describe the system model, introduce the definitions of interference constraints and QoS requirements, and finally formulate the operator optimization problem.

#### 3.1.1 System model

Figure 3.1 shows the system model of one channel CogCell. The BS is located at the center of the cell and provides services for SUs. A number of PUs including PRs and primary transmitters (PTs) are distributed in this cell. PRs are receiving while PTs are transmitting. This CogCell employs Code-Division Multiple Access (CDMA), so that SUs can access the same spectrum band simultaneously. We consider the situation that the spectrum used by SUs are licensed to PUs. Hence, PRs receive interference from SUs which are transmitting data to the BS, while the BS receives interference from PTs. We further assume that the BS can measure the interference from PTs.

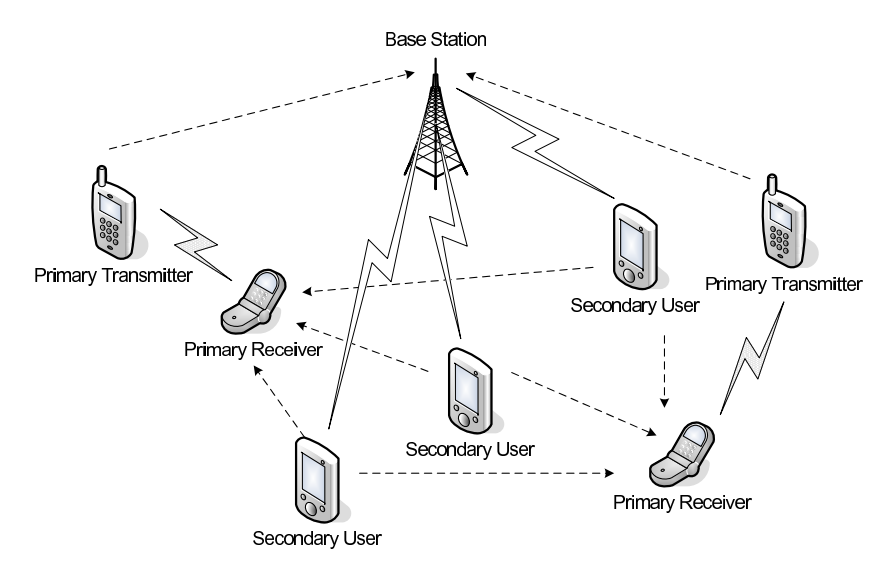


Figure 3.1: System model of one-channel cognitive radio cellular networks

Table 3.1 lists the notations in this chapter. We denote the interference generated by PTs to the BS as  $I_p$ , which can be dynamically changed according to the movements and other activities of PTs. Let  $\mathcal{N}_s$  denote the set of SUs,  $\mathcal{N}_p$  represent the set of PRs, respectively. Let  $n_s = |\mathcal{N}_s|$  and  $n_p = |\mathcal{N}_p|$ . Namely,  $n_s$  and  $n_p$  denote the number of SUs and PRs in the cell, respectively. The network service provider receives the revenue from the accumulated payment by every admitted SU. Suppose that SU i ( $i \in \mathcal{N}_s$ ) pays

 $r_i$  for the operator with the QoS demand in terms of minimal Data Transmission Rate (DTR)  $\bar{\lambda}_i$ . On the other hand, SU i generates interference  $\tau_{ij}$  to PU j if SU i is allowed to access the channel. The interference to PU j from all the active SUs cannot exceed the threshold  $\Gamma_j$ .

**Table 3.1:** Table of notations for one-channel CogCell

Symbol	Meaning
$\mathcal{N}_s$	the set of SUs
$\mathcal{N}_p$	the set of PRs
$I_s$	the interference received at the BS from all SUs
$I_p$	the interference power received by the BS from PTs
$n_s$	the number of SUs
$n_p$	the number of PRs
$\hat{P}_i$ $\hat{P}$	the transmission power at SU $i$
$\hat{P}$	the maximum transmission power at SUs
$r_i$	the revenue from SU $i$
$   au_{ij}  $	the interference from SU $i$ to PR $j$
$\Gamma_j$	the threshold of interference power at PR $j$
$h_i$	the power attenuation from SU $i$ to the BS
$h_{ij}$	the power attenuation from SU $i$ to PR $j$
$d_i$	the distance between SU $i$ and the BS
$d_{ij}$	the distance between SU $i$ and PR $j$
$ar{\lambda_i}$	the minimum uplink DTR required by SU $i$
$\begin{bmatrix} d_{ij} \\ \bar{\lambda}_i \\ \bar{\xi}_i \end{bmatrix}$	the minimum uplink SINR required by SU $i$

#### 3.1.2 Interference power

While SUs share the spectrum with PUs (including PTs and PRs), SUs causes interferences to the PRs. Let  $T_j^I$  denote the interference power received by PR j.

$$T_j^I = \sum_{i=1}^{n_s} h_{ij} P_i x_i \tag{3.1}$$

where the indicator  $x_i$  shows whether SU i is admitted or not.  $x_i = 1$  represents that SU i is admitted, zero otherwise.  $P_i$  refers to the transmission power at SU i.  $h_{ij}$  denotes the power attenuation from SU i to PU j and is

#### Power and Admission Control for One-channel Cognitive Radio Cellular Networks

given by

$$h_{ij} = \frac{G_i^s G_j^p}{(d_{ij})^n} (3.2)$$

where  $d_{ij}$  denotes the distance from SU i to PR j. The exponent n is the path fading factor.  $G_i^s$  and  $G_j^p$  denote the antenna gains of SU i and PR j, respectively. Therefore, according to (3.1) and (3.2), the interference power caused by SU i is expressed as

$$\tau_{ij} = h_{ij} P_i = \frac{G_i^s G_j^p P_i}{(d_{ij})^n}.$$
 (3.3)

#### 3.1.3 QoS definition and requirement

In CogCell, different SUs may have different QoS requirements, and make different payment (e.g., SU i pays  $r_i$  to the operator at the BS). In this chapter, we employ DTR as the major QoS metric. According to Shannon's channel capacity formula, the uplink maximum data transmission rate from SU i to the BS is given by

$$\lambda_i = Blog_2(1 + \xi_i) \tag{3.4}$$

where  $\xi_i$  is the uplink SINR of SU *i* measured at the BS. In the CogCell network, different SUs may require different traffic demands, e.g. voice, video and web browsing. For different types of traffic, the required data rates are different. Let  $\bar{\lambda}_i$  denote the minimum required DTR by SU *i*. Let  $\bar{\xi}_i$  denote the required SINR for SU *i*. Therefore, based on (3.4), we can obtain the required SINR as

$$\bar{\xi_i} = 2^{\frac{\bar{\lambda_i}}{B}} - 1 \tag{3.5}$$

Let  $I_s$  denote the accumulated interference at the BS caused by all active SUs, i.e.,  $I_s = \sum_{i=1}^{n_s} h_i P_i x_i$ . According to the definition of SINR in [34], we can calculate the uplink SINR of an active SU i as following

$$\xi_{i} = \frac{\text{received power at the BS for SU}i}{\text{noise plus interference}}$$

$$= \frac{h_{i}P_{i}}{N_{0} + I_{p} + \sum_{j=1, j \neq i}^{n_{s}} h_{j}^{sb}P_{j}^{s}x_{j}}$$

$$= \frac{h_{i}P_{i}}{N_{0} + I_{p} + I_{s} - h_{i}P_{i}}$$
(3.6)

#### 3.1 System model and problem formulation

where  $h_i$  denotes the power attenuation from SU i to the BS. Similarly, we have

$$h_i = \frac{G_i^s G^b}{(d_i)^n} \tag{3.7}$$

where  $G^b$  stands for the antenna gain of the BS.  $d_i$  refers to the distance from SU i to the BS.

#### 3.1.4The operator problem

The operator problem in CogCell is to maximize the revenue obtained by the operator of the BS. We define the revenue received by the operator on the BS from the SUs as the secondary revenue. The objective is to find the optimal subset of admitted SUs such that the secondary revenue is maximized. At the same time, both the interference power at PUs and the QoS requirements of SUs should be guaranteed. The problem is formulated as follows

$$\text{maximize } \sum_{i=1}^{n_s} r_i x_i \tag{3.8}$$

subject to:

$$\sum_{i=1}^{n_s} \tau_{ij} x_i \le \Gamma_j, \quad \forall j \in \mathcal{N}_p$$
 (3.9)

$$x_i \in \{0, 1\}, \quad \forall i \in \mathcal{N}_s$$
 (3.10)

$$\xi_i \ge \bar{\xi_i}, \quad \text{if } x_i = 1, \forall i \in \mathcal{N}_s$$
 (3.11)

$$x_{i} \in \{0, 1\}, \quad \forall i \in \mathcal{N}_{s}$$

$$\xi_{i} \geq \bar{\xi}_{i}, \quad \text{if } x_{i} = 1, \forall i \in \mathcal{N}_{s}$$

$$P_{i} \in [0, \hat{P}], \quad \forall i \in \mathcal{N}_{s}$$

$$(3.10)$$

$$(3.11)$$

where  $\hat{P}$  is the maximal transmission power for each SU. Constraint (3.9) represents that the interference from all SUs to PUs cannot exceed the interference threshold. Constraint (3.11) represents that the QoS (in terms of SINR, which is determined by DTR) requirement of active SUs should be satisfied. Constraint (3.12) represents the power limitation of SUs.

The defined optimization problem should solve the transmission power of SUs and find out the optimal subset of SUs. Only considering the constraints (3.9) and (3.10), the defined problem (3.8) is a typical 0-1 linear problem, which is NP-Complete [97]. However,  $\tau_{ij}$  ( $\forall i \in \mathcal{N}_s, j \in \mathcal{N}_p$ ) is dynamically changed with different power allocation schemes of SUs based on the constraints (3.11) and (3.12). Thereafter, the dynamics of  $\tau_{ij}$  ( $\forall i \in \mathcal{N}_s, j \in \mathcal{N}_p$ ) makes the original 0-1 linear problem even more challenging. In the following section, we propose a joint admission and power control scheme to solve this problem.

### 3.2 Joint admission and power control schemes

In this section, we propose a joint admission and power control scheme using minimal revenue efficiency removal algorithm called JAPC-MRER to address the operator problem. In order to compare the performance of different schemes, we also introduce JAPC-MSRA and JAPC-Rand, wherein JAPC-MSRA uses an algorithm proposed in [39] to remove the SUs with minimal SINR, while JAPC-Rand remove SU randomly when the constraints are not satisfied.

#### 3.2.1 JAPC-MRER

JAPC-MRER runs in a heuristic way by several iterative operations. Let  $\mathcal{N}_s^*$  and  $\mathcal{N}_p^*$  denote the possible set of admitted SUs and the valid set of PUs, respectively. Initially, all SUs are admitted by the BS, i.e.,  $\mathcal{N}_s^* = \mathcal{N}_s$ , and all PUs should be taken into account, i.e.,  $\mathcal{N}_p^* = \mathcal{N}_p$ . Let  $P_i^{min}$   $(i \in \mathcal{N}_s^*)$  denote the minimum transmission power of SU i to achieve the required minimum SINR  $\bar{\xi}_i$ . The ratio relationship of  $P_i^{min}$  between all SUs can be represented in the following:  $P_1^{min}: P_2^{min}: \ldots: P_{n_s}^{min} = y_1: y_2: \ldots: y_{n_s}$ , where  $y_i$   $(i \in \mathcal{N}_s^*)$  can be calculated by (3.6) and (3.11) as follows

$$y_i = \frac{1}{(1 + \bar{\xi}_i^{-1})h_i} \tag{3.13}$$

Therefore, we can temporally allocate the power  $\beta \hat{P}$  to the SU which has the largest power ratio  $\hat{y}$ . Here,  $\beta$  is a power scaling factor ( $\beta \in (0,1]$ ).

$$\hat{y} = \max\{y_i | \forall i \in \mathcal{N}_s^*\}$$
(3.14)

The power used by other SUs can be assigned based on the ratio to the SU with the transmission power  $\beta \hat{P}$  as follows

$$P_i^{min} = \frac{\beta \hat{P}}{\hat{y}} y_i \tag{3.15}$$

We choose  $P_i$  equal to  $P_i^{min}$ , for all i in the set of  $\mathcal{N}_s^*$ . The reasoning is as follows. If there exists any i in the set of  $\mathcal{N}_s^*$ , wherein  $P_i$  is greater than  $P_i^{min}$ , SU i causes more interferences to any other SU j ( $\forall j \in \mathcal{N}_s^*, j \neq i$ ) than using the transmission power  $P_i^{min}$ . According to (3.6), the SINR of SU j decreases if SU j does not increase its transmission power accordingly. Therefore, all SUs in the set of  $\mathcal{N}_s^*$  other than SU i should increase their transmission power to keep their SINRs non-decreasing. On the other hand, if SUs increase the transmission power, PUs will receive more interference. Due to the constraint

of interference threshold, fewer SUs can be admitted, which will result in smaller secondary revenue. This will be worse than the situation when each SU uses  $P_i^{min}$  as the transmission power. As a consequence, the power of SUs  $P_i$  should be set as  $P_i^{min}$  ( $\forall i \in \mathcal{N}_s^*$ ) to achieve the maximal secondary revenue. After allocating the power to every active SU, we can calculate the interference from every SU to every PU. We use  $\varphi_j$  ( $j=1,...,n_p$ ) to record the difference between the total interference on PU j and its interference threshold.

$$\varphi_j = \sum_{i \in \mathcal{N}_s^*} \tau_{ij} - \Gamma_j \tag{3.16}$$

If  $\varphi_j$  is not greater than 0, the total interference experienced by PU j is less than its threshold. In this situation, PU j should be removed from  $\mathcal{N}_p^*$  (the set of valid PUs) since the interference constraint has been already satisfied on this PU. Otherwise, i.e.  $\varphi_j$  is greater than 0, the positive value of  $\varphi_j$  can physically represent the importance of PU j to the admission set. Consequently, we introduce the revenue efficiency factor as follows

$$e_i = \frac{r_i}{\sum\limits_{j \in \mathcal{N}_s^*} \varphi_j \tau_{ij}}, \quad \forall i \in \mathcal{N}_s^*$$
 (3.17)

The SU with higher revenue efficiency factor is able to provide higher revenue for the operator while generating lower interference to PUs. In order to achieve higher secondary revenue with guaranteed interference at PUs, we can remove the SU with the minimal revenue efficiency factor in the next iteration. The detailed algorithm is shown in Algorithm 1. It terminates if either  $\mathcal{N}_n^*$  or  $\mathcal{N}_s^*$  becomes empty.

The time complexity is dominated by the operation of calculating  $P_i$ ,  $\varphi_j$  and  $e_i$ . There are maximum  $n_s$  iterations for the main loop. After each main loop, the number of admitted SUs is reduced by one. The time complexity can be calculated as follows.

$$T(n_{s}, n_{p}) = (n_{s} + (n_{s} - 1) + (n_{s} - 2) + ...)$$
 calculate power 
$$+(n_{s} + (n_{s} - 1) + (n_{s} - 2) + ...)n_{p}$$
 calculate  $\varphi_{j}$  
$$+(n_{s} + (n_{s} - 1) + (n_{s} - 2) + ...)n_{p}$$
 calculate  $e_{i}$  
$$= (n_{s} + (n_{s} - 1) + (n_{s} - 2) + ...)(2n_{p} - 1)$$
 
$$\leq \frac{n_{s}(1+n_{s})(2n_{p}-1)}{2}$$
 
$$= O(n_{s}^{2}n_{p})$$
 (3.18)

Therefore the time complexity is  $O(n_s^2 n_p)$ .

#### Algorithm 1 JAPC-MRER

```
Input: \mathcal{N}_s, \mathcal{N}_p, \{\lambda_i\}, \{\Gamma_j\}, \{d_{ij}\}, \{d_i\}.
Output: \mathcal{N}_s^*, \{P_i\}
  1: Initialization: \mathcal{N}_s^* \leftarrow \mathcal{N}_s, \mathcal{N}_p^* \leftarrow \mathcal{N}_p.
  2: Calculate y_i, \forall i \in \mathcal{N}_s^*, according to (3.13)
  3: while \mathcal{N}_p^* \neq \emptyset do
                 Select \hat{y} according to (3.14)
  4:
                 Calculate P_i^{min}, \forall i \in \mathcal{N}_s^*, according to (3.15). P_i \leftarrow P_i^{min}, \forall i \in \mathcal{N}_s^*.
  5:
  6:
             for j \in \mathcal{N}_p^* do
  7:
                        Calculate \varphi_i according to (3.16)
  8:
                   if \varphi_i \leq 0 then
  9:
                         \mathcal{N}_p^* \leftarrow \mathcal{N}_p^* - j
10:
                         \mathbf{if}^{r} \mathcal{N}_{n}^{*} = \stackrel{r}{=} \emptyset \mathbf{then}
11:
                                "All the Interference constraints are satisfied"
12:
                                Return:
13:
                         end if
14:
                   end if
15:
             end for
16:
                 Calculate e_i, \forall i \in \mathcal{N}_s^*, according to (3.17).
17:
                 Choose an SU i, where e_i = \min\{e_i | \forall j \in \mathcal{N}_s^*\},\
18:
                 P_i \leftarrow 0
19:
                \mathcal{N}_s^* \leftarrow \mathcal{N}_s^* - i
20:
             if \mathcal{N}_s^* == \emptyset then
21:
                   "No SU can be admitted"
22:
                   Return;
23:
             end if
24:
25: end while
```

#### 3.2.2 JAPC-MSRA

JAPC-MSRA is also a joint admission and power control scheme. Instead, it uses a minimal SINR removal algorithm which is proposed in [39].

The details are shown in Algorithm 2, where, the set of SUs  $\mathcal{N}_s^*$  is updated by removing the SU with the minimal SINR in each iteration of the main loop.

The time complexity is dominated by the operation of calculating the power  $P_i$ ,  $\xi_i$ , and the verification about the interference threshold constraints in each iteration of the main loop. The time complexity can be calculated as follows.

#### Algorithm 2 JAPC-MSRA

```
Input: \mathcal{N}_s, \mathcal{N}_p, \{\lambda_i\}, \{\Gamma_i\}, \{d_{ij}\}, \{d_i\}.
Output: \mathcal{N}_s^*, \{P_i\}
  1: Initialization: \mathcal{N}_s^* \leftarrow \mathcal{N}_s, \mathcal{N}_p^* \leftarrow \mathcal{N}_p.
 2: Calculate y_i, \forall i \in \mathcal{N}_s^*, according to (3.13)
 3: while \mathcal{N}_p^* \neq \emptyset do
                Select \hat{y} according to (3.14)
 4:
                Calculate P_i^{min}, \forall i \in \mathcal{N}_s^*, according to (3.15).
 5:
                P_i \leftarrow P_i^{min}, \forall i \in \mathcal{N}_s^*.
 6:
            if All interference threshold constraints are valid then
 7:
 8:
                  Break;
            end if
 9:
                Calculate \xi_i, \forall i \in \mathcal{N}_s^*, according to (3.6).
10:
                Choose an SU i, where \xi_i = \min\{\xi_j | \forall j \in \mathcal{N}_s^*\},
11:
12:
                P_i \leftarrow 0
               \mathcal{N}_s^* \leftarrow \mathcal{N}_s^* - i
13:
            if \mathcal{N}_s^* == \emptyset then
14:
                  Echo "No SU can be admitted"
15:
                  Break;
16:
            end if
17:
18: end while
```

$$T(n_{s}, n_{p}) = (n_{s} + (n_{s} - 1) + (n_{s} - 2) + ...)$$
 calculate power 
$$+(n_{s} + (n_{s} - 1) + (n_{s} - 2) + ...)n_{p}$$
 verify interference thresholds 
$$+(n_{s} + (n_{s} - 1) + (n_{s} - 2) + ...)$$
 calculate  $\xi_{i}$  
$$= (n_{s} + (n_{s} - 1) + (n_{s} - 2) + ...)(n_{p} + 2)$$
 
$$\leq \frac{n_{s}(1+n_{s})(n_{p}+2)}{2}$$
 
$$= O(n_{s}^{2}n_{p})$$
 (3.19)

Therefore the time complexity of this algorithm is  $O(n_s^2 n_p)$ , which is the same as JAPC-MRER.

#### 3.2.3 JAPC-Rand

JAPC-Rand is also a joint admission and power control scheme. It randomly removes an SU in each iteration. The implementation of JAPC-Rand is based on the Algorithm 2 with minor modification that the line 10 and 11 are modified to randomly select an SU. In consequence, the set of SUs is updated by randomly removing an SU in each iteration operation.

#### Power and Admission Control for One-channel Cognitive Radio Cellular Networks

The time complexity is dominated by the operation of calculating power  $P_i$  in each loop, and the verification of the interference threshold constraints. The time complexity can be calculated as follows.

$$T(n_s, n_p) = (n_s + (n_s - 1) + (n_s - 2) + \dots)$$
 calculate power 
$$+ (n_s + (n_s - 1) + (n_s - 2) + \dots)n_p$$
 verify interference thresholds 
$$\leq \frac{n_s(1+n_s)(n_p+1)}{2}$$
 
$$= O(n_s^2 n_p)$$
 (3.20)

Therefore the time complexity of this algorithm is  $O(n_s^2 n_p)$ , which is the same as JAPC-MSRA and JAPC-MRER.

### 3.2.4 Simulation results and analysis

In this section, we provide the simulation results to demonstrate the performance of the three joint admission and power control schemes JAPC-MRER, JAPC-MSRA, and JAPC-Rand.

We have implemented a CogCell simulator using Matlab [36]. In the simulator, there is a BS located at the center of a cell. The parameters used in this simulation are summarized in Table 3.2. Where  $R_{max}$  denotes the radius of the cell and is set as 1000m. The minimal distance from the BS to any SUs or PUs is denoted by  $R_{min}$ . In our simulation, we choose  $R_{min} = 100m$ . The topologies of SUs and PUs are generated in the way as follows. The distance between SUs (or PUs) and the BS are randomly chosen from  $[R_{min}, R_{max}]$ , The angles from any SUs (or PUs) to the BS are randomly chosen from  $[0, 2\pi]$ . The uplink channel bandwidth B is set as 5MHz. The DTR demand required by every SU i ( $i \in N_s$ ) is randomly chosen from Table 3.3. We also show the DTR and SINR mapping in Table 3.3, where the required SINR demands are calculated by (3.5).

The path fading factor n is set as 4. The antenna gains of all SUs, PUs, and the BS are equal to 1. The power scaling factor  $\beta$  is set as 1.

The revenue  $r_i$  obtained from SU i ( $i \in N_s$ ) is dependent on the DTR. The SU with higher DTR pays more and hence generate higher revenue for the service provider. Without loss of generality and for the sake of illustration, we allocate the revenue and DTR according to Table 3.3.

In the following, we evaluate the performance in terms of the secondary revenues in three different cases, i.e., changing the number of PUs, changing the number of SUs, and changing the interference threshold. We randomly generate 100 topologies. In each topology, we randomly generate the DTR demands. In each case, we run the three schemes, i.e., JAPC-MRER, JAPC-

Table 3.2: Simulation parameters for admission control in CogCell

Symbol	Value	Symbol	Value
$R_{max}$	1000m	$R_{min}$	100m
В	5 MHz	$\hat{P}$	0.28 W
n	4	β	1
$G_i^{sb}$	1	$G^b$	1

**Table 3.3:** Revenue allocation table with DTR and SINR mapping

Revenue	1	2	4	8	16	32
DTR (kbps)	16	32	64	128	256	512
Required SINR	0.0022	0.0043	0.0087	0.0175	0.0353	0.0718

MSRA, and JAPC-Rand to obtain the secondary revenue. Then, we calculate the average secondary revenue based on the results in these 100 topologies.

#### Effect of the number of PUs

In this case, we fix the number of SUs and the interference threshold while changing the number of PUs. Particularly, there are 50 SUs in the CogCell. The interference threshold for each PU is -90dBW.

Figure 3.2 shows the secondary revenue in terms of the number of PUs with three different schemes JAPC-MRER, JAPC-MSRA, and JAPC-Rand.

The secondary revenue decreases with the increasing number of PUs. Because more PUs in the cell result in more stringent interference constraints. This leads to fewer admittable SUs and hence lower revenue. In Fig. 3.2, when  $n_p = 1$ , the secondary revenue obtained by JAPC-MRER, JAPC-MSRA, and JAPC-Rand is 512.6, 478.2, and 463.2, respectively. When  $n_p$  increases to 50, the secondary revenue obtained by JAPC-MRER, JAPC-MSRA, and JAPC-Rand decreases to 384.5, 68.96, and 43.17, respectively. The secondary revenue obtained by JAPC-MRER, when  $n_p$  increases to 50, is more than 5 times of that obtained by JAPC-MSRA, and is almost 9 times of that obtained by JAPC-Rand.

The JAPC-Rand generates the lowest revenue since the JAPC-Rand does not consider the payment differentiation and may remove the SU with high revenue for the operator. The operator can receive more revenue by employ-

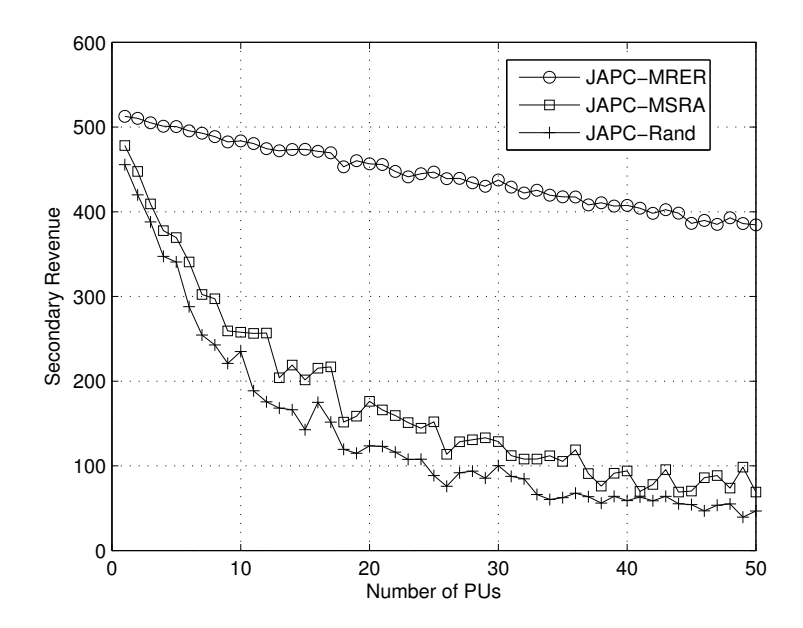


**Figure 3.2:** The secondary revenue in terms of the number of PUs

ing JAPC-MSRA than by using JAPC-Rand since JAPC-MSRA iteratively removes SUs with the minimal SINR, which gives minimal payment to the operator. However, only considering the payment is not enough to achieve the maximum secondary revenue. The interference constraints should be also taken into account. In JAPC-MRER, the introduced revenue efficiency factor considers not only the generated revenue but also the interference to all PUs. Following this advantage, we can see that the operator can obtain much more secondary revenue by employing JAPC-MRER than the other two schemes.

#### Effect of the number of SUs

In this case, we change the number of SUs while fixing the interference threshold and the number of PUs. Especially, the interference threshold for each PU is the same as in the previous case, which is -90dBW. The number of PUs is 6.

Figure 3.3 shows the secondary revenue in terms of the number of SUs with three different schemes JAPC-MRER, JAPC-MSRA, and JAPC-Rand.

The secondary revenue increases with the increasing number of SUs. When the number of SUs is less than 4, all these schemes achieve the same revenue. In this situation, the number of SUs is so few that the interference on all the PUs are too small to exceed the threshold. With the increasing number of SUs, the schemes perform differently. For instance, when  $n_s$  increases

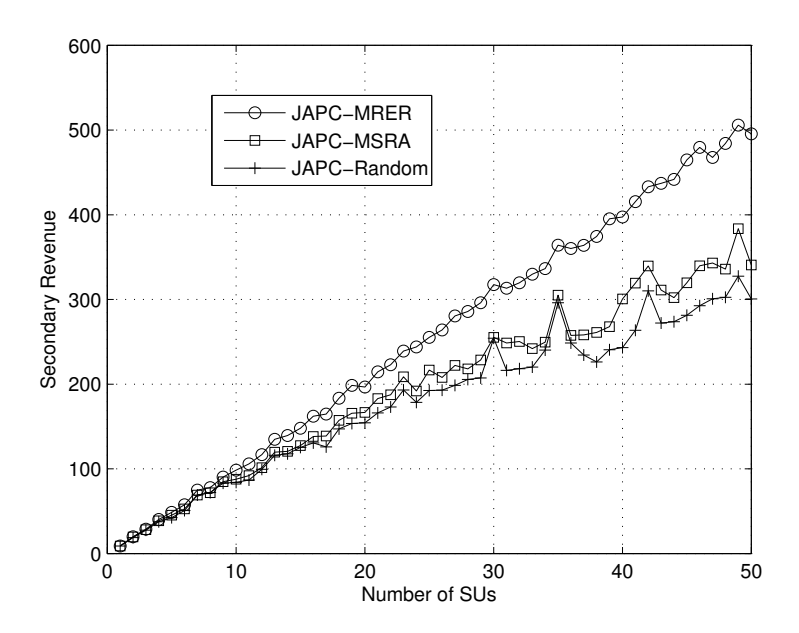


Figure 3.3: The secondary revenue in terms of the number of SUs

to 50, the secondary revenue obtained by JAPC-MRER, JAPC-MSRA, and JAPC-Rand is 495.4, 340.7, and 300.5, respectively. Again, JAPC-Rand achieves the least secondary revenue because it may remove the SUs with high revenue but low interference. JAPC-MSRA achieves more revenue than JAPC-Rand for the operator because it can keep the SUs with high revenue. However, the SUs with high revenue and also high interference to PUs may be admitted. Our proposed scheme JAPC-MRER achieve the balance between the revenue and the interference, and can achieve the highest revenue.

#### Effect of the interference threshold

In this case, we fix the number of PUs and SUs while changing the interference threshold for PUs. Specially, there are 6 PUs and 50 SUs in the BS. The interference thresholds of all PUs are changed from -150dBW to -10dBW.

The results are shown in Fig. 3.4, where JAPC-MRER achieves a slightly lower revenue than the optimal when the interference threshold is less than -100dBW. There are two extreme situations when all the schemes achieve nearly same performance. In this example, when the threshold is less than -130dBW, the interference thresholds are too small to admit any SU while guaranteeing the limited interference to PUs. When the threshold is greater than -50dBW, the interference thresholds are sufficiently large and hence all SUs can be admitted while guaranteeing the interference to PUs. When the

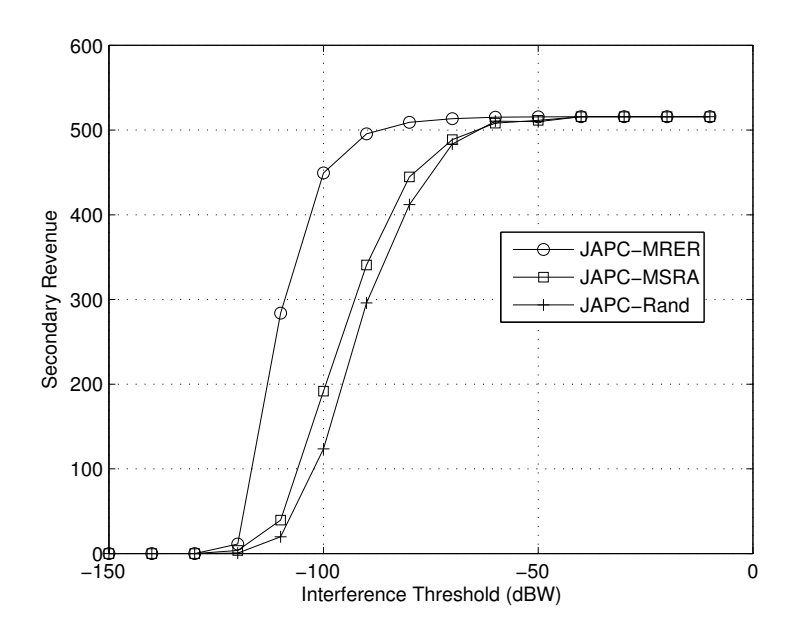


Figure 3.4: The secondary revenue in terms of the interference threshold

interference threshold is greater than -130dBW and smaller than -50dBW, JAPC-MSRA and JAPC-Rand perform very similarly, because these two schemes do not consider the interference to PUs. Since JAPC-MRER considers the influence of the interference, it removes the SUs with high interference to PUs and low revenue to the operator. Following this, JAPC-MRER is capable of achieving the highest among these schemes.

# 3.3 Discussions on power control and pre-admission schemes

In this section, we further discuss the power scaling factor  $\beta$  in the power control schemes in the previous section and propose three pre-admission control schemes.

For any admitted SU i, according to the SINR constraints and the power allocation strategy in (3.15), we have

$$\xi_{i} = \frac{h_{i}P_{i}}{N_{0} + I_{p} + I_{s} - h_{i}P_{i}}$$

$$= \frac{h_{i}\frac{\beta\hat{P}}{\hat{y}}y_{i}}{N_{0} + I_{p} + \sum_{k \in \mathcal{N}_{s}^{*}} y_{k}\frac{\beta\hat{P}}{\hat{y}}y_{k} - h_{i}\frac{\beta\hat{P}}{\hat{y}}y_{i}}$$

$$\geq \bar{\xi}_{i}$$
(3.21)

Then, we obtain

$$\beta \ge \frac{\hat{y}(N_0 + I_p)}{\hat{P}\left(\frac{h_i y_i}{\bar{\xi}_i} - \sum_{k \in \mathcal{N}_s^*, k \ne i} h_k y_k\right)}$$
(3.22)

where

$$\frac{h_i y_i}{\bar{\xi}_i} - \sum_{k \in \mathcal{N}_s^*, k \neq i} h_k y_k > 0$$

Moreover, since  $\beta \in (0, 1]$ , we have

$$0 < \frac{\hat{y}(N_0 + I_p)}{\hat{P}\left(\frac{h_i y_i}{\xi_i} - \sum_{k \in \mathcal{N}_s^*, k \neq i} h_k y_k\right)} \le 1$$
(3.23)

Then we can obtain

$$\frac{h_i y_i}{\bar{\xi}_i} - \sum_{k \in \mathcal{N}^* \ k \neq i} h_k y_k \ge \hat{y} (N_0 + I_p) \hat{P}^{-1}$$
(3.24)

which is equivalent to the following inequality

$$\frac{1}{1+\bar{\xi_i}} - \sum_{k \in \mathcal{N}_*^*, k \neq i} \frac{1}{1+\bar{\xi_k}^{-1}} \ge \hat{y}(N_0 + I_p)\hat{P}^{-1}$$
(3.25)

where the left side of the inequality can be further transformed as follow.

$$\frac{1}{1+\bar{\xi_i}} - \sum_{k \in \mathcal{N}_s^*, k \neq i} \frac{1}{1+\bar{\xi_k}^{-1}} = \left(1 - \frac{1}{1+\bar{\xi_i}^{-1}}\right) - \sum_{k \in \mathcal{N}_s^*, k \neq i} \frac{1}{1+\bar{\xi_k}^{-1}}$$

$$= 1 - \sum_{k \in \mathcal{N}_s^*} \frac{1}{1+\bar{\xi_k}^{-1}}$$

$$= 1 - \sum_{i \in \mathcal{N}_s^*} \frac{1}{1+\bar{\xi_i}^{-1}}$$
(3.26)

#### Power and Admission Control for One-channel Cognitive Radio Cellular Networks

Therefore, substituting (3.26) into (3.25), we have

$$\left(1 - \sum_{i \in \mathcal{N}_s^*} \frac{1}{1 + \bar{\xi}_i^{-1}}\right) \hat{y}^{-1} \ge (N_0 + I_p) \hat{P}^{-1}$$
(3.27)

If the inequality (3.27) is not true, the SINR constraints (3.11) cannot be satisfied. Therefore, some pre-admission procedures should be carried out. In this study, we consider the following three metrics.

- Maximum y removal: The maximum y removal scheme will remove SUs with maximum value of y until the inequality (3.27) are true.
- Minimum SINR removal: The minimum SINR removal scheme will remove SUs with minimum SINR  $\xi$  until the inequality (3.27) are true.
- Minimum channel gain removal: The minimum channel gain removal scheme will remove SUs with minimum channel gain h until the inequality (3.27) are true.

After the above pre-admission procedures, we can have an updated set of SUs  $\mathcal{N}_s^*$ . Then, according to (3.22) and (3.26) we can obtain the value of power scale factor.

$$\beta \ge \frac{\hat{y}(N_0 + I_p)}{\hat{P}\left(1 - \sum_{i \in \mathcal{N}_s^*} \frac{1}{1 + \bar{\xi}_i^{-1}}\right)}$$
(3.28)

Since the bigger  $\beta$  is, the higher the power is, which will result more interference to PUs. Therefore, we will choose  $\beta$  as small as possible.

$$\beta = \frac{\hat{y}(N_0 + I_p)}{\hat{P}\left(1 - \sum_{i \in \mathcal{N}_s^*} \frac{1}{1 + \bar{\xi}_i^{-1}}\right)}$$
(3.29)

By applying different pre-admission control metrics (maximum y removal, minimum SINR removal, or minimum channel gain removal), removal algorithms (MRER or MSRA), power control scaling update strategies (fixed or keep updating after each removal), we have in total twelve schemes as shown in Table 3.4. The flow chart of all the joint admission and power control schemes are shown in Fig. 3.5.

These schemes can be treated as variants from JAPC-MRER and JAPC-MSRA described in Section 3.2. Specially, the schemes in Section 3.2 is a

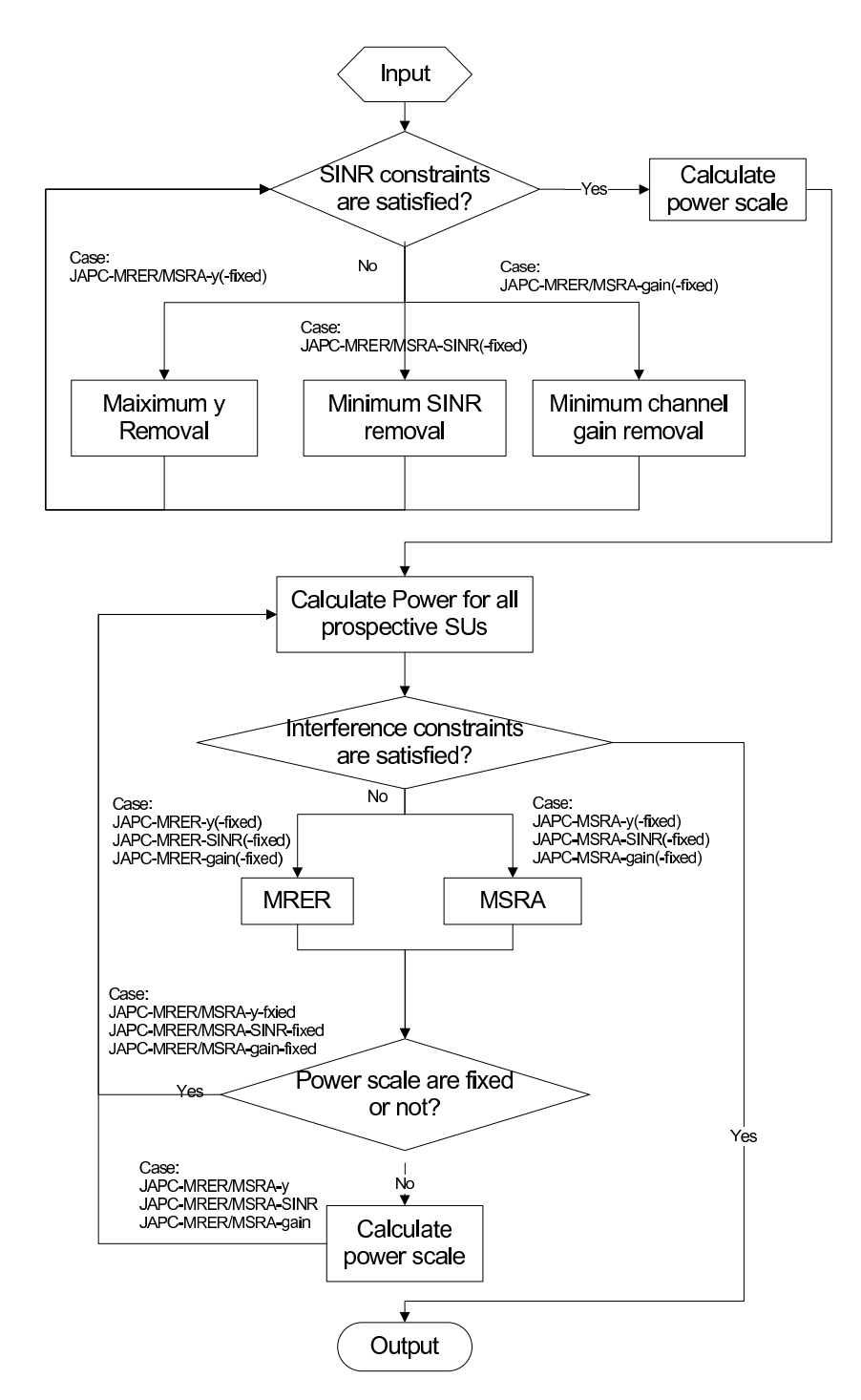


**Figure 3.5:** The flow chart of joint admission and power control schemes for one-channel CogCell

#### Power and Admission Control for One-channel Cognitive Radio Cellular Networks

Table 3.4: Joint admission and power control schemes for one-channel CogCell

Main	Sub Category	Schemes	Pre-admission met-
Category			rics
	JAPC-MRER-	JAPC-MRER-y-	Maximum $y$ removal
	fixed	fixed	
		JAPC-MRER-	Minimum SINR re-
		SINR-fixed	moval
JAPC-	$\beta$ is fixed after	JAPC-MRER-	Minimum channel
MRER	each removal)	gain-fixed	gain removal
	JAPC-MRER-	JAPC-MRER-y	Maximum $y$ removal
	dynamic		
		JAPC-MRER-	Minimum SINR re-
		SINR	moval
	$\beta$ updates after	JAPC-MRER-	Minimum channel
	each removal)	gain	gain removal
	JAPC-MSRA-	JAPC-MSRA-y-	Maximum $y$ removal
	fixed	fixed	
		JAPC-MSRA-	Minimum SINR re-
		SINR-fixed	moval
JAPC-	$\beta$ is fixed after	JAPC-MSRA-	Minimum channel
MSRA	each removal)	gain-fixed	gain removal
	JAPC-MSRA-	JAPC-MSRA-y	Maximum $y$ removal
	dynamic		
		JAPC-MSRA-	Minimum SINR re-
		SINR	moval
	$\beta$ updates after	JAPC-MSRA-	Minimum channel
	each removal)	gain	gain removal

special case when we fix  $\beta$  after each removal. We denote the general fixed  $\beta$  schemes as JAPC-MRER-fixed and JAPC-MSRA-fixed, respectively. On the other hand, if  $\beta$  keeps updating after each removal, we denote such schemes as JAPC-MRER-dynamic and JAPC-MSRA-dynamic, respectively. In the case of fixing  $\beta$ , when we apply the maximum y removal pre-admission metric, we get JAPC-MRER-y-fixed and JAPC-MSRA-y-fixed, when we apply the minimum SINR removal pre-admission metric, we get JAPC-MRER-SINR-fixed and JAPC-MSRA-SINR-fixed, when we apply the minimum channel gain removal, we get JAPC-MRER-gain-fixed and JAPC-MSRA-gain-fixed.

Otherwise, if  $\beta$  keeps on updating after each removal, we get JAPC-MRER-y and JAPC-MSRA-y (when applying maximum y removal pre-admission metric), JAPC-MRER-SINR and JAPC-MSRA-SINR (when applying minimum SINR removal pre-admission metric), JAPC-MRER-gain and JAPC-MSRA-gain (when applying minimum channel gain removal pre-admission metric).

### 3.4 Further improvements

In this section, we improve the algorithm proposed in the previous sections by transforming the formulation. We rewrite the original problem formulation as follows.

$$\text{maximize } \sum_{i=1}^{n_s} r_i x_i \tag{3.30}$$

subject to:

$$\sum_{i=1}^{n_s} h_{ij} P_i x_i \le \Gamma_j, \quad \forall j \in \mathcal{N}_p$$
 (3.31)

$$x_i \in \{0, 1\}, \quad \forall i \in \mathcal{N}_s$$
 (3.32)

$$\xi_i \ge \bar{\xi}_i, \quad \text{if } x_i = 1, \forall i \in \mathcal{N}_s$$
 (3.32)

$$P_i \in [0, \hat{P}], \quad \forall i \in \mathcal{N}_s$$
 (3.34)

Let  $\mathcal{N}_s^*$  denote the optimal solution for admitted SUs is a subset of  $\mathcal{N}_s$ . Thus,

$$x_i = \begin{cases} 1, & i \in \mathcal{N}_s^* \\ 0, & \text{otherwise} \end{cases}$$

From (3.33), we have

$$\xi_i = \frac{h_i P_i}{N_0 + I_p + I_s - h_i P_i} \ge \bar{\xi}_i, \forall i \in \mathcal{N}_s^*$$

When any admitted SU i achieves the required SINR,

$$\frac{h_i P_i}{N_0 + I_p + I_s - h_i P_i} = \bar{\xi_i}, \quad \forall i \in \mathcal{N}_s^*$$

Thus

$$h_i P_i = (N_0 + I_p + I_s)/(1 + \bar{\xi_i}^{-1}), \quad \forall i \in \mathcal{N}_s^*$$

#### Power and Admission Control for One-channel Cognitive Radio Cellular Networks

Let  $a_i$  denote  $1 + \bar{\xi_i}^{-1}$ , we have

$$h_i P_i = (N_0 + I_p + I_s)/a_i, \quad \forall i \in \mathcal{N}_s^*$$
(3.35)

We add up all the admitted SUs as follows

$$\sum_{i \in \mathcal{N}_s^*} h_i P_i = \sum_{i \in \mathcal{N}_s^*} (N_0 + I_p + I_s) / a_i$$

The left side is equal to  $I_s$ , thus

$$I_s = (N_0 + I_p + I_s) \sum_{i \in \mathcal{N}_s^*} a_i^{-1}, \quad \forall i \in \mathcal{N}_s^*$$

After solving the above equation for  $I_s$ , we can get

$$I_s = \frac{N_0 + I_p}{\left(\sum_{i \in \mathcal{N}_s^*} a_i^{-1}\right)^{-1} - 1}$$
(3.36)

Substituting (3.36) into (3.35), we can get the solution of power

$$P_{i} = \frac{N_{0} + I_{p} + I_{s}}{h_{i}a_{i}}$$

$$= \left(N_{0} + I_{p} + \frac{N_{0} + I_{p}}{\left(\sum_{k \in \mathcal{N}_{s}^{*}} a_{k}^{-1}\right)^{-1}}\right) / (h_{i}a_{i})$$

$$= \frac{N_{0} + I_{p}}{h_{i}a_{i}\left(1 - \sum_{k \in \mathcal{N}_{s}^{*}} a_{k}^{-1}\right)}$$
(3.37)

Substituting (3.37) into the constraint in (3.31), we have

$$\sum_{i \in \mathcal{N}_s^*} h_{ij} \frac{N_0 + I_p}{h_i a_i \left(1 - \sum_{k \in \mathcal{N}_s^*} a_k^{-1}\right)} \le \Gamma_j, \quad \forall j \in \mathcal{N}_p$$

Therefore,

$$\sum_{i \in \mathcal{N}_s^*} h_{ij} h_i^{-1} a_i^{-1} (N_0 + I_p) \le \Gamma_j \left( 1 - \sum_{k \in \mathcal{N}_s^*} a_k^{-1} \right), \quad \forall j \in \mathcal{N}_p$$

Then, we can obtain the following constraint

$$\sum_{i \in \mathcal{N}_s^*} \left( h_{ij} h_i^{-1} \Gamma_j^{-1} (N_0 + I_p) + 1 \right) a_i^{-1} \le 1, \quad \forall j \in \mathcal{N}_p$$

It is equal to the following constraint

$$\sum_{i \in \mathcal{N}_{-}} \left( h_{ij} h_i^{-1} \Gamma_j^{-1} (N_0 + I_p) + 1 \right) a_i^{-1} x_i \le 1, \quad \forall j \in \mathcal{N}_p$$
 (3.38)

To obey constraint (3.34), we have

$$0 \le \frac{N_0 + I_p}{h_i a_i \left(1 - \sum_{k \in \mathcal{N}_s^*} a_k^{-1}\right)} \le \hat{P}, \quad \forall i \in \mathcal{N}_s^*$$

which turns out to be

$$\sum_{k \in \mathcal{N}_s^*} a_k^{-1} \le 1 - \frac{N_0 + I_p}{h_i a_i \hat{P}} \quad \forall i \in \mathcal{N}_s^*$$
(3.39)

#### 3.4.1 Lower and upper bounds

We introduce z, where  $z = \min\{h_i a_i, \forall i \in \mathcal{N}_s^*\}$ . According to (3.39) we have

$$\sum_{k \in \mathcal{N}^*} a_k^{-1} \le 1 - \frac{N_0 + I_p}{z\hat{P}}$$

It is equal to the following constraint

$$\sum_{i \in \mathcal{N}_s} a_i^{-1} x_i \le 1 - \frac{N_0 + I_p}{z\hat{P}} \tag{3.40}$$

In summary, the original optimization problem can be transformed into the following formulated problem.

maximize 
$$\sum_{i \in \mathcal{N}_s} r_i x_i$$
subject to 
$$\sum_{i \in \mathcal{N}_s} \left( h_{ij} h_i^{-1} \Gamma_j^{-1} (N_0 + I_p) + 1 \right) a_i^{-1} x_i \le 1, \qquad \forall j \in \mathcal{N}_p \quad (3.41)$$

$$\sum_{i \in \mathcal{N}_s} a_i^{-1} x_i \le 1 - \frac{N_0 + I_p}{z \hat{P}}, \qquad z = \min_{x_i = 1} h_i a_i \quad (3.42)$$

$$x_i \in \{0, 1\} \qquad \forall i \in \mathcal{N}_s$$

The constraint (3.42) dynamically changes according to different admitted SUs.

#### **Constraints Reduction**

We can further examine the relationship between the two constraints in (3.41) and (3.42).

$$\sum_{i \in \mathcal{N}_s} a_i^{-1} x_i \leq 1 - \sum_{i \in \mathcal{N}_s} h_{ij} h_i^{-1} \Gamma_j^{-1} (N_0 + I_p) a_i^{-1} x_i, \quad \forall j \in \mathcal{N}_p \quad (3.43)$$

$$\sum_{i \in \mathcal{N}_c} a_i^{-1} x_i \le 1 - \frac{N_0 + I_p}{z\hat{P}} \tag{3.44}$$

In the right of the above two constraints, we need to show the constraint that has higher value. Since both are larger than 0, we can compare the ratio to 1.

$$R = \frac{\sum_{i \in \mathcal{N}_s} h_{ij} h_i^{-1} \Gamma_j^{-1} (N_0 + I_p) a_i^{-1} x_i}{\frac{N_0 + I_p}{z \hat{P}}}$$

$$= z \hat{P} \sum_{i \in \mathcal{N}_s} h_{ij} h_i^{-1} \Gamma_j^{-1} a_i^{-1} x_i$$
(3.45)

The lower bound of the ratio can be calculated as follows,

$$R = z\hat{P} \sum_{i \in \mathcal{N}_s} h_{ij} h_i^{-1} \Gamma_j^{-1} a_i^{-1} x_i$$

$$= \hat{P} h_{kj} \Gamma_j^{-1} + \hat{P} \sum_{i \in \mathcal{N}_s^*} h_{ij} \Gamma_j^{-1} \frac{h_k a_k}{h_i a_i}, \quad z = h_k a_k, k \in \mathcal{N}_s^*$$

$$\geq \hat{P} h_{kj} \Gamma_j^{-1}$$

$$\geq \hat{P} \Gamma_j^{-1} \min_{i \in \mathcal{N}_s^*} h_{ij}$$

$$\geq \hat{P} \Gamma_j^{-1} \min_{i \in \mathcal{N}_s} h_{ij}, \quad \forall j \in \mathcal{N}_p$$

$$(3.46)$$

Let  $R_L$  represent the lower bound of R

$$R_L = \max_{j \in \mathcal{N}_p} \left( \Gamma_j^{-1} \min_{i \in \mathcal{N}_s} h_{ij} \right) \hat{P}$$
 (3.47)

The upper bound of the ratio can be calculated as follows,

$$R = z\hat{P} \sum_{i \in \mathcal{N}_{s}^{*}} h_{ij} h_{i}^{-1} \Gamma_{j}^{-1} a_{i}^{-1}$$

$$= \hat{P} \Gamma_{j}^{-1} \sum_{i \in \mathcal{N}_{s}^{*}} \frac{h_{k} a_{k}}{h_{i} a_{i}} h_{ij}$$

$$\leq \hat{P} \Gamma_{j}^{-1} \sum_{i \in \mathcal{N}_{s}^{*}} h_{ij}$$

$$\leq \hat{P} \Gamma_{j}^{-1} \sum_{i \in \mathcal{N}_{s}} h_{ij}, \quad \forall j \in \mathcal{N}_{p}$$

$$(3.48)$$

Let  $R_U$  represent the upper bound of R

$$R_U = \min_{j \in \mathcal{N}_p} \left( \Gamma_j^{-1} \sum_{i \in \mathcal{N}_s} h_{ij} \right) \hat{P}$$
 (3.49)

Then we have the following three cases.

• If  $R_L \geq 1$ , then  $R \geq 1$ , the problem formulation can be modified as follows.

maximize 
$$\sum_{i \in \mathcal{N}_s} r_i x_i$$
subject to 
$$\sum_{i \in \mathcal{N}_s} \left( h_{ij} h_i^{-1} \Gamma_j^{-1} (N_0 + I_p) + 1 \right) a_i^{-1} x_i \le 1, \quad \forall j \in \mathcal{N}_p$$
$$x_i \in \{0, 1\}, \qquad \forall i \in \mathcal{N}_s$$
$$(3.50)$$

• If  $R_U \leq 1$ , then  $R \leq 1$ , the problem formulation can be modified as follows.

maximize 
$$\sum_{i \in \mathcal{N}_s} r_i x_i$$
subject to 
$$\sum_{i \in \mathcal{N}_s} a_i^{-1} x_i \le 1 - \frac{N_0 + I_p}{z\hat{P}}, \quad z = \min_{x_i = 1} h_i a_i$$
$$x_i \in \{0, 1\}, \qquad \forall i \in \mathcal{N}_s$$
 (3.51)

• Otherwise, all the original constraints should be considered.

#### The lower bound with tightening of constraints

In (3.42), a tighter constraint can be obtained, if we get the value z from all the SUs no matter it is admitted or not.

$$z \ge \min_{i \in \mathcal{N}_s} h_i a_i$$

#### Power and Admission Control for One-channel Cognitive Radio Cellular Networks

Therefore, we can obtain the following tighter constraint when z is equal to  $\min_{i \in \mathcal{N}} h_i a_i$ .

$$\sum_{i \in \mathcal{N}_s} a_i^{-1} x_i \le 1 - \frac{N_0 + I_p}{\min_{i \in \mathcal{N}_s} h_i a_i \hat{P}}$$
 (3.52)

Thus,

maximize 
$$\sum_{i \in \mathcal{N}_s} r_i x_i$$
subject to 
$$\sum_{i \in \mathcal{N}_s} \left( h_{ij} h_i^{-1} \Gamma_j^{-1} (N_0 + I_p) + 1 \right) a_i^{-1} x_i \le 1, \quad \forall j \in \mathcal{N}_p$$

$$\sum_{i \in \mathcal{N}_s} a_i^{-1} x_i \le 1 - \frac{N_0 + I_p}{\min_{i \in \mathcal{N}_s} h_i a_i \hat{P}}$$

$$x_i \in \{0, 1\}, \qquad \forall i \in \mathcal{N}_s$$

$$(3.53)$$

#### The upper bound with relaxation of constraints

In (3.42), a looser constraint can be obtained, if we get the value z as the maximal value of the product of  $h_i$  and  $a_i$  from all the SUs no matter it is admitted or not.

$$z \le \max_{i \in \mathcal{N}_s} h_i a_i$$

Therefore, we can obtain the following relaxed constraint when z is equal to  $\max_{i \in \mathcal{N}_-} h_i a_i$ .

$$\sum_{i \in \mathcal{N}_s} a_i^{-1} x_i \le 1 - \frac{N_0 + I_p}{\max_{i \in \mathcal{N}_s} h_i a_i \hat{P}}$$

$$\tag{3.54}$$

Thus,

maximize 
$$\sum_{i \in \mathcal{N}_s} r_i x_i$$
subject to 
$$\sum_{i \in \mathcal{N}_s} \left( h_{ij} h_i^{-1} \Gamma_j^{-1} (N_0 + I_p) + 1 \right) a_i^{-1} x_i \le 1, \quad \forall j \in \mathcal{N}_p$$

$$\sum_{i \in \mathcal{N}_s} a_i^{-1} x_i \le 1 - \frac{N_0 + I_p}{\max_{i \in \mathcal{N}_s} h_i a_i \hat{P}}$$

$$x_i \in \{0, 1\}, \qquad \forall i \in \mathcal{N}_s$$

$$(3.55)$$

# 3.4.2 Multidimensional knapsack problem modeling and solutions

According to (3.39) we have

$$\sum_{k \in \mathcal{N}^*} a_k^{-1} + \frac{N_0 + I_p}{h_i a_i \hat{P}} \le 1, \quad \forall i \in \mathcal{N}_s^*$$

#### 3.4 Further improvements

which is equal to the following inequality,

$$\sum_{k \in \mathcal{N}_s} a_k^{-1} x_k + \frac{N_0 + I_p}{\hat{P}} h_i^{-1} a_i^{-1} x_i \le 1, \quad \forall i \in \mathcal{N}_s$$

Then we have

$$\sum_{k \in \mathcal{N}_s, k \neq i} a_k^{-1} x_k + \left( 1 + \frac{N_0 + I_p}{\hat{P}} h_i^{-1} \right) a_i^{-1} x_i \le 1, \quad \forall i \in \mathcal{N}_s$$
 (3.56)

Therefore, the reformulated problem is as follows.

maximize 
$$\sum_{i \in \mathcal{N}_s} r_i x_i$$
subject to 
$$\sum_{i \in \mathcal{N}_s} \left( h_{ij} h_i^{-1} \Gamma_j^{-1} (N_0 + I_p) + 1 \right) a_i^{-1} x_i \le 1, \quad \forall j \in \mathcal{N}_p$$

$$\sum_{k \in \mathcal{N}_s, k \neq i} a_k^{-1} x_k + \left( 1 + \frac{N_0 + I_p}{\hat{P}} h_i^{-1} \right) a_i^{-1} x_i \le 1, \quad \forall i \in \mathcal{N}_s$$

$$x_i \in \{0, 1\}, \quad \forall i \in \mathcal{N}_s$$

$$(3.57)$$

The above formulation can be further written in a canonical matrix form, which is useful for computer aided optimization tools, such as MOSEK [37] and CPLEX [98].

maximize 
$$\mathbf{C}\mathbf{x}$$
  
subject to  $\mathbf{A}\mathbf{x} \leq \mathbf{1}$   
 $\mathbf{x} \in \{0, 1\}$  (3.58)

where

$$\mathbf{1} = (1, 1, ..., 1)^T$$

$$\mathbf{x} = (x_1, x_2, ..., x_{n_s})^T$$

$$\mathbf{C} = (r_1, r_2, ..., r_{n_s})$$

The above formulation is a 0-1 integer linear programming, and can be analogous to a multidimensional knapsack problem, where there are  $(n_s+n_p)$  constraints as the dimensions.

maximize 
$$\sum_{i \in \mathcal{N}_s} r_i x_i$$
subject to 
$$\sum_{i \in \mathcal{N}_s} w_{ij} x_i \le 1, \quad j = 1, ..., n_s + n_p$$
$$x_i \in \{0, 1\}, \qquad \forall i \in \mathcal{N}_s$$
 (3.59)

where

$$w_{ij} = \begin{cases} \left(h_{ij}h_i^{-1}\Gamma_j^{-1}(N_0 + I_p) + 1\right)a_i^{-1} & 1 \le j \le n_p \\ a_i^{-1} & 1 + n_p \le j \le n_s + n_p, j \ne (i + n_p) \\ \left(1 + \frac{N_0 + I_p}{\hat{P}}h_i^{-1}\right)a_i^{-1} & j = i + n_p \end{cases}$$

$$(3.60)$$

The multidimensional knapsack problem is classified as an NP-hard optimization problem, which cannot be solved in polynomial time [99]. Many algorithms, which can be categorized into two types: exact algorithms and heuristic algorithms, have been proposed to solve this problem. The branch-and-bound method [100], and dynamic programming [101] [102] can be used

to find the exact optimal solution of the problem. However, these methods have high computation load [99]. Heuristic algorithms, which aim to compute feasible solutions of "reasonable quality" within "reasonable running time" [99], is more feasible than the optimal algorithms. Typical heuristic algorithms include greedy-type heuristic algorithm, relaxation-based heuristic algorithm, etc.

#### 3.4.3 Proposed efficiency based heuristics method

In this study, we propose an efficiency based heuristics algorithm called JAPC-MKP. The heuristics method proceeds iteratively. Let  $\mathcal{N}_{cs}$  denote the original set of constraints index from 1 to  $n_s + n_p$ , which follows the same sequence of the row index for the matrix  $\mathbf{A}$ . In each iteration, it will exam the valid constraints, and remove one SU in each constraint. Let  $\mathcal{N}_{cs}^*$  denote the valid constraints, and  $\mathcal{N}_s^*$  represent the set of admitted SUs in each iteration.

The order to remove one SU in each iteration is according to the *efficiency* which is defined as follows.

$$e_i = \frac{r_i}{\sum_{j \in \mathcal{N}_{s}^*} \alpha_j w_{ij}} \tag{3.61}$$

The smaller the efficiency is, the higher probability to remove that SU. In each iteration, we remove the SU with the minimal efficiency. In equation (3.61)  $\alpha_j$  is called relevance value of constraint j. It shows the importance to every constraint. The higher the relevance value of a constraint, the higher the scarcity of the corresponding resource is. It then becomes less attractive to pack an SU which consumes a lot of that resource. In our study, we define  $\alpha_j$  as follows.

$$\alpha_j = \sum_{i \in \mathcal{N}_s^*} w_{ij} - 1, \quad j \in \mathcal{N}_{cs}^*$$
 (3.62)

This method is shown in Algorithm 3. The complexity is dominated by the calculation of  $\alpha_j$  in each iteration. In the worst case, it has maximal  $n_s + n_p$  iteration, the cardinality of  $|\mathcal{N}_s^*|$  reduces by one at each iteration from  $n_s$  to 1. The time complexity can be calculated as follows.

$$T(n_{s}, n_{p}) = (n_{s} + (n_{s} - 1) + (n_{s} - 2) + ...)(n_{s} + n_{p})$$
 calculate  $\alpha_{j}$   

$$\leq (n_{s} + (n_{s} - 1) + (n_{s} - 2) + ... + 1)(n_{s} + n_{p})$$
  

$$= \frac{n_{s}(1+n_{s})}{2}(n_{s} + n_{p})$$
  

$$= O(n_{s}^{2}(n_{s} + n_{p}))$$
(3.63)

Thus the time complexity at worst case is  $O(n_s^2(n_s + n_p))$ .

```
Algorithm 3 JAPC-MKP
```

```
\overline{\text{Input: } \mathcal{N}_s, \, \mathcal{N}_p, \, \mathcal{N}_{cs}}
Output: \mathcal{N}_s^*, \{P_i\}
  1: Initialization: \mathcal{N}_s^* \leftarrow \mathcal{N}_s, \mathcal{N}_p^* \leftarrow \mathcal{N}_p, \mathcal{N}_{cs}^* \leftarrow \mathcal{N}_{cs}.
  2: Calculate w_{ij}, \forall i \in \mathcal{N}_s^*, j \in \mathcal{N}_{cs}^*, according to (3.60)
      while \mathcal{N}_{cs}^* \neq \emptyset do
             for j \in \mathcal{N}_{cs}^* do
  4:
                        Calculate \alpha_i according to (3.62)
  5:
                   if \alpha_i \leq 0 then
  6:
                         \mathcal{N}_{nc}^* \leftarrow \mathcal{N}_{nc}^* - j
if \mathcal{N}_{nc}^* == \emptyset then
  7:
  8:
                                "All constraints are satisfied"
  9:
10:
                                Return;
                          end if
11:
                   end if
12:
             end for
13:
             for i \in \mathcal{N}_s^* do
14:
                        Calculate e_i according to (3.61).
15:
             end for
16:
                 Choose an SU i^*, where e_{i^*} = \min_{\forall i \in \mathcal{N}_{nc}^*} e_i
17:
18:
                 x_{i^*} \leftarrow 0
19:
                 P_{i^*} \leftarrow 0
                 \tilde{\mathcal{N}_s^*} \leftarrow \mathcal{N}_s^* - i^*
20:
             if \mathcal{N}_s^* == \emptyset then
21:
                   "No SU can be admitted"
22:
                   Return;
23:
             end if
24:
25: end while
26: for i \in \mathcal{N}_s^* do
27:
                  x_i \leftarrow 1
                  Calculate P_i according to (3.37).
28:
29: end for
```

## 3.5 Simulation results

In this section, we evaluate the performance of all the proposed schemes in Section 3.3 and Section 3.4. The schemes in Section 3.2 is a special case of the

fixed β updating schemes in Section 3.3. In the convenience for comparison in this simulation, we denote the JAPC-MRER and JAPC-MSRA schemes in Section 3.2 as JAPC-MRER-fixed and JAPC-MSRA-fixed, respectively. Where JAPC-MRER-fixed includes JAPC-MRER-y-fixed, JAPC-MRER-SINR-fixed, and JAPC-MRER-gain-fixed, while JAPC-MSRA-fixed includes JAPC-MSRA-gain-fixed for the three different pre-admission control metrics. We denote the schemes proposed in Section 3.3 as JAPC-MRER-dynamic and JAPC-MSRA-dynamic, respectively. Where JAPC-MRER-dynamic includes JAPC-MRER-y, JAPC-MRER-SINR, and JAPC-MRER-gain, while JAPC-MSRA-dynamic includes JAPC-MSRA-y, JAPC-MSRA-sinR, JAPC-MSRA-gain for the three different pre-admission control metrics.

We use the CogCell simulator specified in Section 3.2.4, where we generate 100 random topologies. In each topology, we randomly generate the DTR demands. In addition, we use the same DTR and SINR mapping table as Table 3.3. The noise power  $N_0$  is set as  $10^{-14}$  W. The other simulation parameters are the same as in Table 3.2 except the power scaling factor  $\beta$ . In this simulation, the power scaling factor is calculated by (3.29) after the pre-admission procedures for the schemes proposed in Section 3.3. For JAPC-MKP proposed in Section 3.4, there is no need for this parameter.

In the following simulation, we evaluate the performance in terms of the secondary revenues in four different cases, i.e., changing the number of PUs, changing the number of SUs, changing the interference threshold ( $\Gamma$ ), and changing the interference to BS from primary systems ( $I_p$ ).

In each case, with the given number of PUs and SUs, the value of  $\Gamma$  and and  $I_p$ , we solve the optimization problem by MOSEK software [37], and run the joint admission and power control schemes, i.e., JAPC-MKP, JAPC-MRER-dynamic, JAPC-MRER-fixed, and JAPC-MSRA-dynamic. Then, we calculate the average secondary revenue based on the results in the 100 random topologies.

## 3.5.1 Effect of the number of primary users

In the following, we evaluate the secondary revenue when changing the number of PUs. The other parameters are fixed as follows,  $n_s = 50$ ,  $\Gamma = -100dBW$ , and  $I_p = -110dBW$ .

The results are shown in Fig. 3.6, where the secondary revenue decreases with the increasing number of PUs. The reason is that more PUs will add more constraints on interference generated by SUs. We can see that our proposed JAPC-MKP can approach the optimal results obtained by the

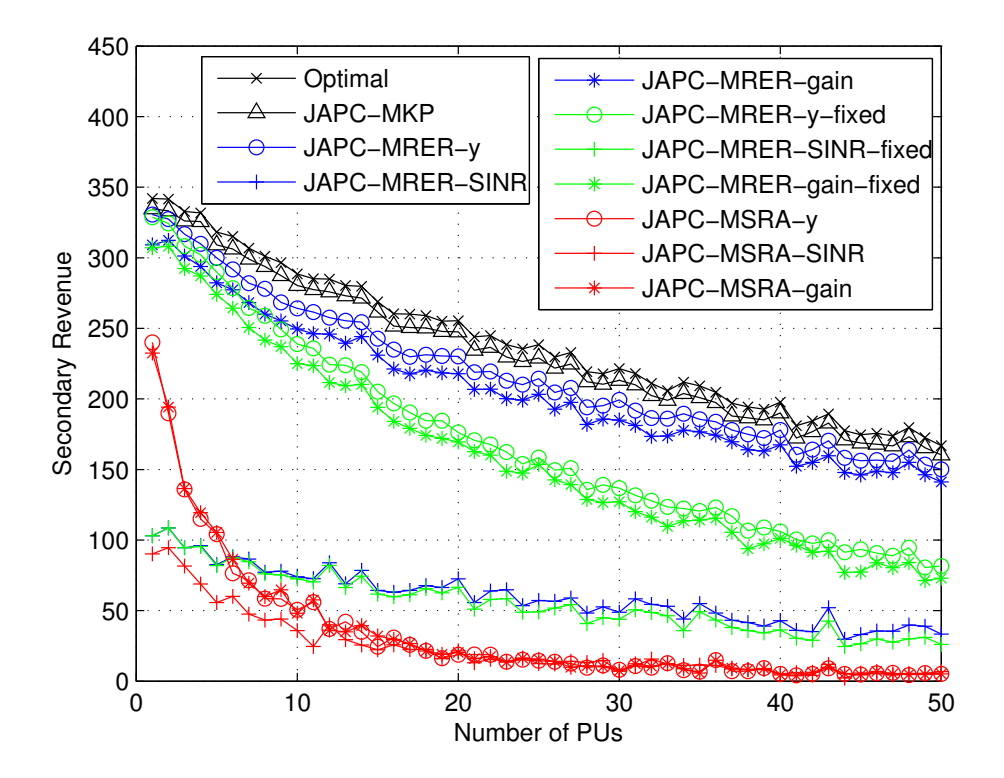


**Figure 3.6:** Secondary Revenue in terms of number of PUs ( $n_s=50$ ,  $\Gamma=$ -100dBW, and  $I_p = -110dBW$ )

optimization software MOSEK, and achieve higher revenue than all other schemes. JAPC-MRER-SINR achieves the least revenue than all the other schemes, the reason is as follows. From (3.27), we see that if the constraints

cannot be satisfied, parts of the left side of that inequality  $\left(1 - \sum_{i \in \mathcal{N}_s^*} \frac{1}{1 + \bar{\xi_i}^{-1}}\right)$ 

is too large. To reduce the value of  $\left(1-\sum_{i\in\mathcal{N}_s^*}\frac{1}{1+\bar{\xi_i}^{-1}}\right)$ , we may need to re-

move more SUs with minimal SINR metric, since the smaller SINR is, the smaller  $\sum_{i \in \mathcal{N}_s^*} \frac{1}{1 + \bar{\xi_i}^{-1}}$  is. JAPC-MRER-y achieves the highest revenue among

all the three pre-admission control metrics. The reason can be found from (3.27), where  $\hat{y}$  reduces after removing the SU with maximum y, thus the left part of the inequality can increase more efficiently than other two metrics. The dynamic  $\beta$  updating strategy can achieve higher revenue than the fixed  $\beta$  strategy in all kinds of pre-admission control schemes. This is because that with the updated  $\beta$  calculated by (3.29) after each removal,  $\beta$  decreases and results in power decreasing for all prospective SUs, which further results in less interference to PUs. Therefore, more SUs can be admitted comparing to the fixed  $\beta$  scheme. JAPC-MRER can achieve higher revenue than JAPC-MSRA for all kinds of pre-admission schemes in the case of dynamic updating  $\beta$  strategy.

#### 3.5.2 Effect of the number of secondary users

In the following, we evaluate the secondary revenue when changing the number of SUs. The other parameters are fixed as follows,  $n_p=50,~\Gamma=-100dBW,$  and  $I_p=-110dBW.$ 

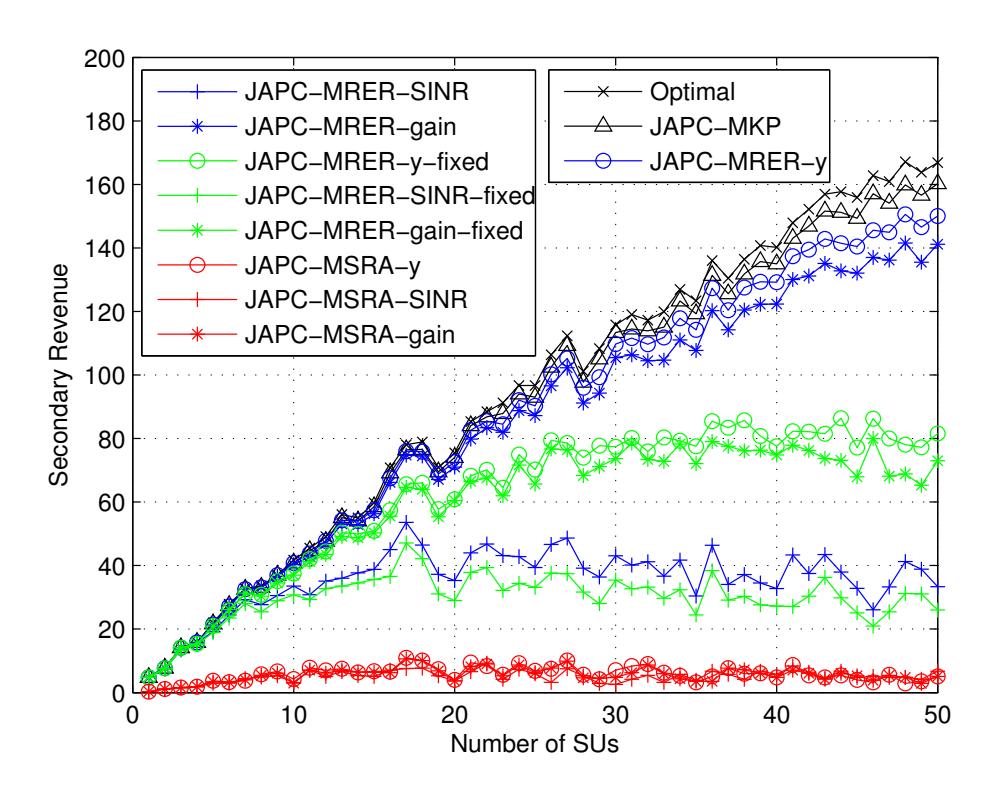


Figure 3.7: Secondary revenue in terms of number of SUs ( $n_p=50$ ,  $\Gamma=-100dBW$ , and  $I_p=-110dBW$ )

The results are shown in Fig. 3.7, where the secondary revenue increases with the increasing number of SUs. The reason is that with the increasing number of SUs, the number of SUs with trivial interference can increase and contribute on the increasing revenue to BS. We can see that our proposed JAPC-MKP can approach the optimal results obtained by the optimiza-

tion software MOSEK, and achieve higher revenue than all other schemes. With the same reason as explained in the previous case, JAPC-MRER-SINR achieves the least revenue than all the other schemes, and JAPC-MRER-y achieves the highest revenue among all the three pre-admission control metrics, and the dynamic  $\beta$  updating strategy can achieve higher revenue than the fixed  $\beta$  strategy in all kinds of pre-admission control schemes. JAPC-MRER can achieve higher revenue than JAPC-MSRA for all kinds of pre-admission schemes in the case of dynamic updating  $\beta$  strategy.

# 3.5.3 Effect of the interference threshold on primary users

In the following, we evaluate the secondary revenue when changing  $\Gamma$ , which is the interference threshold on PUs. The other parameters are fixed as follows, there are 50 SUs, 50 PUs, and  $I_p = -110dBW$ .

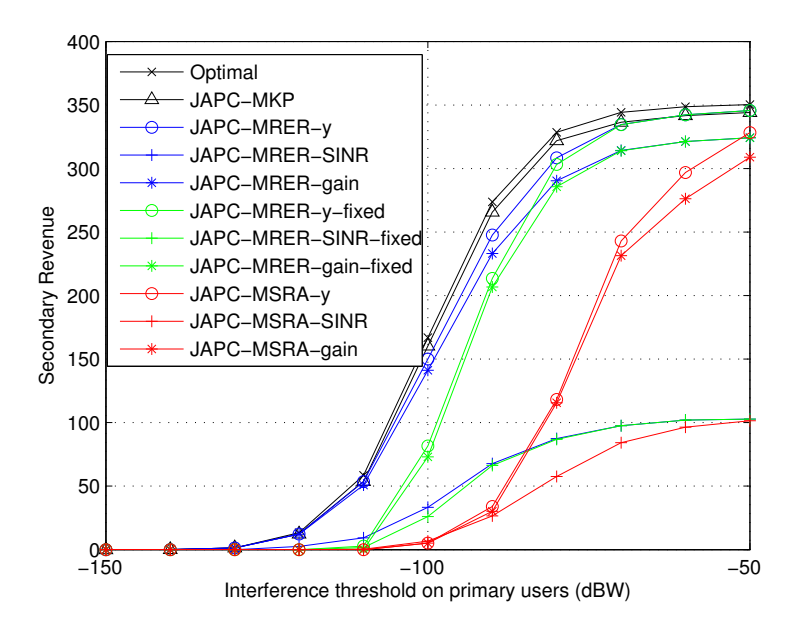


Figure 3.8: Secondary Revenue in terms of  $\Gamma$  ( $n_s=50$ ,  $n_p=50$ , and  $I_p=-110dBW$ )

The results are shown in Fig. 3.8. Again, JAPC-MKP achieves revenue closely to the optimal result from MOSEK, and outperform all other schemes. When  $\Gamma$  is less than -130dBW, the interference constraints are too strict that no SUs can be admitted into the system. When using JAPC-MRER the

dynamic  $\beta$  updating schemes achieve higher revenue than the fixed  $\beta$  updating scheme when  $\Gamma$  is less than -70dBW and larger than -130dBW. The maximum y removal pre-admission control scheme always outperform the minimal SINR and channel gain removal schemes using either JAPC-MRER or JAPC-MSRA. JAPC-MRER outperforms JAPC-MSRA when using the same pre-admission control scheme by using either dynamic or fixed  $\beta$  updating strategy.

# 3.5.4 Effect of the interference to BS from primary systems

In the following, we evaluate the secondary revenue when changing  $I_p$ , which is the interference to BS from primary systems. The other parameters are fixed as follows,  $n_s = 50$ ,  $n_p = 50$ , and  $\Gamma = -100 dBW$ .

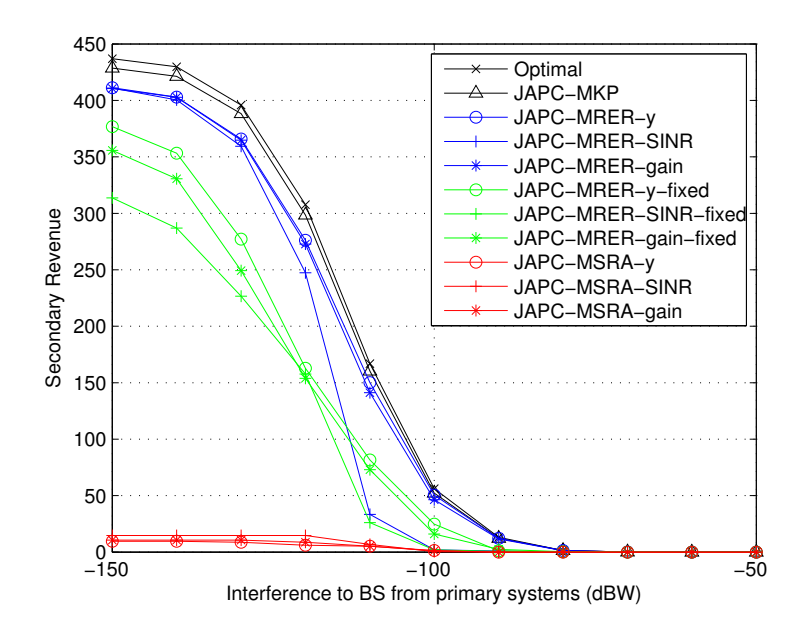


**Figure 3.9:** Secondary Revenue in terms of  $I_p$  ( $n_s=50$ ,  $n_p=50$ , and  $\Gamma=-100dBW$ )

The results are shown in Fig. 3.9. Again, JAPC-MKP achieves revenue closely to the optimal result from MOSEK, and outperform all other schemes. When  $I_p$  is greater than -80dBW, the interference to BS is too strong that no SUs can be admitted into the system. When  $I_p$  is less than -80dBW, the dynamic  $\beta$  updating schemes achieve higher revenue than the fixed  $\beta$  updating scheme using JAPC-MRER. The maximum y removal pre-admission con-

trol scheme always outperform the minimal SINR and channel gain removal schemes using either JAPC-MRER or JAPC-MSRA. JAPC-MRER outperforms JAPC-MSRA when using the same pre-admission control scheme by using either dynamic or fixed  $\beta$  updating strategy.

### 3.6 Conclusion

In this chapter, we have investigated the problem of maximizing the secondary revenue of the CogCell, while satisfying the QoS (in terms of DTR) requirements on SUs and guaranteeing the interference constraints on PUs. To solve this optimization problem, we first introduced a revenue efficiency factor to search for the SUs with high revenue and also low interference, and proposed JAPC-MRER. The time complexity is  $O(n_s^2 n_p)$ , which is the same as the other two algorithms used in JAPC-MSRA and JAPC-Rand. Simulation results indicated that our proposed JAPC-MRER can achieve much higher secondary revenue for the operator than the other two schemes. We further improved our proposed JAPC-MRER by pre-admission control schemes and dynamic updating the power scale after each removal. Simulation results showed that JAPC-MRER-dynamic schemes can achieve higher secondary revenue than JAPC-MRER-fixed schemes with all kinds of pre-admission control schemes. The minimal y removal pre-admission control scheme can achieve higher secondary revenue than other pre-admission control schemes. In the end, we transformed the operator problem to an instance of multidimensional knapsack problem, and proposed a heuristic scheme called JAPC-MKP with  $O(n_s^2(n_s + n_p))$  time complexity. Simulation results showed that JAPC-MKP can approach the optimal results obtained by the optimization software MOSEK, and achieve higher secondary revenue than all other proposed schemes.

## Chapter 4

## Resource Optimization for Multi-channel Cognitive Radio Cellular Networks

In the previous chapter, we focused on the power and admission control for one-channel CogCell. We now consider the multi-channel CogCell, where channel allocation strategies should be taken into account. In this chapter, we study the operator problem again to maximize the secondary revenue in multi-channel CogCell. We formulate this problem as an instance of multi-dimensional multiple knapsack problem, and proposed a heuristic method.

The rest of this chapter is organized as follows. We introduce the system model and formulate the optimization problem in Section 4.1. In Section 4.2, we model the operator problem as an MMKP. We then transfer the MMKP to MKP in Section 4.3, and present our proposed heuristic scheme in Section 4.4. In Section 4.5, we introduce a traditional channel allocation scheme based on SINR together with JAPC-MKP which has been proposed in Chapter 3. In Section 4.6, we evaluate the performance of different schemes by simulation. Finally, we draw the conclusions in Section 4.7.

## 4.1 System model and problem formulations

In this section, we introduce the system model, the coexistence condition of PUs and SUs, the definition of interference from SUs to PUs, and the uplink throughput of SUs. At the end of this section, we formulate the operator problem.

#### 4.1.1 System model

We consider a multi-channel CDMA CogCell in a certain area with multiple PUs, SUs, and channels as illustrated in Fig. 4.1. The set of channels is denoted as  $\mathcal{N}_c$ . These channels are licensed to the primary systems in that area. A secondary BS is deployed to serve a set of SUs (denoted by  $\mathcal{N}_s$ ) using the channels from  $\mathcal{N}_c$ . For a given channel m ( $m \in \mathcal{N}_c$ ), a set of  $\mathcal{N}_{pm}$  PUs will receive interference from SUs working in the same channel m. Those PUs are not part of the CogCell users, but existing in the CogCell area. They may be fixed or mobile. The interference power received by BS from the primary transmitters can be measured by the BS, and we denote it as  $I_{pm}$  for any channel m. BS will allocate a channel for each SU. The allocation rule should guarantee that the interference to those PUs in any channel m should not exceed the tolerable interference threshold.

This model is different with OFDMA mode as follows. In OFDMA mode, wideband channels are divided into several sub-carriers, which logically form subchannels. Each subchannel are further allocated to one user at one time. The BS should decide how to allocate the subchannels to SUs, and each SU can utilize several subchannels at the same time. But in multi-channel CDMA mode, the BS should decide how to allocate the wideband channels to each SU, which can only use one of the wideband channels.

Table 4.1 lists the notations used in this chapter. Channel gain information between SUs and BS, between SUs and PUs in receiving mode is assumed to be estimated by the same method as in [79].

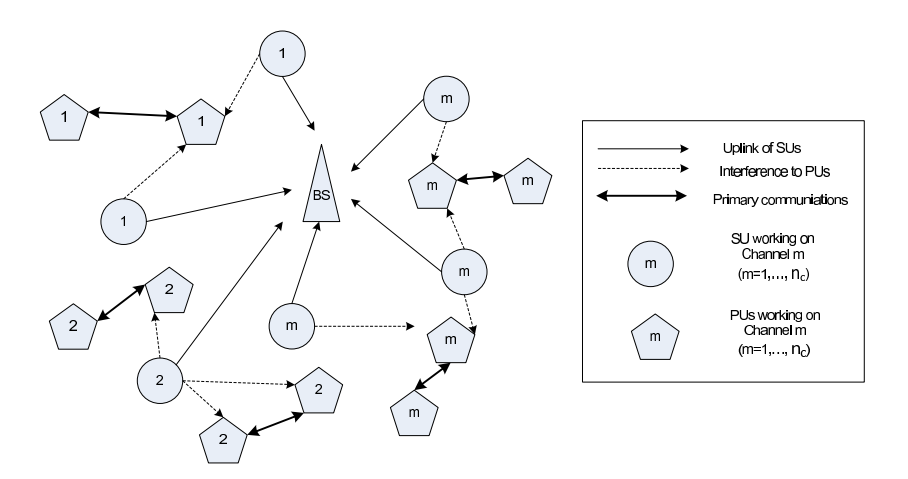


Figure 4.1: System model of multi-channel cognitive radio cellular networks

Table 4.1: Table of notations for multi-channel CogCell

Symbol	Meaning
$\mathcal{N}_s$	the set of SUs
$\mathcal{N}_c$	the set of Channels
$\mathcal{N}_{sm}$	the set of SUs on channel $m$
$\mathcal{N}_{pm}$	the set of PUs on channel $m$
$n_s$	the number of SUs, equal to $ \mathcal{N}_s $
$n_c$	the number of Channels, equal to $ \mathcal{N}_c $
$n_{pm}$	the number of PUs in receiving mode on channel $m$
$n_p$	the total number of PUs in receiving mode on all channels
$P_{mi}$	the transmission power of SU $i$ on channel $m$
$P_{mi}$ $\hat{P}$	the maximum transmission power of every SU
$I_{pm} \ rac{\xi_{mi}}{ar{\xi}_i} \ ar{\lambda}_i$	the interference on channel $m$ measured at BS from primary systems
$\xi_{mi}$	the SINR of SU $i$ on channel $m$ measured at the BS
$ar{\xi_i}$	the minimum uplink SINR requirement of SU $i$
$ar{\lambda}_i$	the data rate required by SU $i$
$ au_{mij}$	the interference from SU $i$ to PU $j$ on channel $m$
$\Gamma_{mj}$	the interference threshold of PU $j$ on channel $m$
$r_i$	the payment from SU $i$ (the revenue got from SU $i$ )
$g_{mi}$	the channel gain from SU $i$ to the BS on channel $m$
$h_{mij}$	the channel gain from SU $i$ to PU $j$ on channel $m$

#### 4.1.2 Interference from SUs to PUs

While SUs and PUs are coexistent in the underlay mode, SUs cause interference to the PUs which are receiving data from their primary transmitters. On channel m ( $m \in \mathcal{N}_c$ ), the interference power  $\tau_{mij}$  received by PU j ( $j \in \mathcal{N}_{pm}$ ) caused by SU i ( $i \in \mathcal{N}_s$ ) is given by

$$\tau_{mij} = h_{mij} P_{mi} \tag{4.1}$$

where  $P_{mi}$  is the transmission power of SU i on channel m.  $h_{mij}$  is the channel gain from SU i to PU j on channel m.

According to the coexisting rule in the underlay mode, the total interference power received by any PU j on channel m should be no more than the predefined threshold  $\Gamma_{mj}$ . That is

$$\sum_{i \in \mathcal{N}_s} h_{mij} P_{mi} \le \Gamma_{mj}, \quad \forall j \in \mathcal{N}_{pm}. \tag{4.2}$$

### 4.1.3 Uplink capacity of SUs

Let  $\xi_{mi}$  denote the Signal-Interference-plus-Noise-Ratio (SINR) at the BS for the transmitter SU i ( $i \in \mathcal{N}_{sm}$ ) on channel m. According to the definition of SINR, we can obtain

$$\xi_{mi} = \beta_{mi} P_{mi} \tag{4.3}$$

where

$$\beta_{mi} = \frac{g_{mi}}{N_0 + I_{pm} + I_{-i}^m}$$

$$= \frac{g_{mi}}{N_0 + I_{pm} + \sum_{k \in \mathcal{N}_{sm}, k \neq i}^{m}} g_{mk} P_{km}$$

$$= \frac{g_{mi}}{N_0 + I_{pm} + I_s^m - g_{mi} P_{mi}}$$
(4.4)

where  $g_{mi}$  is the channel gain from SU i to the BS on channel m.  $N_0$  denotes the average power of background noise received by the BS at every channel.  $I_{pm}$  represents the interference on channel m at the BS caused by PUs.  $I_{-i}^m$  denotes the interference power received by the BS from all the SUs on channel m except SU i. In practice, as explained in [103],  $I_{pm}$  and  $I_{-i}^m$  can be measured at the BS.

Suppose that the bandwidth of the channel m is  $B_m$ , according to Shannon's capacity theory, we can obtain the capacity for SU i on channel m as follows.

$$\lambda_{mi} = B_m log_2(1 + \xi_{mi}), \quad \forall m \in \mathcal{N}_c \tag{4.5}$$

If SU i is allowed to access from channel m, the data rate is satisfied as follows,

$$\lambda_{mi} \geq \bar{\lambda}_i$$

It is then equivalent to the following SINR requirements according to (4.5).

$$\xi_{mi} \geq \bar{\xi}_i$$

## 4.1.4 The operator problem

We call the sum of revenue got from all admitted SUs Secondary Revenue. The operator problem is how to admit a subset of SUs and allocate a channel for each SU and control its transmission power such that the secondary revenue can be maximized. In the mean time, the solution should obey the constraints of maximum transmission power, minimum SINR for SUs, and maximum interference to every PU. In the following, we denote this problem as Maximization of Revenue from SUs (MRS) problem for short. It can be formulated as follows.

MRS:

maximize 
$$\sum_{i \in \mathcal{N}_s} \sum_{m \in \mathcal{N}_c} r_i x_{mi} \tag{4.6}$$

subject to:

$$\sum_{i \in \mathcal{N}_s} h_{mij} P_{mi} \leq \Gamma_{mj}, \quad \forall j \in \mathcal{N}_{pm}, m \in \mathcal{N}_c$$

$$x_{mi} \in \{0, 1\}, \quad \forall i \in \mathcal{N}_s, m \in \mathcal{N}_c$$

$$\sum_{m \in \mathcal{N}_c} x_{mi} \leq 1, \quad \forall i \in \mathcal{N}_s$$

$$\xi_{mi} \geq \bar{\xi}_i, \quad \text{if } x_{mi} = 0, \forall i \in \mathcal{N}_s, m \in \mathcal{N}_c$$

$$P_{mi} \in [0, \hat{P}], \quad \forall i \in \mathcal{N}_s, m \in \mathcal{N}_c$$

$$(4.10)$$

$$x_{mi} \in \{0, 1\}, \quad \forall i \in \mathcal{N}_s, m \in \mathcal{N}_c$$
 (4.8)

$$\sum_{m \in \mathcal{N}} x_{mi} \le 1, \quad \forall i \in \mathcal{N}_s$$
 (4.9)

$$\xi_{mi} \ge \bar{\xi}_i, \quad \text{if } x_{mi} = 0, \forall i \in \mathcal{N}_s, m \in \mathcal{N}_c$$
 (4.10)

$$P_{mi} \in [0, \hat{P}], \quad \forall i \in \mathcal{N}_s, m \in \mathcal{N}_c$$
 (4.11)

$$P_{mi} = 0, \quad \text{if } x_{mi} = 0, \forall i \in \mathcal{N}_s, m \in \mathcal{N}_c$$
 (4.12)

where  $x_{mi}$  is a binary variable,  $x_{mi} = 1$  if SU i works on channel m, zero otherwise. Constraint (4.7) means that the interference from SUs to PUs can not exceed the predefined threshold. Constraint (4.8) and (4.9) indicate that every SU can only occupy one channel at most. Constraint (4.10) represents the minimum SINR requirement of all SUs working on channel m. Constraint (4.11) shows the power constraint of SUs, wherein  $\hat{P}$  is the maximum transmission power that can be used at SUs.

The solution is to find the value of the binary variables  $x_{mi}$  and every SU's transmission power  $P_{mi}$ , which may not be an integer. Moreover, the objective function (4.6) is linear to the binary variables. Therefore, this optimization problem is a Mixed Integer Non-linear Programming (MINLP) problem, which is NP-hard in general.

#### MMKP modeling 4.2

For constraint (4.10) in MRS problem, we can use the result from Chapter 3. According to (3.37) about the power calculation in one-channel CogCell, we can have the similar calculation for an SU in any channel m.

$$P_{mi} = \frac{N_0 + I_{pm} + I_{sm}}{g_{mi}a_i}$$

$$= \left(N_0 + I_{pm} + \frac{N_0 + I_{pm}}{\left(\sum\limits_{k \in \mathcal{N}_{sm}} a_k^{-1}\right)^{-1}}\right) / (g_{mi}a_i)$$

$$= \frac{N_0 + I_{pm}}{g_{mi}a_i \left(1 - \sum\limits_{k \in \mathcal{N}_{sm}} a_k^{-1}\right)}$$
(4.13)

#### Resource Optimization for Multi-channel Cognitive Radio Cellular Networks

where  $a_i$  denotes  $1 + \bar{\xi_i}^{-1}$ . Substitute (4.13) into the constraint in (4.7), we have

$$\sum_{i \in \mathcal{N}_{sm}} h_{mij} \frac{N_0 + I_{pm}}{g_{mi} a_i \left(1 - \sum_{k \in \mathcal{N}_{sm}} a_k^{-1}\right)} \le \Gamma_{mj}, \quad \forall j \in \mathcal{N}_{pm}, m \in \mathcal{N}_c$$

Therefore,

$$\sum_{i \in \mathcal{N}_{sm}} h_{mij} g_{mi}^{-1} a_i^{-1} (N_0 + I_{pm}) \le \Gamma_{mj} \left( 1 - \sum_{k \in \mathcal{N}_{sm}} a_k^{-1} \right), \quad \forall j \in \mathcal{N}_{pm}, m \in \mathcal{N}_c$$

Then.

$$\sum_{i \in \mathcal{N}_{sm}} \left( h_{mij} g_{mi}^{-1} \Gamma_{mj}^{-1} (N_0 + I_{pm}) + 1 \right) a_i^{-1} \le 1, \quad \forall j \in \mathcal{N}_{pm}, m \in \mathcal{N}_c$$

It is equivalent to the following constraint

$$\sum_{i \in \mathcal{N}_c} \left( h_{mij} g_{mi}^{-1} \Gamma_{mj}^{-1} (N_0 + I_{pm}) + 1 \right) a_i^{-1} x_{mi} \le 1, \quad \forall j \in \mathcal{N}_{pm}, m \in \mathcal{N}_c \quad (4.14)$$

On the other hand, to obey constraint (4.11), we have

$$0 \le \frac{N_0 + I_{pm}}{g_{mi}a_i \left(1 - \sum_{k \in \mathcal{N}_{sm}} a_k^{-1}\right)} \le \hat{P}, \quad \forall i \in \mathcal{N}_{sm}, m \in \mathcal{N}_c$$

It can be rewritten as

$$\sum_{k \in \mathcal{N}_{sm}} a_k^{-1} + \frac{N_0 + I_{pm}}{g_{mi} a_i \hat{P}} \le 1, \quad \forall i \in \mathcal{N}_{sm}, m \in \mathcal{N}_c$$

which is equivalent to the following constraint

$$\sum_{k \in \mathcal{N}_c} a_k^{-1} x_{km} + (N_0 + I_{pm}) \hat{P}^{-1} g_{mi}^{-1} a_i^{-1} x_{mi} \le 1, \quad \forall i \in \mathcal{N}_s, m \in \mathcal{N}_c \quad (4.15)$$

Combining (4.14) and (4.15), we have the following constraint.

$$\sum_{i \in \mathcal{N}_c} w_{mij} x_{mi} \le 1, \quad \forall j = 1, 2, \cdots, n_s + n_{pm}, m \in \mathcal{N}_c$$
 (4.16)

where, for each i in  $\mathcal{N}_s$ , and m in  $\mathcal{N}_c$ , we have

$$w_{mij} = \begin{cases} (h_{mij}g_{mi}^{-1}\Gamma_{mj}^{-1}(N_0 + I_{pm}) + 1) a_i^{-1} & j = 1, 2, \dots, n_{pm} \\ a_i^{-1} & j = n_{pm} + 1, n_{pm} + 2, \dots, \\ & n_{pm} + n_s; j \neq n_{pm} + i \\ (1 + (N_0 + I_{pm})\hat{P}^{-1}g_{mi}^{-1}) a_i^{-1} & j = n_{pm} + i \end{cases}$$

$$(4.17)$$

Therefore, the reformulated problem is as follows. *MMKP Formulation:* 

maximize 
$$\sum_{i \in \mathcal{N}_s} \sum_{m \in \mathcal{N}_c} r_i x_{mi}$$
subject to 
$$\sum_{i \in \mathcal{N}_s} w_{mij} x_{mi} \leq 1, \quad j = 1, 2, \dots, n_s + n_{pm}, m \in \mathcal{N}_c$$
$$\sum_{m \in \mathcal{N}_c} x_{mi} \leq 1, \quad \forall i \in \mathcal{N}_s$$
$$x_{mi} \in \{0, 1\}, \quad \forall i \in \mathcal{N}_s, m \in \mathcal{N}_c$$
$$(4.18)$$

The above formulation is a 0-1 integer linear programming, and can be analogous to a multidimensional multiple knapsack problem (MMKP), where there are  $n_c$  knapsacks, while any knapsack m ( $m = 1, \dots, n_c$ ) has  $(n_s + n_{pm})$  constraints as the dimensions.

## 4.3 MKP modeling by matrix transformation

In order to solve the MMKP in (4.18) by MOSEK, we need to describe it in a general matrix form as follows.

maximize 
$$\mathbf{RX}$$
  
subject to  $\mathbf{AX} \leq \mathbf{U}$   
 $\mathbf{X} \in \zeta$  (4.19)

where, 
$$\zeta = \{0, 1\}$$
, and  $\mathbf{U} = (\underbrace{1, 1, \cdots, 1})^T$ .  $\mathbf{R} = (\underbrace{\mathbf{R}_{1 \times n_s}, \mathbf{R}_{1 \times n_s}, \cdots, \mathbf{R}_{1 \times n_s}}_{n_c})$   
(wherein  $\mathbf{R}_{1 \times n_s} = (\underbrace{r_1, r_2, \cdots, r_{n_s}}_{n_s})$ ), and  $\mathbf{X} = (\underbrace{\mathbf{X}_1, \mathbf{X}_2, \cdots, \mathbf{X}_{n_c}}_{n_c})^T$  (wherein  $\mathbf{X}_m = (\underbrace{x_{m,1}, x_{m,2}, \cdots, x_{m,n_s}}_{n_s})$ ,  $\forall m \in \mathcal{N}_c$ ).

According to the constraints in (4.18) that every SU can only use maximum one channel, we have the following matrix form constraint.

#### Resource Optimization for Multi-channel Cognitive Radio Cellular Networks

$$\begin{pmatrix}
\mathbf{1}_{1\times n_c} & 0 & \cdots & 0 \\
0 & \mathbf{1}_{1\times n_c} & \cdots & 0 \\
\vdots & \vdots & \ddots & \vdots \\
0 & 0 & \cdots & \mathbf{1}_{1\times n_c}
\end{pmatrix} \cdot \begin{pmatrix}
\mathbf{X}_1' \\
\mathbf{X}_2' \\
\vdots \\
\mathbf{X}_{n_s}'
\end{pmatrix} \le \mathbf{U}$$
(4.20)

where,  $\mathbf{X}'_i = (\underbrace{x_{1,i}, x_{2,i}, \cdots, x_{n_c,i}})^T, \forall i \in \mathcal{N}_s.$ 

The inequality of (4.20) is further equivalent to the following

$$(\underbrace{\mathbf{A}_0, \mathbf{A}_0, \cdots, \mathbf{A}_0}_{n_c})\mathbf{X} \le \mathbf{U} \tag{4.21}$$

where,

$$\mathbf{A}_0 = \begin{pmatrix} 1 & 0 & \cdots & 0 \\ 0 & 1 & \cdots & 0 \\ \vdots & \vdots & \ddots & \vdots \\ 0 & 0 & \cdots & 1 \end{pmatrix}_{n_s \times n_s}$$

Then, we define the following matrix  $\mathbf{A}$ ,

$$\mathbf{A} = \begin{pmatrix} \mathbf{A}_1 & 0 & \cdots & 0 \\ 0 & \mathbf{A}_2 & \cdots & 0 \\ \vdots & \vdots & \ddots & \vdots \\ 0 & 0 & \cdots & \mathbf{A}_{n_c} \\ \mathbf{A}_0 & \mathbf{A}_0 & \cdots & \mathbf{A}_0 \end{pmatrix}_{(n_s(n_c+1)+n_p) \times n_c n_s}$$

where, for each  $m \in \mathcal{N}_c$   $(m \neq 0)$ ,

where, for each 
$$m \in \mathcal{N}_c$$
  $(m \neq 0)$ ,
$$\mathbf{A}_m = \begin{pmatrix}
\frac{(N_0 + I_{pm})h_{m,1,1}}{h_{m,1}\Gamma_{m,1}} + 1 & \frac{(N_0 + I_{pm})h_{m,2,1}}{h_{m,2}\Gamma_{m,1}} + 1 & \cdots & \frac{(N_0 + I_{pm})h_{m,n_s,1}}{h_{m,n_s}\Gamma_{m,1}} + 1 \\
\frac{1}{a_1} & a_2 & \cdots & \frac{(N_0 + I_{pm})h_{m,n_s,1}}{h_{m,n_s}\Gamma_{m,2}} + 1 \\
\frac{1}{a_1} & a_2 & \cdots & \frac{(N_0 + I_{pm})h_{m,n_s,2}}{h_{m,n_s}\Gamma_{m,2}} + 1 \\
\frac{1}{a_1} & a_2 & \cdots & \frac{(N_0 + I_{pm})h_{m,n_s,n_s,2}}{h_{m,n_s}\Gamma_{m,n_pm}} + 1 \\
\frac{N_0 + I_{pm}}{h_{m,1}\Gamma_{m,pm}} + 1 & \frac{(N_0 + I_{pm})h_{m,2,n_{pm}}}{h_{m,2}\Gamma_{m,n_{pm}}} + 1 \\
\frac{1}{a_1} & a_2 & \cdots & \frac{1}{a_{n_s}} \\
\frac{1}{a_1} & \frac{1}{a_2} & \cdots & \frac{1}{a_{n_s}} \\
\vdots & \vdots & \ddots & \vdots \\
\frac{1}{a_1} & \frac{1}{a_2} & \cdots & \frac{N_0 + I_{pm}}{h_{m,n_s}} + 1 \\
\frac{1}{a_2} & \cdots & \frac{N_0 + I_{pm}}{h_{m,n_s}} + 1 \\
\frac{1}{a_1} & \frac{1}{a_2} & \cdots & \frac{N_0 + I_{pm}}{h_{m,n_s}} + 1 \\
\frac{1}{a_{n_s}} & \cdots & \frac{N_0 + I_{pm}}{h_{m,n_s}} + 1 \\
\frac{1}{a_{n_s}} & \cdots & \frac{N_0 + I_{pm}}{h_{m,n_s}} + 1 \\
\frac{1}{a_1} & \frac{1}{a_2} & \cdots & \frac{N_0 + I_{pm}}{h_{m,n_s}} + 1 \\
\frac{1}{h_{m,n_s}} & \cdots & \frac{N_0 + I_{pm}}{h_{m,n_s}} + 1 \\
\frac{1}{h_{m,n_s}\Gamma_{m,n_s}} & \cdots & \frac{N_0 + I_{pm}}{h_{m,n_s}} + 1 \\
\frac{1}{h_{m,n_s}\Gamma_{m,2}} & \cdots & \frac{N_0 + I_{pm}}{h_{m,n_s}} + 1 \\
\frac{1}{h_{m,n_s}\Gamma_{m,2}} & \cdots & \frac{N_0 + I_{pm}}{h_{m,n_s}} + 1 \\
\frac{1}{h_{m,n_s}\Gamma_{m,2}} & \cdots & \frac{N_0 + I_{pm}}{h_{m,n_s}} + 1 \\
\frac{1}{h_{m,n_s}\Gamma_{m,2}} & \cdots & \frac{N_0 + I_{pm}}{h_{m,n_s}} + 1 \\
\frac{1}{h_{m,n_s}\Gamma_{m,2}} & \cdots & \frac{N_0 + I_{pm}}{h_{m,n_s}} & \cdots & \frac{N_0 + I_{pm}}{h_{m,n_s}} + 1 \\
\frac{1}{h_{m,n_s}\Gamma_{m,2}} & \cdots & \frac{N_0 + I_{pm}}{h_{m,n_s}} & \cdots & \frac{N_0 + I_{pm}}{h_{$$

We employ i' ( $i'=1,2,\cdots,n_cn_s$ ) to denote the index of any member in **X**. i' is a combination of m and i as follows.

$$i' = (m-1)n_s + i, \quad m = 1, 2, \dots, n_c; i = 1, 2, \dots, n_s.$$
 (4.22)

Reversely, given i' we get

$$\begin{cases}
 m = \lceil i'/n_s \rceil \\
 i = \begin{cases}
 n_s & i' \mod n_s = 0 \\
 i' \mod n_s & \text{Otherwise}
\end{cases}$$
(4.23)

Then, the MMKP in (4.18) can be represented as the following MKP . MKP Formulation:

maximize 
$$\sum_{\substack{i'=1\\n_c n_s}}^{n_c n_s} \hat{r}_{i'} y_{i'}$$
subject to 
$$\sum_{\substack{i'=1\\i'=1}}^{n_c n_s} \omega_{j'i'} y_{i'} \le 1, \quad j' = 1, 2, \cdots, (n_c + 1) n_s + n_p$$
$$y_{i'} \in \{0, 1\}, \qquad \forall i' = 1, 2, \cdots, n_c n_s$$
 (4.24)

where,  $\hat{r}_{i'} = r_i$  (*i* is calculated from i' by (4.23)).  $\omega_{j'i'}$  has different expressions with different j'.

• when 
$$j' \leq n_c n_s + n_p$$
, let  $j'_m = (m-1)n_s + \sum_{k=1}^{m-1} n_{pk}$ , for any  $m = 1, 2, \dots, n_c$ ,

- if 
$$j' = j'_m + 1, j'_m + 2, \dots, j'_m + n_{pm}$$
, we have

$$\omega_{j'i'} = \begin{cases} \frac{\frac{(N_0 + I_{pm})h_{mij}}{g_{mi}\Gamma_{mj}} + 1}{a_i}, & i' = (m-1)n_s + i; j = 1, 2, \dots, n_{pm} \\ 0, & \text{Otherwise} \end{cases}$$
(4.25)

- if  $j' = j'_m + n_{pm} + 1, j'_m + n_{pm} + 2, \dots, j'_m + n_{pm} + n_s$ , and  $j' \neq j'_m + n_{pm} + i$ , where  $i = 1, 2, \dots, n_s$ , we have

$$\omega_{j'i'} = \begin{cases} \frac{1}{a_i}, & i' = (m-1)n_s + i\\ 0, & \text{Otherwise} \end{cases}$$
 (4.26)

- if  $j' = j'_m + n_{pm} + i$ , where  $i = 1, 2, \dots, n_s$ , we have

$$\omega_{j'i'} = \begin{cases} \frac{\frac{N_0 + I_{pm}}{\hat{P}g_{mi}} + 1}{a_i}, & i' = (m-1)n_s + i\\ 0, & \text{Otherwise} \end{cases}$$
(4.27)

• when  $j' > n_c n_s + n_p$ , for any  $m = 1, 2, \dots, n_c$ , we have

$$\omega_{j'i'} = \begin{cases} 1, & i' = (m-1)n_s + j' - n_c n_s - n_p \\ 0, & \text{Otherwise} \end{cases}$$
 (4.28)

In this MKP, there is only one knapsack. But it has  $n_c n_s$  items and  $(n_c + 1)n_s + n_p$  dimensions.

## 4.4 Proposed heuristic algorithm to MKP

In this section, we will introduce two lemmas and definitions, then we will describe our proposed heuristic algorithm to MKP.

**Lemma 1.** Given a set of constraints  $\mathcal{CS}$ , we say the i'-th decision variable  $y_{i'}$  is equal to 0, if there exist a  $j' \in \mathcal{CS}$  that  $\omega_{j'i'} > 1$ .

*Proof.* We use proof by contradiction. Suppose y' is equal to 1, and all the constraints are satisfied. Assume there is a j' where  $\omega_{j'i'} > 1$ , thus  $\sum_{i' \in \mathcal{D}} \omega_{j'i'} > \omega_{j'i'} > 1$ . Which means the constraint will never be satisfied.

The contradiction happens, and the hypothesis is wrong. Thus y' should be equal to 0.

**Lemma 2.** Given a selected set of decision variables as  $\mathcal{D}$ , the j'-th constraint can be removed if the constraint is satisfied when  $y_{i'}$  is equal to 1 for all i' in  $\mathcal{D}$ .

*Proof.* Assume j'-th constraint  $(j' = 1, ..., (n_c + 1)n_s + n_p)$  is satisfied when  $y_{i'}$  is equal to 1 for all i' in  $\mathcal{D}$ . It means  $\sum_{i' \in \mathcal{D}} \omega_{j'i'} \leq 1$ 

Because  $\omega_{j'i'}$  is non-negative and  $y_{i'}$  is equal to either 0 or 1, we have,  $\sum_{i'\in\mathcal{D}}\omega_{j'i'}y_{i'}\leq\sum_{i'\in\mathcal{D}}\omega_{j'i'}$ . Thus  $\sum_{i'\in\mathcal{D}}\omega_{j'i'}y_{i'}\leq 1$ . It means that the j'-th constraint is always satisfied whatever the final solution is for all decision variables.

From Lemma 2, we have the following definition for valid constraints.

Valid Constraints Given a selected set of decision variables as  $\mathcal{D}$ , we say the j'-th constraint is *valid*, if for all i' in  $\mathcal{D}$  the constraints do not meet. The set of all valid constraints is noted as  $\mathcal{CS}$ . In another word,

$$CS := \left\{ j' \middle| \sum_{i' \in \mathcal{D}} \omega_{j'i'} > 1 \right\}$$

$$(4.29)$$

Relevance of a valid constraint We say  $\alpha_{j'}$  is the reference for a valid constraint j'  $(j' \in \mathcal{CS})$ .

$$\alpha_{j'} := \sum_{i' \in \mathcal{D}} \omega_{j'i'} - 1 \tag{4.30}$$

Since j is a valid constraint, according to Definition 4.4, we have  $\alpha_{j'} > 0$ . The higher the relevance of a valid constraint, the higher the "scarcity" of the corresponding resource and the less attractive it becomes to pack an item which consumes a lot of that resource [99].

Efficiency for an item i' We say  $e_{i'}$  is the efficiency for the i'-th decision variable  $y_{i'}$ .

$$e_{i'} := \frac{\hat{r}_{i'}}{\sum\limits_{j' \in \mathcal{CS}} \alpha_{j'} \omega_{j'i'}} = \frac{\hat{r}_{i'}}{\sum\limits_{j' \in \mathcal{CS}} \left(\sum\limits_{i' \in \mathcal{D}} \omega_{j'i'} - 1\right) \omega_{j'i'}}$$
(4.31)

The core of our proposed heuristic algorithm is minimal efficiency removal. The major steps are as follows.

- In the beginning, we set  $\mathcal{CS}$  to  $\{1, 2, \dots, (n_c + 1)n_s + n_p\}$ , and  $\mathcal{D}$  to  $\{1, 2, \dots, n_c n_s\}$ . Every decision variable  $y_{i'}$   $(\forall i' \in \mathcal{D})$  is equal to 1.
- Then, we go through all  $i' \in \mathcal{D}$  by Lemma 1 to set  $y_{i'}$  to 0, if there exist  $j' \in \mathcal{CS}$  that  $\omega_{j'i'} > 1$ . i' is then removed from  $\mathcal{D}$  where  $y_{i'} = 0$ .
- We then select a variable with index of  $i^*$  where  $e_{i^*} = \arg\min_{i' \in \mathcal{D}} e_{i'}$ , remove  $i^*$  from  $\mathcal{D}$ , set  $y_{i^*}$  to 0, and update the valid constraints set  $\mathcal{CS}$ .
- We repeat this selection and removal procedure until either  $\mathcal{D}$  or  $\mathcal{CS}$  is empty. If  $\mathcal{D}$  is empty, it means no SU can be admitted. The reason is either the interference constraint or QoS constraint is too strict to all SUs for all channels.

The flow chart of the algorithm is shown in Fig. 4.2. We show more details in Algorithm 4 and 5.

The time complexity is dominated by the procedure of Minimal Efficien-cyRemoval. It will call the function of  $Update Constraints And Efficiencies(CS, <math>\mathcal{D}$ ) maximum  $n_c n_s$  times in the worst case. In the function  $Update Constraints And Efficiencies(CS, <math>\mathcal{D}$ ), updating efficiency dominates the procedure. It takes maximum  $(n_c+1)n_s+n_p$  to calculate in the worst case if no constraint

#### Algorithm 4 Proposed MKP Heuristic Algorithm for MMKP: Part 1

```
Input: \mathcal{N}_c, \mathcal{N}_s, \{\mathcal{N}_{pm} | \forall m \in \mathcal{N}_c\}.
Output: \{x_{mi}\}, \{P_{mi}\}
  1: procedureInitialization
  2: for m=1 \rightarrow n_c do
            for i=1 \rightarrow n_s do
 3:
                 P_{mi} \leftarrow 0; x_{mi} \leftarrow 0
  4:
                 i' \leftarrow (m-1)n_s + i; y_{i'} \leftarrow 1
  5:
                 for j = 1 \to (n_c + 1)n_s + n_p \ do
  6:
  7:
                       \omega_{i'i'} \leftarrow 0
                 end for
  8:
            end for
 9:
10: end for
11: end procedure
12: procedureCountWeight
13: for m=1 \rightarrow n_c do
           j_m' \leftarrow (m-1)n_s + \sum_{k=1}^{m-1} n_{pk}
14:
            for i = 1 \rightarrow n_s do
15:
                 i' \leftarrow (m-1)n_s + i
16:
                 for j = 1 \rightarrow n_{pm} do
17:
                      j' \leftarrow j'_m + j
\omega_{j'i'} \leftarrow \left(\frac{(N_0 + I_{pm})h_{mij}}{g_{mi}\Gamma_{mj}} + 1\right)/a_i
18:
                                                                                         \triangleright According to (4.25)
19:
                 end for
20:
                 for k=1 \rightarrow n_s do
21:
                      j' \leftarrow j' + 1
22:
                      if k == i then
\omega_{j'i'} \leftarrow \left(\frac{N_0 + I_{pm}}{\hat{P}g_{mi}} + 1\right) / a_i
23:
                                                                                         \triangleright According to (4.27)
24:
25:
                       else
                       \omega_{j'i'} \leftarrow 1/a_i end if
26:
                                                                                         \triangleright According to (4.26)
27:
                 end for
28:
            end for
29:
30: end for
31: for i=1 \rightarrow n_s do
            for m=1 \rightarrow n_c do
32:
                 i^{'} \leftarrow (m-1)n_s + i; \ j^{'} \leftarrow n_c n_s + n_p + i
33:
                 \omega_{i'i'} \leftarrow 1
                                                                                         \triangleright According to (4.28)
34:
            end for
35:
36: end for
37: end procedure
```

#### Algorithm 5 Proposed MKP Heuristic Algorithm for MMKP: Part 2

```
38: CS \leftarrow \{1, 2, \cdots, (n_c + 1)n_s + n_p\}
39: \mathcal{D} \leftarrow \{1, 2, \cdots, n_c n_s\}
40: procedure PreadmissionControl
         for all i' \in \mathcal{D} do
41:
             for all j' \in \mathcal{CS} do
42:
                 if \omega_{i'i'} > 1 then
43:
                     y_{i'} \leftarrow 0
44:
                     Break
45:
                 end if
46:
             end for
47:
        end for
48:
49: end procedure
    function UpdateConstraintsAndEfficiencies(\mathcal{CS}, \mathcal{D})
         for all j' \in \mathcal{CS} do
51:
             Update CS according to (4.29).
52:
        end for
53:
        for all i' \in \mathcal{D} do
54:
             Update e_{i'} according to (4.31).
55:
         end for
56:
57: end function
58: procedure MinimalEfficiencyRemoval
         UPDATECONSTRAINTSANDEFFICIENCIES (CS, D)
59:
         while \mathcal{CS} \neq \emptyset and \mathcal{D} \neq \emptyset do
60:
             i^* \leftarrow \arg\min e_{i'}
             x_{i^*} \leftarrow 0
62:
             \mathcal{D} \leftarrow \mathcal{D} - i^*
63:
             UPDATECONSTRAINTS AND EFFICIENCIES (CS, D)
64:
         end while
65:
66: end procedure
67: procedure GetResult
        if D \neq \emptyset then
68:
             for all i' \in \mathcal{D} do
69:
70:
                 Calculate m and i according to (4.23).
                 x_{mi} \leftarrow 1
71:
             end for
72:
             for m=1 \rightarrow n_c do
73:
                 for i = 1 \rightarrow n_s do
74:
                     Calculate P_{mi} according to (4.13)
75:
                 end for
76:
             end for
77:
        end if
78:
                                              73
79: end procedure
```

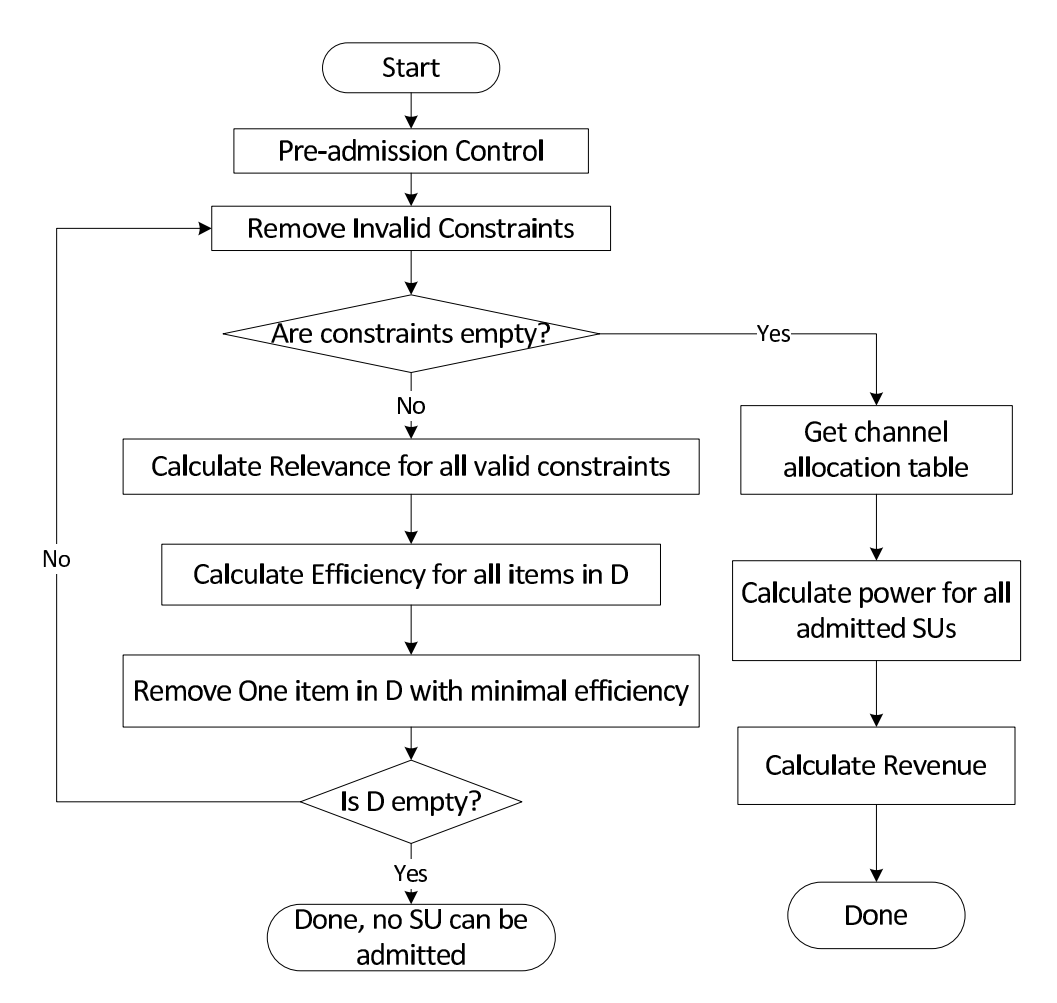


Figure 4.2: Heuristic Algorithm to MKP

removed. We use  $t_i$  (i = 1, 2, ...) to denote the number of constraints removed by the *i*-th calling. The time complexity can be calculated as follows.

$$T(n_{c}, n_{s}, n_{p}) = n_{c}n_{s}((n_{c} + 1)n_{s} + n_{p}) + (n_{c}n_{s} - 1)((n_{c} + 1)n_{s} + n_{p} - t_{1}) + (n_{c}n_{s} - 2)((n_{c} + 1)n_{s} + n_{p} - t_{2}) + \dots$$

$$\leq (n_{c}n_{s} + (n_{c}n_{s} - 1) + (n_{c}n_{s} - 2) + \dots + 1)((n_{c} + 1)n_{s} + n_{p})$$

$$= \frac{n_{c}n_{s}(1 + n_{c}n_{s})}{2}((n_{c} + 1)n_{s} + n_{p})$$

$$= O(n_{c}^{2}n_{s}^{2}(n_{c}n_{s} + n_{p}))$$

$$(4.32)$$

Thus, the time complexity of our proposed scheme is  $O(n_c^2 n_s^2 (n_c n_s + n_p))$ .

### 4.5 Best SINR channel selection scheme

In order to evaluate the performance of our proposed scheme in the previous section, we, hereby, introduce a scheme using traditional channel allocation based on SINR. Wherein, any SU i ( $\forall i \in \mathcal{N}_s$ ) select the channel  $m_i^*$  which can achieve the most SINR with a certain power P.

$$m_{i}^{*} = \arg \max_{\forall m \in \mathcal{N}_{c}} \xi_{mi}$$

$$= \arg \max_{\forall m \in \mathcal{N}_{c}} \frac{h_{mi}P}{N_{0}+I_{pm}}$$

$$= \arg \max_{\forall m \in \mathcal{N}_{c}} \frac{h_{mi}}{N_{0}+I_{pm}}, \quad \forall i \in \mathcal{N}_{s}$$

$$(4.33)$$

After channel allocation, we then use our proposed joint admission and power control scheme JAPC-MKP in Chapter 3. We denote this scheme as BestSINR-JAPC-MKP.

From (3.63), the time complexity using JAPC-MKP on a given channel m is  $O(n_{sm}^2(n_{sm}+n_{pm}))$ , where  $n_{sm}$  and  $n_{pm}$  represent the number of SUs and PUs, respectively. The total time complexity can be calculated as follows.

$$T(n_{c}, n_{s}, n_{p}) = \sum_{m=1}^{n_{c}} n_{sm}^{2} (n_{sm} + n_{pm})$$

$$\leq \sum_{m=1}^{n_{c}} n_{sm}^{2} (n_{sm} + n_{pc}^{max})$$

$$= \sum_{m=1}^{n_{c}} n_{sm}^{3} + \sum_{m=1}^{n_{c}} n_{sm}^{2} n_{pc}^{max})$$

$$\leq (\sum_{m=1}^{n_{c}} n_{sm})^{3} + (\sum_{m=1}^{n_{c}} n_{sm})^{2} n_{pc}^{max}$$

$$= n_{s}^{2} (n_{s} + n_{pc}^{max})$$

$$= O(n_{s}^{2} (n_{s} + n_{pc}^{max}))$$
(4.34)

Thus, the time complexity of our proposed scheme is  $O(n_s^2(n_s + n_{pc}^{max}))$ .

## 4.6 Simulation results and analysis

In this section, we will describe the simulation parameters and present the simulation results. To evaluate the simulation results, we use MOSEK to get the optimal results.

In our CogCell simulator, we generate the topology for 100 times for a given number of channels, SUs and PUs. Each time, the topology is generated randomly as follows. The BS locates at the center of a cell with its radius  $R_{max}$  as 1000m. The minimal distance from the BS to any SUs or PUs,  $R_{min}$ , is set as 100m. The distance between SUs (or PUs) and the BS are randomly

chosen from  $[R_{min}, R_{max}]$ , The angles from any SUs (or PUs) to the BS are randomly chosen from  $[0, 2\pi]$ . The number of channels in this system ranges from 1 to 10, and the bandwidth of each channel is 5MHz. The number of PUs per channel ranges from 1 to  $n_{pc}^{max}$ . The average power of noise is -110dBm. The maximum transmission power of all SUs is 280mW. For the estimation of channel gain in our simulation, we consider a slow fading channel, and the path loss is  $\frac{1}{d^4}$ , where d is the distance between a transmitter and its receiver. For the interference on each channel m, we use  $I_{pm} = n_{pm}I_p$ , where  $I_p$  is the interference contribution from one primary transmitter.

Table 4.2: Simulation parameters for Multi-channel CogCell

Symbol	Value	Symbol	Value
$R_{max}$	1000m	$R_{min}$	100m
В	5 MHz	$n_c$	[1, 10]
$n_{pc}^{max}$	[2, 10]	$n_s$	[1, 100]
$N_0$	-110dBm	$\hat{P}$	280mW

The revenue  $r_i$  obtained from SU i ( $i \in N_s$ ) is dependent on the DTR. The SU with higher DTR pays more and hence generate higher revenue for the service provider. Without loss of generality and for the sake of illustration, we allocate the revenue and DTR according to Table 4.3, which is the same as 3.3 in Chapter 3.

**Table 4.3:** Revenue allocation table for Multi-channel CogCell

Revenue	1	2	4	8	16	32
DTR (kbps)	16	32	64	128	256	512
Required SINR	0.0022	0.0043	0.0087	0.0175	0.0353	0.0718

In the following simulation, we evaluate the performance in terms of the secondary revenues in five different cases, i.e., changing the number of channels, changing the number of SUs, changing the number of PUs per channel, changing the interference threshold ( $\Gamma$ ), and changing the interference to BS from primary systems ( $I_p$ ).

In each case, with the given number of PUs and SUs, the value of  $\Gamma$  and and  $I_p$ , we solve the optimization problem by MOSEK software [37], and run our proposed scheme, and the bestSINR-JAPC-MKP. Then, we calculate the

average secondary revenue based on the results in the 100 random topologies, and 100 random data rate requirements according to Table 4.3.

#### Effect of number of channels

In the following, we evaluate the secondary revenue when changing the number of channels from 1 to 10. The other parameters are fixed as follows,  $n_s = 100$ ,  $n_{pc}^{max} = 10$ ,  $\Gamma = -70dBm$ , and  $I_p = -80dBm$ . The results are shown in Fig. 4.3 and Fig. 4.4.

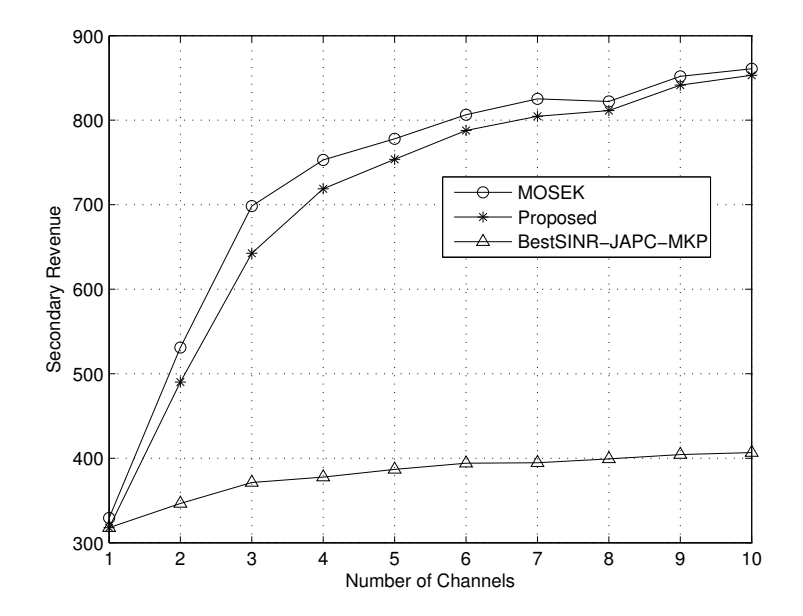


**Figure 4.3:** Revenue in terms of number of channels  $(n_{pc}^{max}=10, \Gamma=-70dBm, I_p=-80dBm, and <math>n_s=100)$ 

Figure 4.3 shows the secondary revenue increases with the increasing number of channels. The reason is the more channels, the more SUs can be admitted. Thus, the revenue to BS increases. When  $n_c$  is equal to 1, the results of three schemes are almost the same. However, when  $n_s$  is greater than 1, the gap between our proposed scheme and BestSINR-JAPC-MKP becomes bigger and bigger. When  $n_s$  is greater than 7, our proposed scheme gets more than twice the revenue got by BestSINR-JAPC-MKP. Moreover, our proposed scheme approaches the results from MOSEK all the time.

Figure 4.4 shows the percentage of optimal solution from MOSEK for both our proposed scheme and BestSINR-JAPC-MKP. BestSINR-JAPC-MKP decreases from 97% when  $n_c$  is equal to 1 to as low as 47% when  $n_c$  is equal

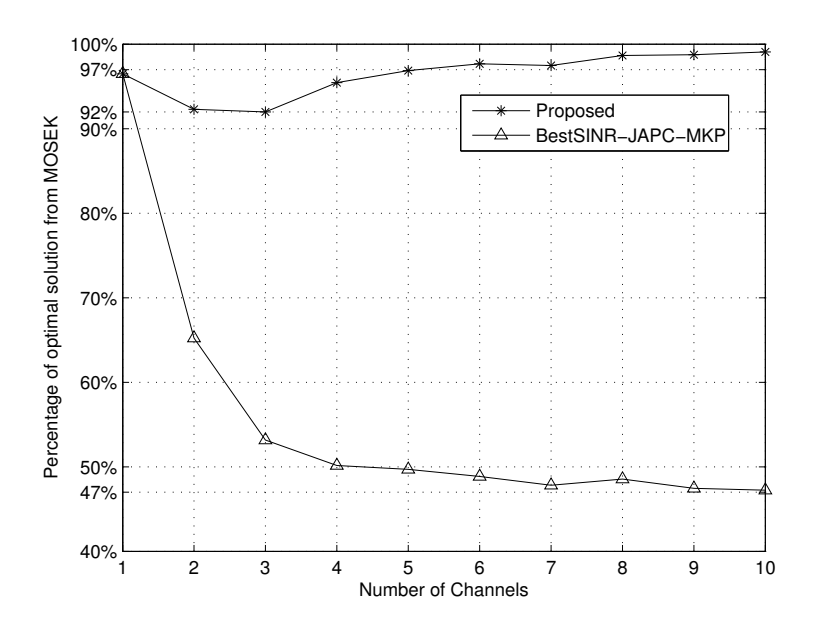


**Figure 4.4:** Percentage of optimal solution from MOSEK in terms of number of channels  $(n_{pc}^{max}=10, \Gamma=-70dBm, I_p=-80dBm, and n_s=100)$ 

to 10. Our proposed scheme decreases from 97% when  $n_c$  is equal to 1 to 92% when  $n_c$  is equal to 3. However, when  $n_c$  is greater than 3, our proposed scheme starts to increase the revenue. When  $n_c$  is great than 7, our proposed scheme achieves more than 97%.

#### Effect of number of SUs

In the following, we evaluate the secondary revenue when changing the number of SUs from 1 to 100. The other parameters are fixed as follows,  $n_c = 10$ ,  $n_{pc}^{max} = 10$ ,  $\Gamma = -70dBm$ , and  $I_p = -80dBm$ . The results are shown in Fig. 4.5 and Fig. 4.6.

Figure 4.5 shows the secondary revenue increases with the increasing number of SUs. The reason is channels in the system are not saturated with lower number of SUs, and can serve more SUs when more SUs are available. Thus, the revenue to BS increases. When  $n_s$  is smaller than 20, the results of three schemes are almost the same, since in that case, almost all the SUs can be admitted. However, when  $n_s$  is greater than 20, the gap between our proposed scheme and BestSINR-JAPC-MKP becomes bigger and bigger. When  $n_s$  is 100, our proposed scheme gets more than twice the revenue got by BestSINR-JAPC-MKP. Moreover, our proposed scheme approaches the results from MOSEK all the time.

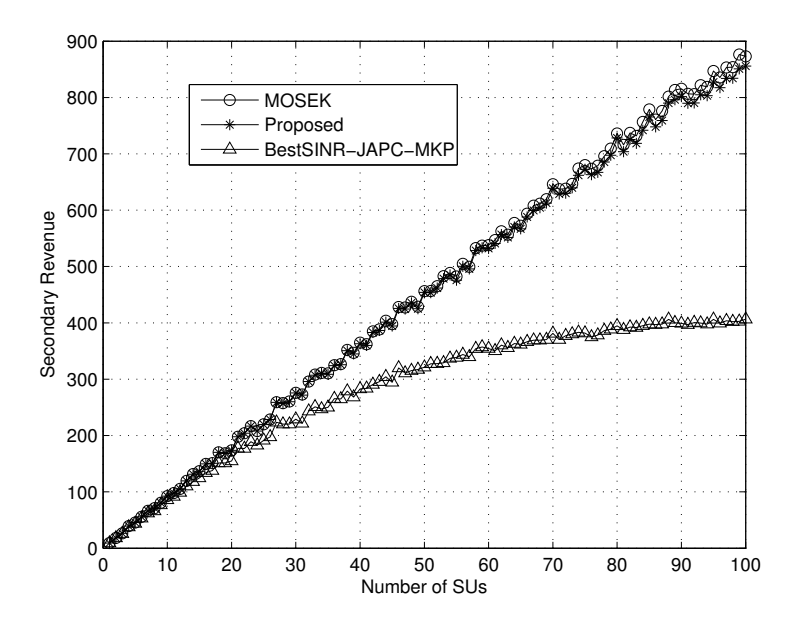
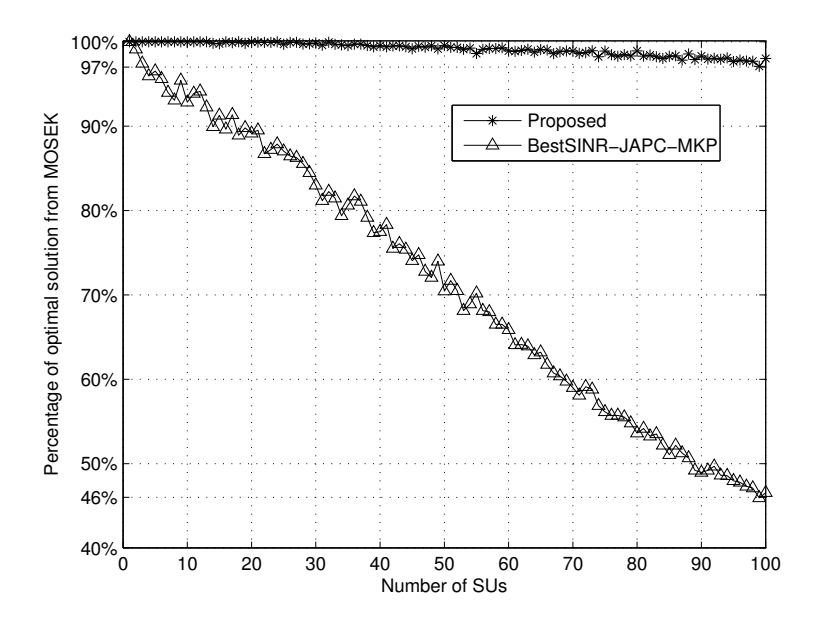


Figure 4.5: Revenue in terms of number of SUs ( $n_{pc}^{max}=10$ ,  $\Gamma=-70dBm$ ,  $I_p=-80dBm$ , and  $n_c=10$ )



**Figure 4.6:** Percentage of optimal solution from MOSEK in terms of number of SUs ( $n_{pc}^{max}=10$ ,  $\Gamma=-70dBm$ ,  $I_p=-80dBm$ , and  $n_c=10$ )

Figure 4.6 shows the percentage of optimal solution from MOSEK decreases for both our proposed scheme and BestSINR-JAPC-MKP with the increasing number of SUs. BestSINR-JAPC-MKP decreases to as low as 46%, while our proposed scheme can still achieve at least 97% of the optimal result from MOSEK.

#### Effect of number of PUs per channel

The number of PUs per channel is randomly generated from 1 to  $n_{pc}^{max}$ . We change  $n_{pc}^{max}$  from 2 to 10, while other parameters are fixed as follows:  $\Gamma = -70dBm$ ,  $I_p = -80dBm$ ,  $n_{SU} = 100$ , and  $n_c = 10$ . The results are shown in Fig. 4.7 and Fig. 4.8.

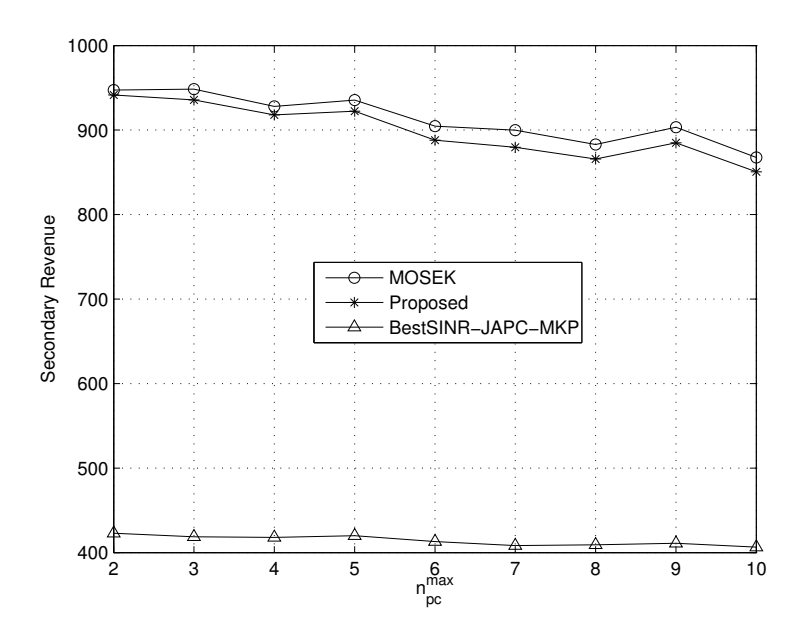


**Figure 4.7:** Revenue in terms of different number of PUs per channel ( $\Gamma = -70dBm$ ,  $I_p = -80dBm$ ,  $n_{SU} = 100$ , and  $n_c = 10$ )

Figure 4.7 shows the secondary revenue decreases with the increasing  $n_{pc}^{max}$ . The reason is the more PUs in a channel, the more interference constraints should be considered. Thus, fewer SUs can be admitted. It then results in less secondary revenue to BS. Our proposed scheme approaches MOSEK in all the cases, and achieves more than twice the revenue got by BestSINR-JAPC-MKP.

Figure 4.8 shows the percentage of optimal solution from MOSEK for both our proposed scheme and BestSINR-JAPC-MKP. BestSINR-JAPC-

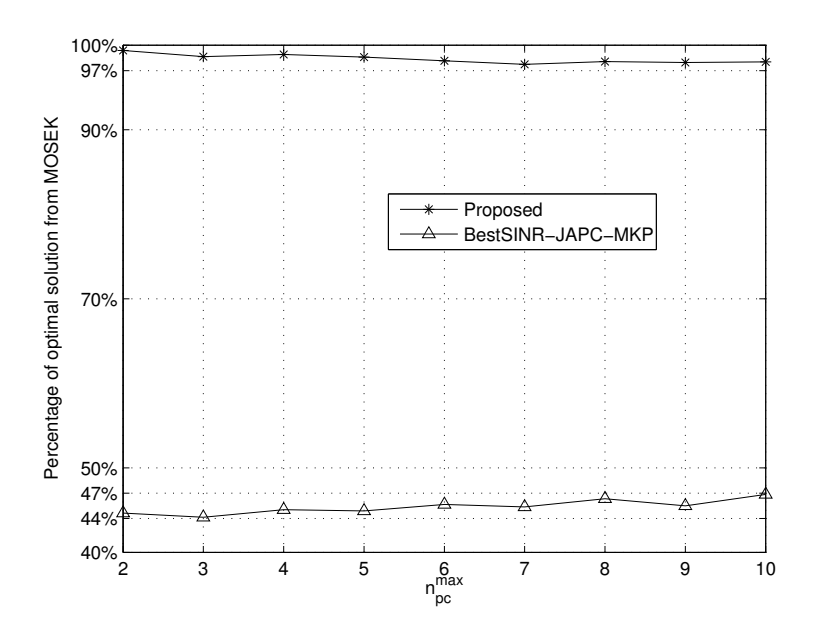


**Figure 4.8:** Percentage of optimal solution from MOSEK in terms of number of maximum PUs per channel ( $n_{pc}^{max}=10$ ,  $\Gamma=-70dBm$ ,  $I_p=-80dBm$ , and  $n_c=10$ )

MKP achieves between 44% and 47%, while our proposed scheme achieves more than 97% of the secondary revenue from MOSEK.

#### Effect of interference from primary system

We change  $I_p$  from -140dBm to -40dBm, while other parameters are fixed as follows:  $n_{pc}^{max} = 10$ ,  $\Gamma = -70dBm$ ,  $n_{SU} = 100$ , and  $n_c = 10$ . The results are shown in Fig. 4.9 and Fig. 4.10.

Figure 4.9 shows the secondary revenue decreases with the increasing interference to BS from each PU transmitter. The reason is the more interference from PU transmitters to BS in a channel, the higher power SUs should use to achieve a certain SINR level. It then results in more interference to PUs. Because the interference to PUs is limited, fewer SUs can be admitted. Thus, the secondary revenue to BS decreases. Our proposed scheme achieves more than twice the revenue got by BestSINR-JAPC-MKP when the interference to BS per PU transmitter is less than  $-80 \, \mathrm{dBm}$ , and approaches MOSEK in all cases.

Figure 4.10 shows the percentage of optimal solution from MOSEK for both our proposed scheme and BestSINR-JAPC-MKP. BestSINR-JAPC-MKP achieves between 40% and 50%, when  $I_p$  is less than -80dBm, and

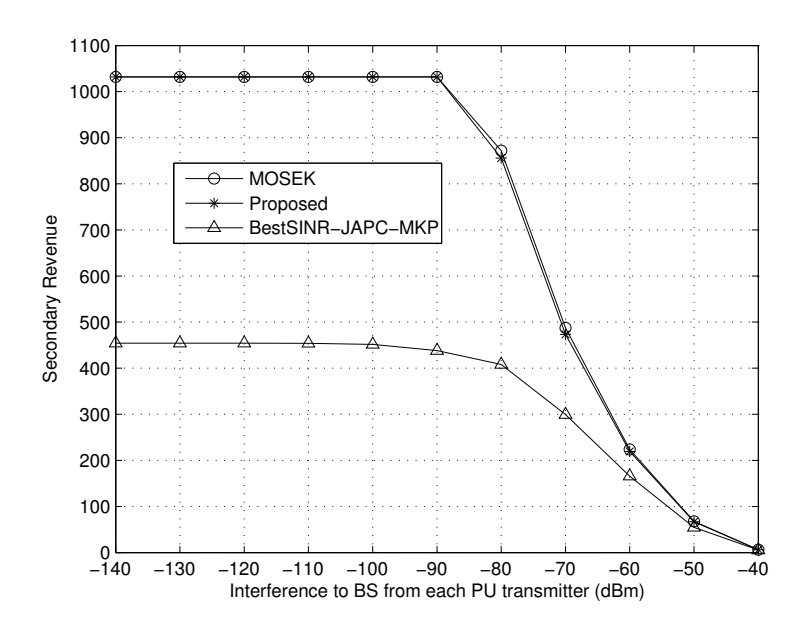


**Figure 4.9:** Revenue in terms of different interference to BS from each PU transmitter ( $n_{pc}^{max}=10$ ,  $\Gamma=-70dBm$ ,  $n_{SU}=100$ , and  $n_c=10$ )

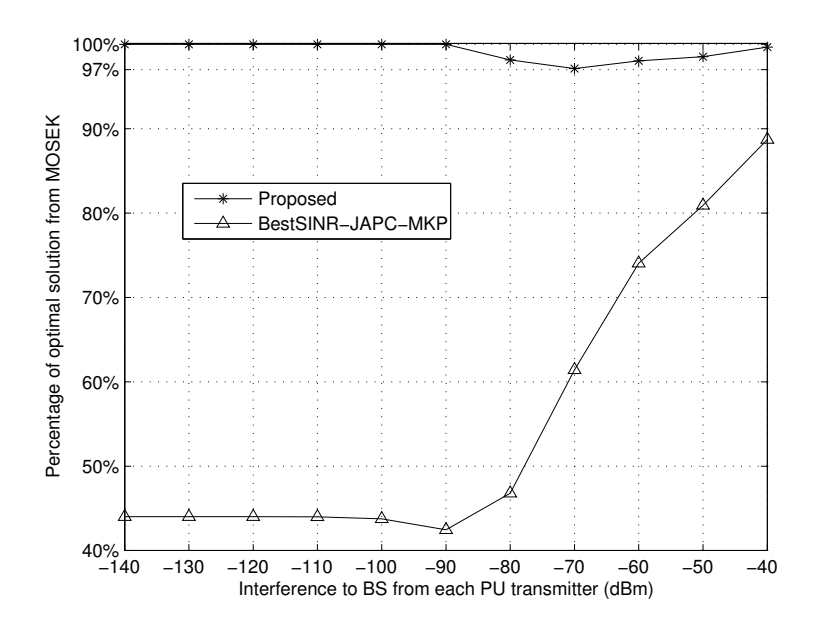


Figure 4.10: Percentage of optimal solution from MOSEK in terms of different interference to BS from each PU transmitter ( $n_{pc}^{max}=10$ ,  $\Gamma=-70dBm$ ,  $n_{SU}=100$ , and  $n_c=10$ )

increase to 90% when  $I_p$  increases to  $-40 \mathrm{dBm}$ . On the other hand, our proposed scheme achieves more than 97% of the secondary revenue from MOSEK, it achieves the same revenue with MOSEK when  $I_p$  is less than  $-90 \mathrm{dBm}$ .

#### Effect of interference threshold on PUs

We change  $\Gamma$  from -140dBm to -40dBm, while other parameters are fixed as follows:  $n_{pc}^{max} = 10$ ,  $I_p = -80dBm$ ,  $n_{SU} = 100$ , and  $n_c = 10$ . The results are shown in Fig. 4.11 and Fig. 4.12.

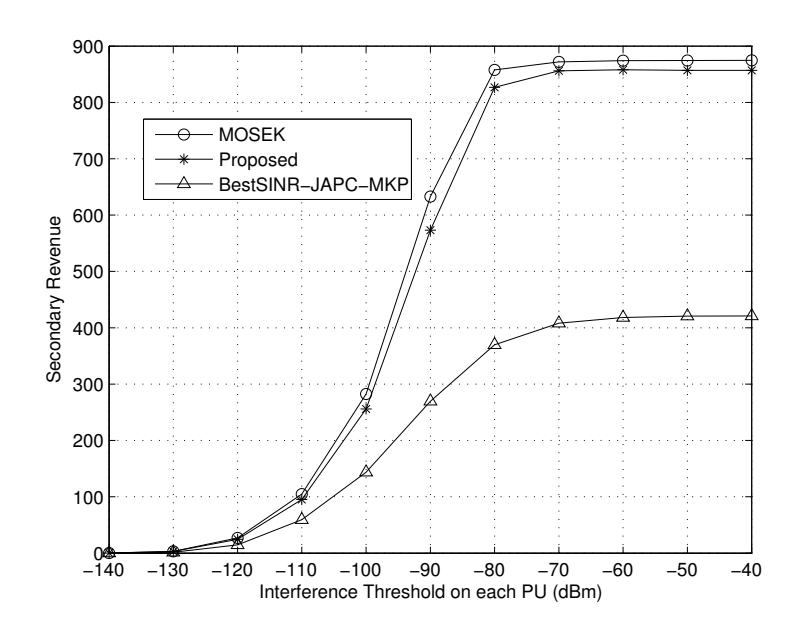
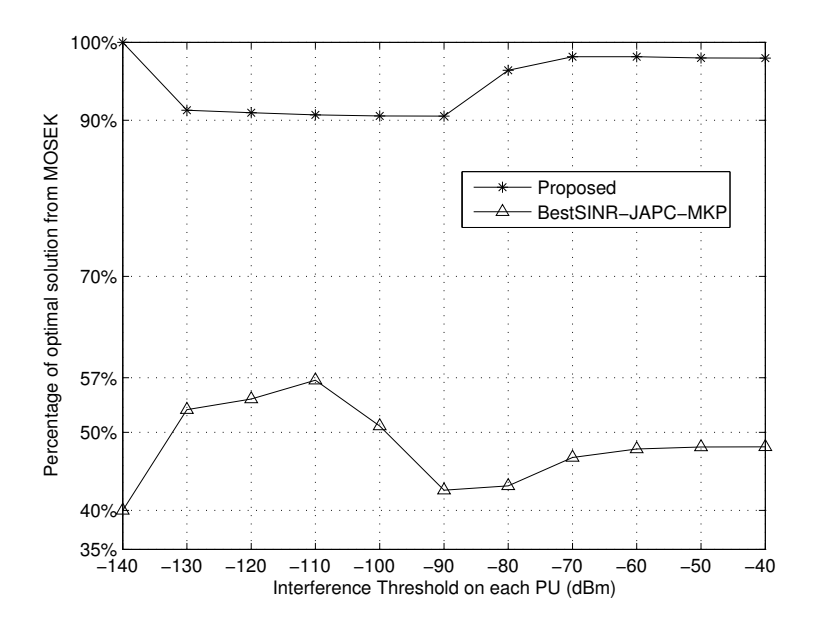


Figure 4.11: Revenue in terms of different interference level per PU ( $n_{pc}^{max}=10$ ,  $I_p=-80dBm$ ,  $n_{SU}=100$ , and  $n_c=10$ )

Figure 4.11 shows the secondary revenue increases with the increasing interference threshold on PUs. The reason is the higher interference threshold on PUs, the more SUs can be allowed to transmit. Thus, the revenue to BS increases. When  $\Gamma$  is smaller than  $-130 \mathrm{dBm}$ , the results of three schemes are almost the same, since in that case, almost no SUs can be admitted. However, when  $\Gamma$  is greater than  $-130 \mathrm{dBm}$ , the gap between our proposed scheme and BestSINR-JAPC-MKP becomes bigger and bigger until  $\Gamma$  is equal to  $-70 \mathrm{dBm}$ . When  $\Gamma$  is greater than  $-70 \mathrm{dBm}$ , the gap between our proposed scheme and BestSINR-JAPC-MKP stays almost the same. It also shows, when  $\Gamma$  is greater than  $-90 \mathrm{dBm}$ , our proposed scheme gets more than twice



**Figure 4.12:** Percentage of optimal solution from MOSEK in terms of different interference level per PU  $(n_{pc}^{max} = 10, I_p = -80dBm, n_{SU} = 100, \text{ and } n_c = 10)$ 

the revenue got by BestSINR-JAPC-MKP. Moreover, our proposed scheme approaches the results from MOSEK very closely.

Figure 4.12 shows the percentage of optimal solution from MOSEK for both our proposed scheme and BestSINR-JAPC-MKP. Our proposed scheme achieves more than 90% of optimal solution from MOSEK, while BestSINR-JAPC-MKP achieves only 40% to 57%.

## 4.7 Conclusions and discussions

#### 4.7.1 Conclusions

In this chapter, we have investigated the operator problem of maximization the secondary revenue, while satisfying the power limitation, minimum SINR and interference constraints. We modeled the problem as MMKP, and then transfer it to MKP. Then, we proposed a heuristic algorithm based on the MKP formulation. Simulation results showed our proposed heuristic scheme archive much more secondary revenue than BestSINR-JAPC-MKP, and is close to the optimal results from MOSEK.

#### 4.7.2 Discussions

The problem we studied in this chapter can be extended and applied in many ways.

- Different revenue formulations. In our simulation, revenue is proportional to the data rate of each SU. In practice, the revenue can be customized by the service providers.
- Different path loss models. In our simulation, we consider a slow fading channel, and the path loss is  $\frac{1}{d^4}$ , where d is the distance between a transmitter and its receiver. In practice, we can use any suitable path loss models.
- When SU can use multiple channels in the same time.
   In case every SU has the ability to use multiple channels at the same time, say maximum K, we can modify our formulations as follows.

maximize 
$$\sum_{i \in \mathcal{N}_s} \sum_{m \in \mathcal{N}_c} r_i x_{mi}$$
subject to 
$$\sum_{i \in \mathcal{N}_s} w_{mij} x_{mi} \leq 1, \quad j = 1, 2, \cdots, n_s + n_{pm}, m \in \mathcal{N}_c$$
$$\sum_{m \in \mathcal{N}_c} x_{mi} \leq K, \qquad \forall i \in \mathcal{N}_s$$
$$x_{mi} \in \{0, 1\}, \qquad \forall i \in \mathcal{N}_s, m \in \mathcal{N}_c$$

$$(4.35)$$

## Chapter 5

## Spectrum Sharing in Cognitive Radio Femtocell Networks

In the previous chapters, we have investigated the resource optimization problems in the underlay spectrum sharing mode. From this chapter on, we study the resource optimization in the overlay spectrum sharing mode. Specially in this chapter, we study the resource optimization problem in cognitive radio femtocell networks.

Femtocell is envisioned as a highly promising solution for indoor wireless communications. The spectrum allocated to femtocells is traditionally from the same licensed spectrum bands of macrocells. In this case, the capacity of femtocell networks may be highly limited due to the finite number of licensed spectrum bands and also the interference with macrocells and other femtocells. In this chapter, we propose a radically new communication paradigm by incorporating cognitive radio in femtocell networks. The cognitive radio enabled femtocells are able to access licensed spectrum bands not only from macrocells but also from other licensed systems (e.g. TV systems). Thus, the co-channel interference in femtocells can be greatly reduced and the network capacity can be significantly improved.

The rest of this chapter is organized as follows. In section 5.1, we introduce the system model and assumptions. Then we formulate the downlink spectrum sharing problem for CogFem in section 5.2. In section 5.3, we employ a mixed primal and dual decomposition method to decompose the problem into a master problem with channel allocation, and several subproblems with power control at each femtocell. Then, we propose a joint channel allocation and fast power control schemes. In section 5.4, we evaluate the performance of our proposed scheme for normal femtocells and CogFem, and compare it to some existing methods. Simulation results also showed that our proposed scheme without any iteration can achieve almost twice of the

average capacity by coloring method when the number of available channels is less than 5. Moreover, our proposed scheme can converge very fast with a typical value of only 5 iterations, and it can achieve around 2% extra average capacity than fixed power control scheme. Finally, we draw conclusions in section 5.5.

## 5.1 System model and assumptions

In this section, we introduce the system model and assumptions for CogFem in the overlay spectrum sharing mode.

The notations used in this chapter are shown in Table 5.1. Suppose that there are a set of  $\mathcal{F}$  femtocells in the coverage of a macrocell. For any FBS i  $(i \in \mathcal{F})$ , there are a set of  $\mathcal{M}_i$  FUs. Normally the number of FUs is between 2 and 4 as indicated in [25]. In this chapter, we also use i as the ID of the femtocell where FBS i is located. There are a set of  $\mathcal{N}_i$  licensed channels that can be used for femtocell i.  $\mathcal{N}_i$  may change dynamically depending on the activities of nearby primary systems. These channels are not only from macrocells but also from other licensed systems. We claim that the definition of this channel could be adapted according to the particular access method. For example, if femtocells use CDMA, the channel is a wide band like 5MHz, 10MHz. If femtocells use OFDMA, the channel could be a narrow band subchannel containing several subcarriers typically 100KHz similar in IEEE 802.22 draft standard [104].

### 5.1.1 System initialization

Whenever an FBS turns on, it will first sense the spectrum environment to initialize an available spectrum list. The FBS will be responsible to allocate spectrum to its users, and inform them the suitable uplink transmission power. The uplink power control is out of the topic in this chapter. Synchronization between neighboring FBSs is not obligatory in CogFem, but it is an option if any FBS wants to synchronize with its neighbors. The synchronization can be implemented by listening to neighboring femtocells information to obtain the frame length and structure.

#### 5.1.2 Number of transceivers

We do not specify the stringent requirement on the number of transceivers on FBS. One transceiver for each FBS is possible. In this situation, each FBS will perform both spectrum sensing and data transmission on this transceiver

Table 5.1: Table of notations for cognitive radio femtocell networks

Symbol	Meaning
$\mathcal{F}$	the set of FBSs
$\mathcal{M}_i$	the set of FUs in FBS $i$
$\mathcal{N}_i$	the set of available channels in FBS $i$
i	the index of FBS
j	the index of FU
c	the index of channel
$m_i$	the number of FUs in FBS $i$
$x_{ijc}$	the binary indicator of channel $c$ on FU $j$ in FBS $i$
$p_{ijc}$	the transmission power for FBS $i$ at channel $c$ on FU $j$
$h_{ijc}$	the channel gain on channel $c$ for FBS $i$ and FU $j$
$I_{ijc}$	the interference at FU $j$ in FBS $i$ on channel $c$
$\psi$	the minimum required SINR for FUs

at different time. To reduce the complexity and improve the throughput, two transceivers for each FBS would be better. In this situation, each FBS is equipped with two transceivers. One is called *sensing radio* used for spectrum sensing, while the other one is called *cognitive radio* used for data communication of both intra-femtocell and inter-femtocell on the selected channels. So that, FBS can do spectrum sensing and data transmission simultaneously.

# 5.1.3 Spectrum sensing and primary system protection

Each FBS is able to sense the available spectrum. The available spectrum list can be stored into a local database or a database in the Internet for the future use. FBSs from other femtocells can access these information from the database, and negotiate with the neighboring FBSs with the available spectrum.

For spectrum sensing, both FBS and FU can support spectrum sensing if the hardware expense is not an issue. In this situation, whenever an FU detects the return of a primary user (PU), it will stop transmission and inform the FBS in the control channel. The FBS will do fine spectrum sensing by itself, and determine the real existence of the PU. If a real PU exists, the FBS will inform the FU to switch to another channel. Otherwise, it will inform FU to continue using the current channel.

To save hardware expense and battery lifetime for FU, we can suppose only FBS would do spectrum sensing. In this situation, whenever an FBS detects the return of a PU, it will stop transmission, and then inform its FUs and the neighboring FBSs about the existence of the PU. It then updates the available channel list, and runs the spectrum sharing algorithms to select new channels and allocates new time-subchannel blocks for its FUs.

The main challenge is the accuracy of spectrum sensing. Due to hardware limitation and spectrum detection schemes, false alarm and miss detection may happen. Specifically, false alarm happens when the spectrum sensing results show that primary signal exists but actually there is no primary signal. Miss detection happens when the spectrum sensing results show that there is no primary signal but actually primary signal do exist. False alarm will cause unnecessary channel switching which results in increased delay and packet loss. Miss detection will cause interference to the primary systems. Cooperative spectrum sensing and decision is a good candidate to reduce the probability of false alarm and miss detection. In this chapter, the details of spectrum sensing is out of the range of this topic, we assume perfect spectrum sensing. For more details on spectrum sensing, please refer to [105].

#### 5.1.4 Control channel

There are two kinds of control channels. One is called *inter-femtocell* control channel, whereby each FBS can communicate with each other. The other one is called *intra-femtocell* control channel, whereby each user in a femtocell can communicate with its FBS to obtain the channel information and allowed transmission power. These control channel could be a dedicated control channel or a rendezvous channel which can be selected according to some metrics such as channel availability. Since every FBS has a broadband connection to the Internet, in spite of using the inter-femtocell control channel, neighboring FBSs can communicate with each other through the broadband connection. Similarly, an additional FBS controller in the Internet can be helpful for the management of FBSs.

#### 5.1.5 Handover between macrocell and femtocell

Whenever an FU moves into a femtocell from a macrocell, it can detect the existence of an FBS by listening to the control channel information, and decide to switch into the femtocell network.

By contrast, whenever an FU moves out of a femtocell, it can detect that the strength from FBS is weaker than the strength from macrocell BS (MBS), then it decides to switch into the macrocell network.

#### 5.1 System model and assumptions

In traditional mobile macrocell networks, handover can be either soft or hard. In soft handover, the mobile user will communicate with the two BSs at the same time, until the signal strength is higher than a threshold. In hard handover, the mobile user will switch to the new BS as soon as the signal is stronger than the old BS.

In CogFem, we can employ both soft and hard handover. Simply, we can use hard handover for instance in this chapter. When the FU detects that the pilot signal is much stronger than the traffic channel, it will switch to the femtocell network. If it detects that the pilot signal from macrocell BS is much higher than current femtocell data traffic channel, it will switch to the macrocell network.

#### 5.1.6 Deployment example

In practice, we can deploy CogFem in a flexible way. As an example shown in Fig. 5.1, an FBS controller can be added in the system architecture to improve the management ability for all the FBSs.

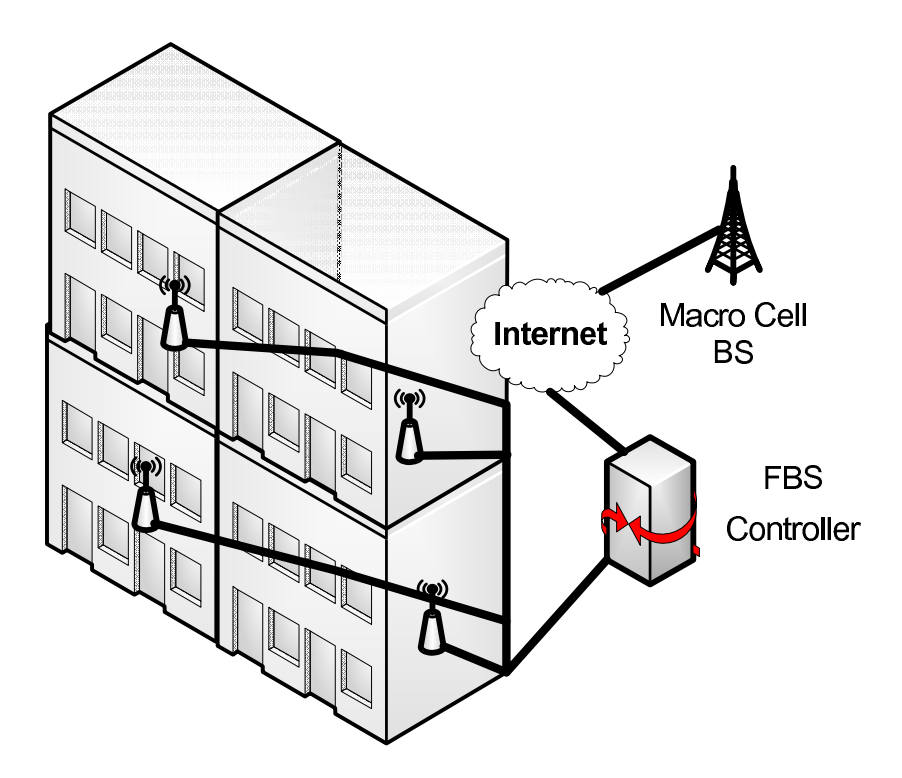


Figure 5.1: An example of deploying CogFem networks with FBS controller

### 5.2 Problem formulations

In this chapter, we consider the downlink spectrum sharing problem in the overlay mode. Femtocells use the licensed channels when they are not occupied by primary systems. Thus, there is no co-channel interference between primary systems and femtocells. The only interference should be managed is amongst femtocells. Suppose each femtocell user in a femtocell i requires one channel. We consider the worst case when all neighboring femtocells are in downlink transmission. In the following, we analyze the downlink capacity and then formulate the spectrum sharing problem.

#### 5.2.1 Channel model

The indoor path loss model in dB is based on the ITU and COST 231 indoor model [106] [107] as follows.

$$G_{ij} = 37 + 30log_{10}d_{ij} + 18.3n_{ij}^{\left(\frac{n_{ij}+2}{n_{ij}+1} - 0.46\right)}$$
(5.1)

where  $d_{ij}$  is the distance between the transmitter i and the receiver j.  $n_{ij}$  denotes the number of floors in the path. We introduce  $h_{ijc}$  as follows to represent the channel gain between FBS i and its FU j on channel c.

$$h_{ijc} = 10^{\left(-\frac{G_{ij}}{10}\right)} \tag{5.2}$$

# 5.2.2 Downlink capacity

Any femtocell user will receive interference from neighboring femtocells using the same channel. We consider an Additive White Gaussian Noise (AWGN) channel. The SINR of the received signal from FBS i at femtocell user j can be denoted as

$$\xi_{ijc} = g_{ijc} p_{ijc} x_{ijc} \tag{5.3}$$

where

$$g_{ijc} = \frac{h_{ijc}}{N_0 + I_{ijc}} \tag{5.4}$$

where  $N_0$  denotes the background noise power.  $I_{ijc}$  represents the interference measured at user j on channel c from femtocells other than i.  $p_{ijc}$  is the downlink transmission power for FBS i on channel c.  $x_{ijc}$  is a binary indicator. If  $x_{ijc} = 1$ , user j in femtocell i works on channel c, zero otherwise.

The downlink capacity of any femtocell user j in femtocell i can be calculated according to Shannon's capacity theory as follows.

$$C_{ij} = \sum_{c \in \mathcal{N}_i} B_c log_2(1 + \xi_{ijc}) \tag{5.5}$$

where  $B_c$  denotes the bandwidth of channel c.  $\xi_{ijc}$  is defined in (5.3). Then, we can calculate the downlink capacity of femtocell i as follows.

$$C_{i} = \sum_{j \in \mathcal{M}_{i}} C_{ij}$$

$$= \sum_{j \in \mathcal{M}_{i}} \sum_{c \in \mathcal{N}_{i}} B_{c} log_{2}(1 + \xi_{ijc}), \quad \forall i \in \mathcal{F}$$
(5.6)

#### 5.2.3 Downlink spectrum sharing problem

The spectrum sharing problem in CogFem downlink transmission is to maximize the downlink capacity of all FBSs while guaranteeing the channel allocation, SINR, and power constraints.

P1

maximize 
$$\sum_{i \in \mathcal{F}} C_i$$
 (5.7)

s.t.

$$x_{ijc} \in \{0, 1\}, \quad \forall i \in \mathcal{F}, j \in \mathcal{M}_i, c \in \mathcal{N}_i$$
 (5.8)

$$\sum_{c \in \mathcal{N}_i} x_{ijc} = 1, \quad \forall i \in \mathcal{F}, j \in \mathcal{M}_i$$
 (5.9)

$$\sum_{j \in \mathcal{M}_i} \sum_{c \in \mathcal{N}_i} x_{ijc} = m_i, \forall i \in \mathcal{F}$$
 (5.10)

$$\xi_{ijc} \ge \psi, \quad if \ x_{ijc} = 1, \forall i \in \mathcal{F}, j \in \mathcal{M}_i, c \in \mathcal{N}_i$$
 (5.11)

$$p_{ijc} = 0, \quad if \ x_{ijc} = 0, \forall i \in \mathcal{F}, j \in \mathcal{M}_i, c \in \mathcal{N}_i$$
 (5.12)

$$p_{ijc} \ge 0, \quad \forall i \in \mathcal{F}, j \in \mathcal{M}_i, c \in \mathcal{N}_i$$
 (5.13)

$$\sum_{j \in \mathcal{M}_i} \sum_{c \in \mathcal{N}_i} p_{ijc} \le P_i^{max}, \quad \forall i \in \mathcal{F}$$
 (5.14)

where  $\psi$  denotes the minimum required SINR for FUs. Constraint (5.9) means every user in a CogFem can only use one channel. Constraint (5.10) means the total number of channels can be used in one femtocell is equal to the number of users in that femtocell  $m_i$ . Constraint (5.11) represents that if channel c is allocated to user j in femtocell i for downlink transmission, the SINR received on user j should be higher than the predefined threshold  $\psi$ . Constraint (5.12) means any FBS i will not allocate any power on channel c, if channel c is not allocated to FBS i. Constraint (5.13) represents the transmission power of any FBS i should be no less than 0, while constraint (5.14) indicates the total transmission power of any FBS i on its FUs can not exceed the maximum power budget  $P_i^{max}$ .

The solution of the formulated spectrum sharing problem is the channel allocation vector  $\mathbf{x}$  and power vector  $\mathbf{p}$ , and the objective function is non-linear. Thus it is a MINLP problem, which is NP-hard in general. In the following sections, we will use decomposition methods to solve it.

# 5.3 Problem decompositions and solutions

In this section, we use mixed primal and dual decomposition methods to solve the downlink spectrum sharing problem based on the decomposition theories in [108] and [109].

### 5.3.1 The master problem

Given a feasible power  $p_{ijc}$  for each FU i, we have the master problem in charge of updating the channel allocation variables  $\{x_{ijc}\}$ , by solving the following problem.

maximize 
$$\sum_{i \in \mathcal{F}} \sum_{j \in \mathcal{M}_i} \sum_{c \in \mathcal{N}_i} B_c log_2 (1 + g_{ijc} p_{ijc} x_{ijc})$$
 (5.15)

s.t.

$$x_{ijc} \in \{0, 1\}, \quad \forall i \in \mathcal{F}, j \in \mathcal{M}_i, c \in \mathcal{N}_i$$
 (5.16)

$$\sum_{c \in \mathcal{N}_i} x_{ijc} = 1, \quad \forall i \in \mathcal{F}, j \in \mathcal{M}_i$$
 (5.17)

$$\sum_{j \in \mathcal{M}_i} \sum_{c \in \mathcal{N}_i} x_{ijc} = m_i, \forall i \in \mathcal{F}$$
 (5.18)

This problem can be solved heuristically in polynomial times. We can observe that the objective function (5.15) is concave and monotonously increasing with  $g_{ijc}p_{ijc}x_{ijc}$ . Intuitively, we can find a solution by assigning 1 to  $x_{ijc}$  with the maximum  $g_{ijc}p_{ijc}$ , and 0 to other channel vector for the same FU j in femtocell i. We repeat this process until all the constraints are satisfied. The detailed implementation is shown in Algorithm 6.

#### Algorithm 6 Channel allocation algorithm for the master problem

```
Input: \{N_i\}, \{M_i\}, \{p_{ijc}\}, \{g_{ijc}\}.
Output: \{x_{ijc}\}.
  1: Initialization: \mathcal{M}_{i}^{'} \leftarrow \mathcal{M}_{i}, \, \mathcal{N}_{i}^{'} \leftarrow \mathcal{N}_{i}.
  2: while \forall \mathcal{M}'_i \neq \emptyset do
                if \mathcal{N}_i^{'} = \emptyset then
  3:
                        Break;
                                                                                     \triangleright not enough channels for femtocell i.
  4:
                else
  5:
                        \{i^*, j^*, c^*\} \leftarrow \arg\max_{\forall i \in \mathcal{F}, j \in \mathcal{M}_i', c \in \mathcal{N}_i'} g_{ijc} p_{ijc}
  6:
                       \mathcal{N}'_{i^*} \leftarrow \mathcal{N}'_{i^*} - c^*
M'_{i^*} \leftarrow M'_{i^*} - j^*
  7:
  8:
                end if
  9:
10: end while
```

The complexity of the Algorithm 6 is  $O(|\mathcal{F}||\mathcal{M}||\mathcal{N}|)$ , where  $|\cdot|$  denotes the cardinal of the set within.  $|\mathcal{M}|$  and  $|\mathcal{N}|$  are the maximum number of FUs and channels per FBS, i.e.,  $|\mathcal{M}| = \max_{\forall i \in \mathcal{F}} |\mathcal{M}_i|$ , and  $|\mathcal{N}| = \max_{\forall i \in \mathcal{F}} |\mathcal{N}_i|$ .

# 5.3.2 Subproblems

#### problem formulation

Given a solution of channel allocation  $\{x_{ijc}\}$ , we can get the following power control subproblem to obtain the transmission power for every FBS i to any of its FU j on the allocated channel  $c_i$ .

maximize 
$$\sum_{i \in \mathcal{F}} \sum_{j \in \mathcal{M}_i} B_c log_2(1 + g_{ijc} p_{ijc^*})$$
 (5.19)

s.t.

$$p_{ijc} \ge 0, \quad \forall i \in \mathcal{F}, j \in \mathcal{M}_i$$
 (5.20)

$$\sum_{j \in \mathcal{M}_i} p_{ijc} \le P_i^{max}, \quad \forall i \in \mathcal{F}$$
 (5.21)

$$g_{ijc}p_{ijc} \ge \psi, \quad \forall i \in \mathcal{F}, j \in \mathcal{M}_i$$
 (5.22)

$$p_{ijc} = 0, \quad if \ c \neq c_j, \forall i \in \mathcal{F}, j \in \mathcal{M}_i, c \in \mathcal{N}_i$$
 (5.23)

#### The Lagrangian

We form the Lagrangian function as follows

$$L(\mathbf{p}, \lambda, \nu) = \sum_{i \in \mathcal{F}} \sum_{j \in \mathcal{M}_i} B_c log_2(1 + g_{ijc} p_{ijc})$$

$$+ \sum_{i \in \mathcal{F}} \lambda_i \left( P_i^{max} - \sum_{j \in \mathcal{M}_i} p_{ijc} \right)$$

$$+ \sum_{i \in \mathcal{F}} \sum_{j \in \mathcal{M}_i} \nu_{ij} \left( g_{ijc} p_{ijc} - \psi \right)$$

$$= \sum_{i \in \mathcal{F}} L_i(\mathbf{p}_i, \lambda_i, \nu_i)$$
(5.24)

where the Lagrangian multiplier vectors of  $\lambda$  and  $\nu$  are non-negative. ( $\lambda = (\lambda_1, \lambda_2, ...)^T$ ,  $\nu = (\nu_1, \nu_2, ...)^T$ ,  $\nu_i = (\nu_{i1}, \nu_{i2}, ...)^T$ ).  $\mathbf{p}_i$  is the power vector for FBS i. And  $L_i(\mathbf{p}_i, \lambda_i, \nu_i)$  is defined as follows.

$$L_{i}(\mathbf{p}_{i}, \lambda_{i}, \nu_{i}) = \sum_{j \in \mathcal{M}_{i}} B_{c}log_{2}(1 + g_{ijc}p_{ijc})$$

$$+ \lambda_{i} \left( P_{i}^{max} - \sum_{j \in \mathcal{M}_{i}} p_{ijc} \right)$$

$$+ \sum_{j \in \mathcal{M}_{i}} \nu_{ij} (g_{ijc}p_{ijc} - \psi)$$

$$(5.25)$$

Thus, the Lagrangian dual can be decomposed into  $|\mathcal{F}|$  subproblems for each FBS i ( $\forall i \in \mathcal{F}$ ). For each given  $\lambda_i$  and  $\nu_i$ , the dual is to solve  $\mathbf{p}_i$ 

$$\mathbf{p}_{i}^{*} = \arg\max_{\mathbf{p}_{i} > 0} L_{i}(\mathbf{p}_{i}, \lambda_{i}, \nu_{i})$$
(5.26)

The decomposed Lagrangian dual function (5.25) is concave on  $\mathbf{p}_i$ , according to Karush-Kuhn-Tucker (KKT) condition [110], we have the following equations for any FBS i.

$$\frac{\partial L_i(\mathbf{p}_i, \lambda_i, \nu_i)}{\partial p_{ijc}} = 0 \tag{5.27}$$

$$\lambda_i \left( P_i^{max} - \sum_{j \in \mathcal{M}_i} p_{ijc} \right) = 0 \tag{5.28}$$

$$\nu_{ij}(g_{ijc}p_{ijc} - \psi) = 0 \tag{5.29}$$

where (5.28) means if  $\sum_{j\in\mathcal{M}_i} p_{ijc} \neq P_i^{max}$ , the Lagrangian multiplier  $\lambda_i$  should be zero. Similarly, (5.29) means if  $g_{ijc}p_{ijc} \neq \psi$ , the Lagrangian multiplier  $\nu_{ij}$  should be zero.

According to (5.27), we have

$$\frac{B_c g_{ijc}}{(1 + g_{ijc} p_{ijc}) ln2} - \lambda_i + \nu_{ij} g_{ijc} = 0$$
 (5.30)

We can obtain  $p_{ijc}$  as follows

$$p_{ijc} = \left[ \frac{B_c}{(\lambda_i - \nu_{ij}g_{ijc})ln2} - \frac{1}{g_{ijc}} \right]_{P_{ijc}^{min}}^{P_i^{max}}$$
(5.31)

where  $[\cdot]_a^b$  denotes the projection onto the area in [a,b]. This solution is only valid when  $x_{ijc} = 1$ . If  $x_{ijc} = 0$ ,  $p_{ijc} = 0$ .  $P_{ijc}^{min}$  is the minimum transmission power at FBS i for FU j on channel c.  $P_{ijc}^{min}$  can be determined by substituting (5.3) into (5.11) as follows.

$$P_{ijc}^{min} = \frac{\psi}{q_{ijc}} \tag{5.32}$$

This minimum value may be changed according to the environment, for example the movement of FUs and the interference from other FBSs. Moreover, the first part in (5.31) should be non-negative, so we have

$$\lambda_i > \nu_{ij} g_{ijc}, \quad \forall j \in \mathcal{M}_i$$
 (5.33)

In addition, we observe that  $P_i^{max}$  should be larger than the sum of  $P_{ijc}^{min}$  in any FBS i. Otherwise, there will be no feasible solution for the problem, which results in not all FUs in the FBS can be served. Therefore,  $P_i^{max}$  should be configured at least  $\sum_{\forall j,c} P_{ijc}^{min}$  in the CogFem deployment.

#### Solution with subgradient methods

In the following, we discuss the updating of Lagrangian multipliers when  $x_{ijc} = 1$ . We employ the projected subgradient method as follows.

$$\lambda_i(t+1) = \left[\lambda_i(t) - \alpha(t) \left(P_i^{max} - \sum_{j \in \mathcal{M}_i} p_{ijc}^*\right)\right]^+$$
 (5.34)

$$\nu_{ij}(t+1) = \left[\nu_{ij}(t) - \alpha(t)(g_{ijc}p_{ijc}^* - \psi)\right]^+$$
 (5.35)

where  $[\cdot]^+$  denotes the projection onto the non-negative area.  $\alpha(t)$  is a positive stepsize for the t times iteration.

**Convergence** Theoretically,  $\alpha(t)$  can be chosen in a manner of either constant or diminishing. The method using constant stepsize  $\alpha(t) = \alpha(0)$ ,  $(\alpha(0) > 0)$  can not guarantee the convergence, it may iterate repeatedly near the optimal solution. By contrast, using the diminishing stepsize, where  $\alpha(t) > 0$ ,  $\lim_{t \to \infty} \alpha(t) = 0$ , and  $\sum_{t=1}^{\infty} \alpha(t) = \infty$ , for example,  $\alpha(t) = \alpha(0)/t$ , the solution will be finally converged.

In our scenario, we can try  $\alpha(0) = 1$ , and  $\alpha(t) = 1/t$ , t = 1, 2, ... For the initial value of  $\lambda$  and  $\nu$ , we can choose  $\lambda_i(0) = P_i^{max}$ . To obey the constraints in (5.33), we can assign

$$\nu_{ij}(0) = \frac{\theta \lambda_i(0)}{g_{ijc}}, \quad \forall j \in \mathcal{M}_i$$

where  $\theta$  is a scale in the range of [0,1).

**Distributed implementation** This scheme can work distributively, where each FBS i updates its own  $\lambda_i$  and  $\nu_{ij}$  until convergence. The details of the power control algorithm for any FBS i is shown in Algorithm 7. We can summarize our decomposition methods in Fig. 5.2, where the Lagrangian multipliers  $\lambda_i$  and  $\nu_{ij}$  serve as the prices for each FBS i.

```
Algorithm 7 Power control algorithms for any FBS i
```

```
Input: i, \{x_{ijc}\}, \mathcal{N}_i, \mathcal{M}_i, \theta.
Output: \{p_{ijc}\}.
 1: Initialization: \alpha \leftarrow 1, \lambda_i \leftarrow P_i^{max}, and \nu_{ij} \leftarrow \frac{\theta \lambda_i}{g_{ijc}}, t \leftarrow 0, p_{ijc} \leftarrow P_{ijc}^{min}
 2: while not converged do
 3:
            Update \lambda_i according to (5.34)
 4:
           for all j \in \mathcal{M}_i do
                 Update \nu_{ij} according to (5.35)
 5:
                 Calculate p_{ijc} according to (5.31)
 6:
           end for
 7:
           t \leftarrow t + 1
 8:
           \alpha \leftarrow 1/t
 9:
10: end while
```

#### Proposed scheme

Although the subgradient method can converge to the optimal solution, it highly depends on the stepsize and initial values. Therefore, it may require

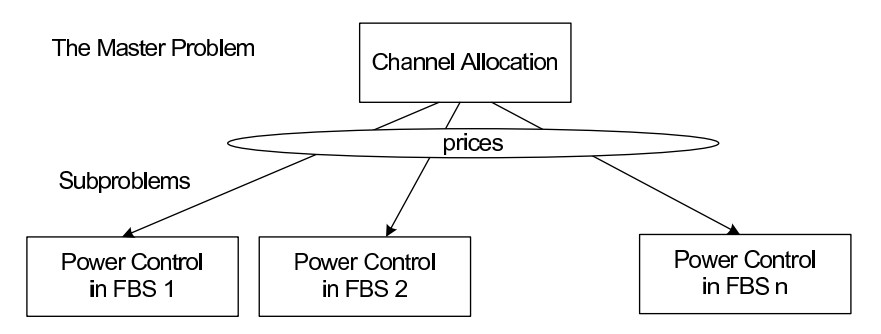


Figure 5.2: The decomposition of spectrum sharing problems in CogFem

lots of iterations and the knowledge of stepsize and Lagrangian multipliers crossing different FBSs. In this study, we are interested in finding a more suitable approach for CogFem. We can rewrite (5.31) as follows

$$p_{ijc} = \frac{1}{\lambda_i'} - \frac{1}{g_{ijc}} \tag{5.36}$$

where

$$\lambda_i' = \frac{\ln 2}{B_c} (\lambda_i - \nu_{ij} g_{ijc}) \tag{5.37}$$

where the Lagrangian multiplier  $\nu_{ij}$  can change accordingly with  $g_{ijc}$ , so that (5.37) is only changed with i instead of both i and j.

Substituting (5.36) to (5.28) when  $x_{ijc} = 1$ , we have

$$\lambda_i' = \frac{m_i}{P_i^{max} + \sum_{k \in \mathcal{M}_i} \frac{1}{g_{ikc_k}}}$$
 (5.38)

where  $c_k$  is the selected channel for FU k. Substituting (5.38) to (5.36) when  $x_{ijc} = 1$ , we have

$$p_{ijc} = \begin{cases} 0, & x_{ijc} = 0\\ \left[\frac{1}{m_i} P_i^{max} + \frac{1}{m_i} \sum_{k \in \mathcal{M}_i} \frac{1}{g_{ikc_k}} - \frac{1}{g_{ijc}}\right]_{P_{ijc}^{min}}^{P_i^{max}}, & x_{ijc} = 1 \end{cases}$$
(5.39)

Similarly,  $p_{ijc}$  should be no less than  $P_{ijc}^{min}$ . This can be guaranteed by the configuration of  $P_i^{max}$ .

In this scheme, we assume Channel State Information (CSI) can be obtained by each FBS. One of the possible way to obtain CSI is as follows: each FU can report the interference measurement result to its FBS. Therefore, each FBS will make the decision of channel selection and power allocation

according to the measurements not only on FBS but also on its users. In practice, each femtocell user is required to negotiate a control channel with its FBS, and reports its measurements to the FBS through this channel. Based on these information, FBS then characterizes the channels with the accurate interference levels for each user, and chooses  $m_i$  channels with lowest interference levels. The channel allocation metric is based on  $g_{ijc}$ . FBS can also use its own measured interference as approximate interference on FUs. Our study in [111] has shown that the network performance in terms of average capacity is quite close to each other by either obtaining the interference from FBS or FUs. The reason behind it is that FBS and its FUs are in the same apartment. Other FBSs, where the interference comes from, get power decay not only because of distance but also because of the penetration of floors and walls.

This scheme goes as follows.

- Channel  $c^*$  is allocated to user  $j^*$ , if  $g_{ij^*c^*}$  has the maximum value in the available channels and users.
- Then the allocated channel and user will be removed from the sets of channels and users.
- We repeat the channel and user selection until there is no user or channel left.
- After channel allocation, the power for each user j in femtocell i is calculated according to (5.39) for the worst case, and according to (5.31) for normal case, respectively.

The details of the joint channel allocation and fast power control are shown in Algorithm 8. This scheme is distributed since each FBS work independently. Moreover, each FBS can periodically updating the joint channel allocation and fast power control schemes by the changing of  $g_{ijc}$  because of the change of other FBSs' interference, the movements of FUs, and so on. We will show the convergence in the simulation results in the next section. The complexity of this scheme depends on the channel selection and power allocation. For any FBS i, it is bounded by  $O((|\mathcal{N}_i| \times |\mathcal{M}_i|)^2)$  by employing quicksort in channel and user selection. Similar as the first scheme, in this scheme, whenever an FBS detects a return of primary users on the licensed channel, it will perform the following procedures sequentially, i.e., inform its user to switch to another channel with the least interference on the available channel list, decide a transmission power according to (5.39), and update the transmission power on other active channels.

**Algorithm 8** Proposed joint channel allocation and fast power control algorithm for FBS i

```
Input: i, \mathcal{N}_i, \mathcal{M}_i.
Output: \{x_{ijc}\}, \{p_{ijc}\}.
  1: Initialization: \mathcal{M}_{i}^{'} \leftarrow \mathcal{M}_{i}, \, \mathcal{N}_{i}^{'} \leftarrow \mathcal{N}.
  2: while \mathcal{M}_{i}^{'} \neq \emptyset do
              if \mathcal{N}_{i}^{'}=\emptyset then
  3:
                    Break;
  4:
                                                                         \triangleright not enough channels for femtocell i.
  5:
              else
                    \{j^*, c_{j^*}\} \leftarrow \arg\max_{j \in \mathcal{M}'_i, c \in \mathcal{N}'_i} g_{ijc}
  6:
                   \mathcal{N}_{i}^{'} \leftarrow \mathcal{N}_{i}^{'} - c_{j^{*}}M_{i}^{'} \leftarrow M_{i}^{'} - j^{*}
  7:
  8:
              end if
  9:
10: end while
11: for j \in \mathcal{M}_i do
              Calculate p_{ijc_i} by (5.39).
12:
              Calculate \xi_{ijc} by (5.3).
13:
              if \xi_{ijc} < \psi then
14:
                    p_{iic_i} \leftarrow 0
                                                          \triangleright power allocation for user j in cell i is failed.
15:
              else
16:
17:
                    x_{ijc} \leftarrow 1
              end if
18:
19: end for
```

#### 5.4 Simulation results and discussion

In this section, we evaluate our proposed downlink spectrum sharing schemes. We have implemented a CogFem simulator based on MATLAB, where we create a dense urban apartment topology as shown in Fig. 5.3. There are maximal 10 rows of apartment buildings. Each row has maximal 10 buildings, while each building has maximal 10 floors. The length, width, height of an apartment are 10, 10, and 3 meters, respectively. We call the gap between neighboring buildings in a row side gap, and set it as 1 meter, while we call the gap between neighboring rows row gap, and set it as 5 meters. Each apartment has an FBS, and has 2 to 4 users suggested by [26]. These users sit randomly in each apartment. Without loss of generality, each FBS is located at the middle of the apartment. The minimum required SINR is 0.01. The average power of noise is -110dBmW. The bandwidth of each channel is 100KHz. For the estimation of channel gain in our simulation, we consider

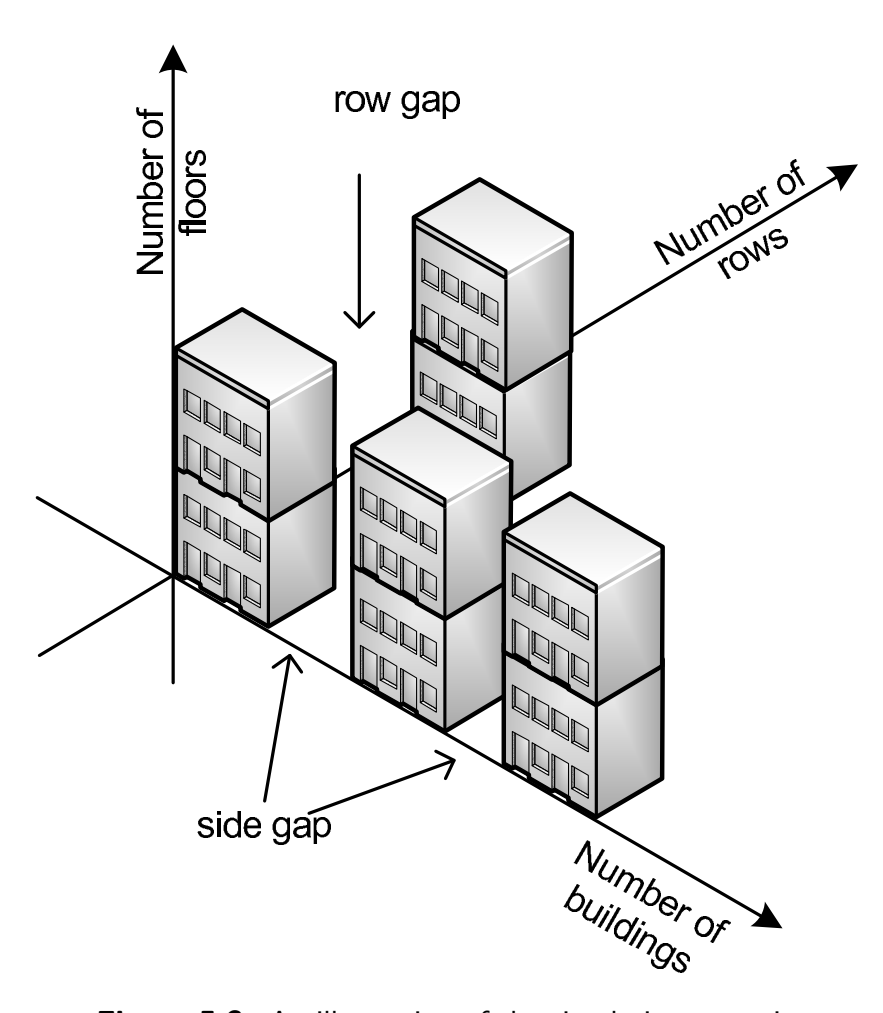


Figure 5.3: An illustration of the simulation scenario

a slow fading channel, and use the COST 231 path loss model in (5.1). We run each case 10 times with different random seeds for the number of users in each femtocell and the number of available channels, and then calculate the average capacity per femtocell.

# 5.4.1 Existing schemes

In this simulation study, we compare our proposed scheme to the existing channel allocation and power allocation schemes. The most popular channel allocation scheme for cellular networks is coloring methods by which no neighboring cells can use the same spectrum at the same time, e.g. in [27]. Regarding the power control method, we consider the fixed power control method by which the total power budget is equally divided by the number

of users in each CogFem.

# 5.4.2 Average capacity with different density of apartments

In the simulation for this purpose, we use power 10mW for the maximum power budget in each FBS. We apply our proposed scheme in normal femtocell networks and cognitive radio femtocell networks, respectively. In the case of normal femtocells, the number of available channels is fixed to 10, while the number of available channels is randomly changed from 10 to 20 in the case of CogFem.

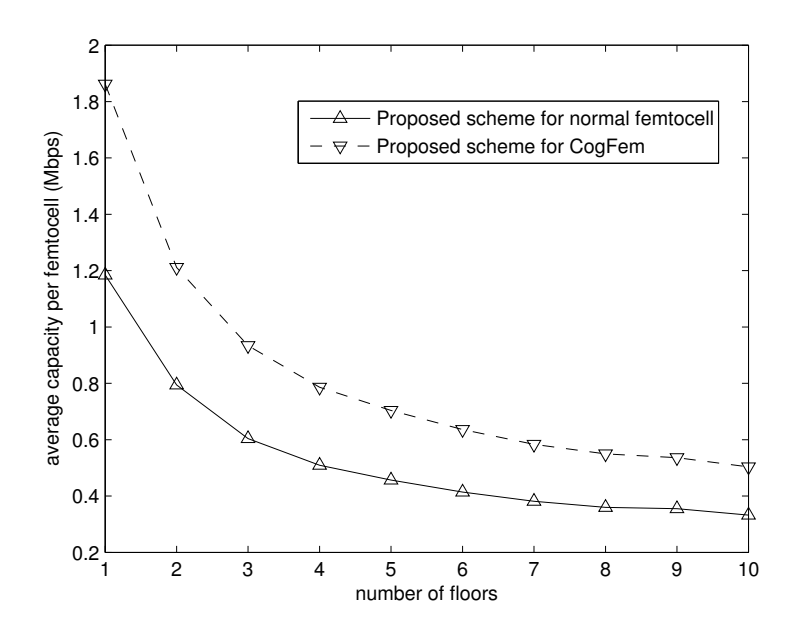


**Figure 5.4:** Average capacity per femtocell in terms of number of floors in each building. (3 rows, and 5 buildings per row)

Figure 5.4, 5.5, and 5.6 show the variation of average capacity per femtocell while changing the number of floors, buildings, and rows, respectively. We can see the average capacity per femtocell decreases while increasing the number of floors, buildings, and rows, respectively. The reason is as follows. When the number of floors, buildings, and rows increases, the number of FBSs also increases. It then leads to more interference amongst femtocells given a limited number of available channels. From the results in Fig. 5.4, 5.5, and 5.6, CogFem achieved almost twice the average capacity of normal femtocells without CR capability by using our proposed scheme. This is essentially

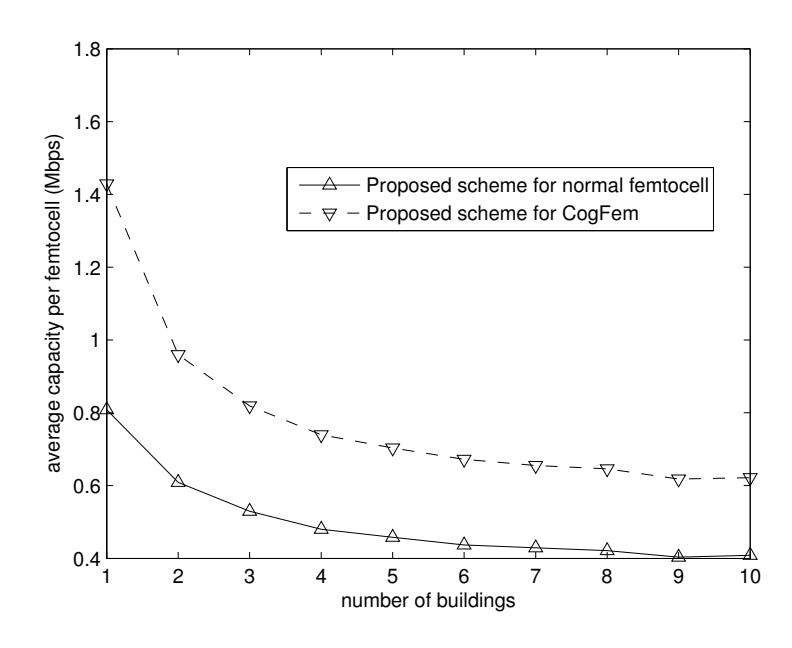


**Figure 5.5:** Average capacity per femtocell in terms of number of buildings in each row. (3 rows, and 5 floors per building)

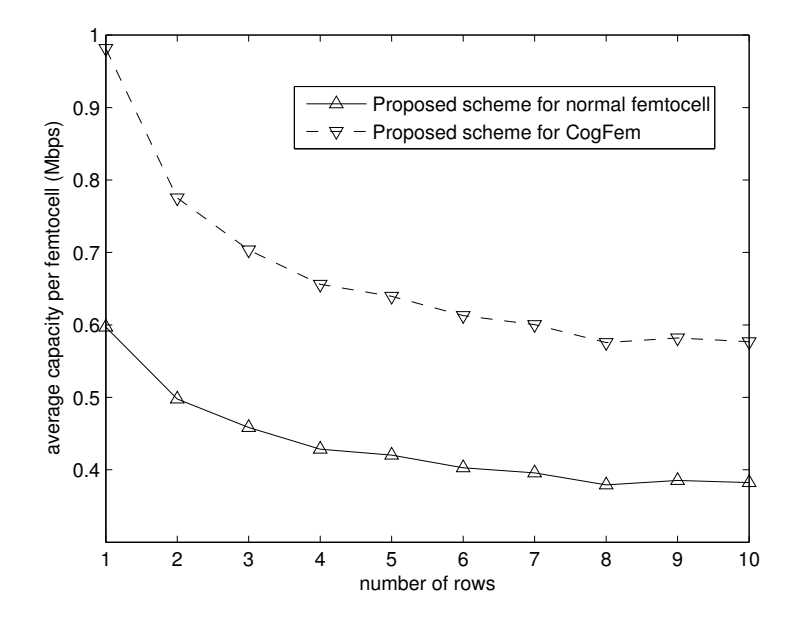


**Figure 5.6:** Average capacity per femtocell in terms of number of rows of buildings. (5 floors per building, and 5 buildings per row)

due to more channel opportunities in CogFem than normal femtocells.

# 5.4.3 System performance with different number of available channels

In the simulation for this purpose, we use power 20mW for the maximum power budget in each FBS.

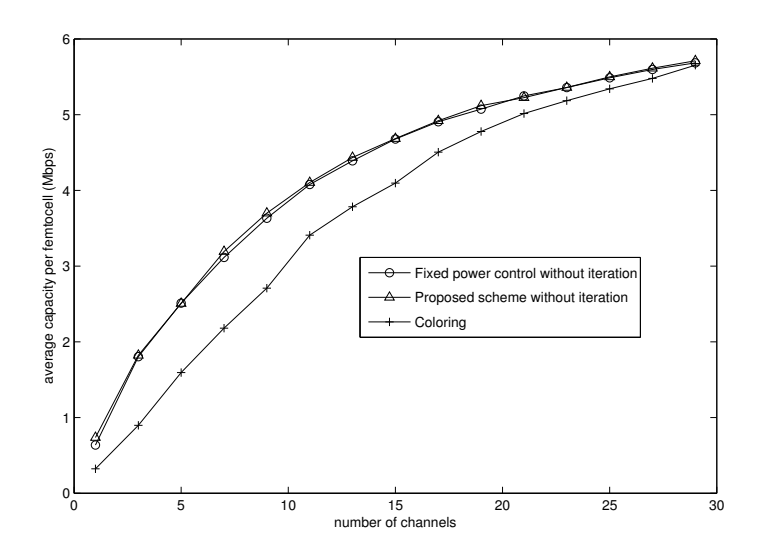


**Figure 5.7:** Average capacity per femtocell in terms of number of channels. (5 rows, 5 buildings per row, 10 floors per building)

Figure 5.7 shows the variation of average capacity per femtocell while changing the available channels. Here, we fix the topology as 5 rows, 5 buildings per row, and 10 floors per building. It shows that the average capacity per femtocell increases while the number of available channels increases. That is because more channel candidates can reduce the interference from neighboring femtocells by allocating different channels to neighboring femtocells. The fixed power control scheme using our channel allocation strategy in Algorithm 6 without any iteration achieved almost the same average capacity of our proposed scheme also without any iteration. Both of these schemes achieved much higher average capacity than coloring method. Specifically, when the number of channels is less than 5, the fixed power control scheme and our proposed scheme can achieve almost twice of the capacity of the coloring method. The performance gap reduced slightly until the number of channels approaches 30.

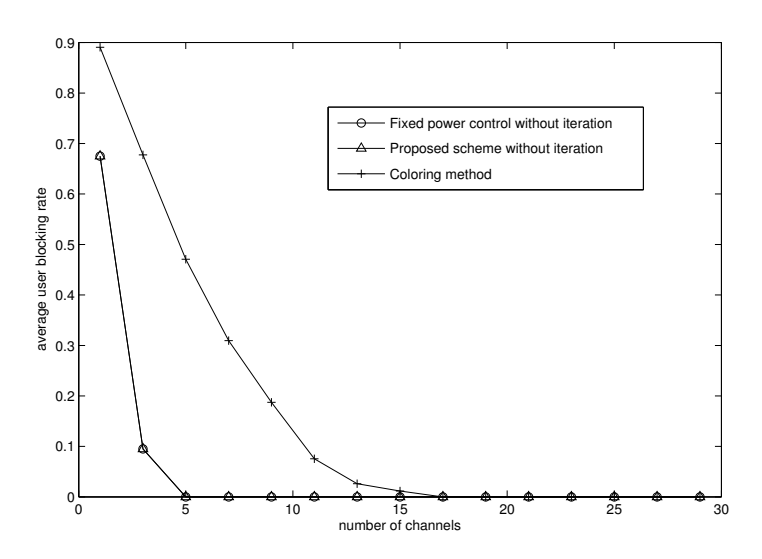


**Figure 5.8:** Average blocking rate in terms of number of channels. (5 rows, 5 buildings per row, 10 floors per building)

The average blocking rate is defined as the ratio of total failed FUs to all FUs. Those failed FUs exist if the SINR at any FU is lower than the required minimum SINR, thus this FU will be not served. Figure 5.8 shows the average blocking rate by using different channel allocation and power control schemes. When the number of available channels is less than 5, the blocking rate for the coloring method is higher than 50%. The blocking rate for fixed power control scheme and our proposed scheme become zero when the number of available channels turns to no less than 5, while the blocking rate for the coloring method stops blocking when the available channels is more than 15. The reason is that the coloring method requires the neighboring CogFem can not use the same channels at the same time. It requires much more channels to allocate all the neighboring FUs. On the contrary, the fixed power control scheme and our proposed scheme are based on the interference related channel allocation, so that neighboring CogFem can utilize the same channel as long as the interference is not unberable for neighboring FBSs and FUs.

## 5.4.4 The convergence

In the simulation for this purpose, we use power 20mW for the maximum power budget in each FBS. We study a scenario with 10 available channels. Figure 5.9 and 5.10 show the convergence of our proposed scheme and the

fixed power control scheme. In each iteration, the channel allocation mechanism will update according to the new interference measured. Figure 5.9 shows that both schemes can converge by a few iterations, e.g., around 5. Our proposed scheme outperforms the fixed power control scheme by obtaining around 2% higher average capacity. Both schemes have zero blocking rate as shown in 5.10.

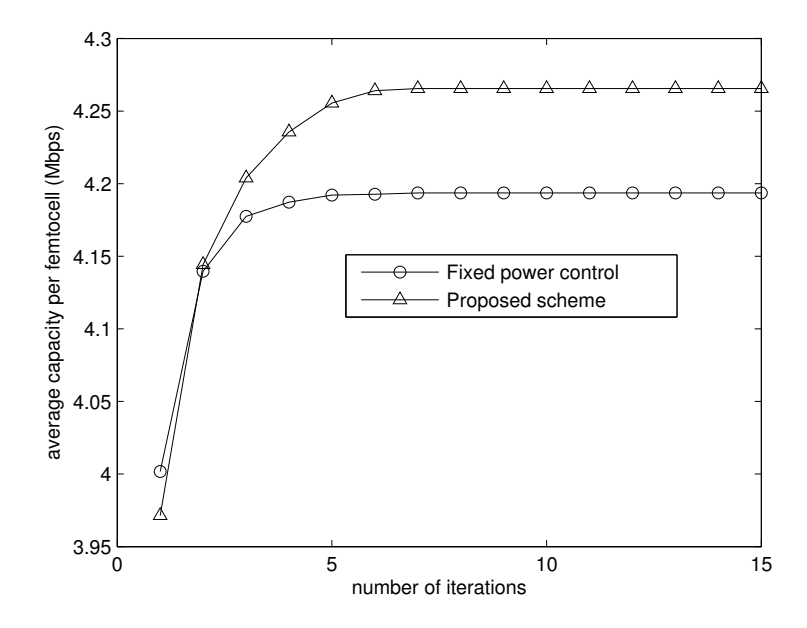


**Figure 5.9:** Average capacity per femtocell in terms of number of Iterations. (10 available channels, 10 floors per building, 5 buildings per row, and 5 rows)

## 5.5 Conclusion

In this chapter, we have investigated the spectrum sharing problem in downlink transmission while applying CR technology into femtocell networks. We formulated this problem as a MINLP problem and then use decomposition methods to solve this problem. According to the solution of the decomposed problem, we proposed a joint channel allocation and fast power control scheme. Simulation results showed that CogFem with more spectrum opportunities could achieve much higher capacity than normal femtocells depending on the number of available of channels. Our proposed scheme converges very fast, and achieves much higher average capacity and lower user blocking rate than the coloring method. Using fixed power control together with

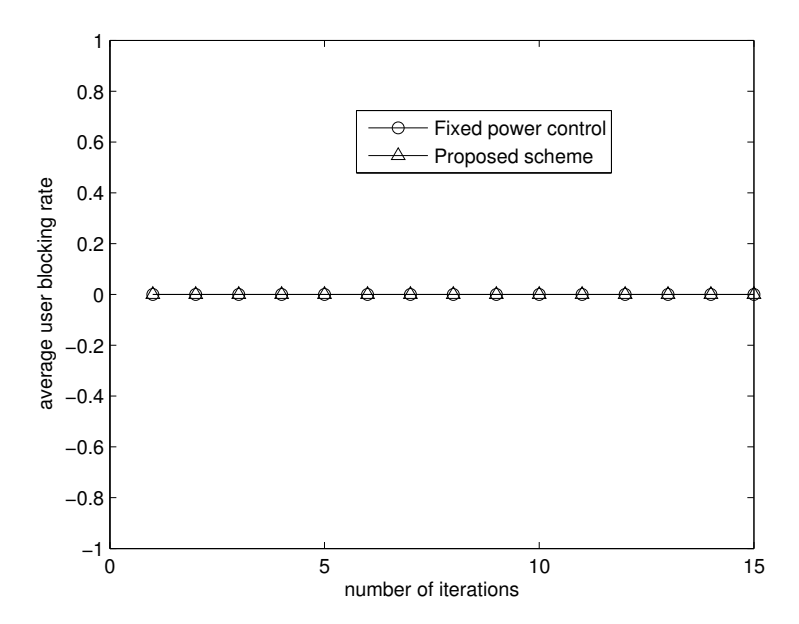


**Figure 5.10:** Average user blocking rate in terms of number of Iterations. (10 available channels, 10 floors per building, 5 buildings per row, and 5 rows)

our proposed channel allocation scheme only sacrifices 2% average capacity comparing to using dynamic power control scheme.

# Chapter 6

# QoS-aware Spectrum Access for Cognitive Radio Mesh Networks

So far, we have investigated the resource optimization problem in one-hop wireless network topology, including macrocell networks in chapter 3 and 4, femtocell networks in chapter 5. In this chapter, we study the optimal channel and route selection problems in multi-hop cognitive radio mesh networks.

In CogMesh, secondary mesh routers (SMRs) can opportunistically utilize the primary licensed spectrum for the traffic of the secondary mesh users (SMUs). We study the QoS problems for real-time communication in CogMesh, where end-to-end delay should be less than a threshold. Moreover, different spectrum bands may have different quality in terms of SINR, due to the spatial, time, and frequency selective fading. SMRs may select an appropriate channel to achieve maximum data rate and minimum transmission latency. However, because of the uncertainty of the primary systems, the channels on use may have to be released frequently, and will cause packet loss and lots of retransmission incidents.

In this chapter, we formulate the optimization problem to select a route and determine the channels on each link to maximize the route availability, while guaranteeing the end-to-end transmission delay. We transform the non-linear programing problem as a variant of Multiple-Choice Knapsack Problem. We propose a channel and route selection scheme based on the Lagrangian methods, and a low-complexity heuristic scheme.

Numerical results show that our proposed method acts much better than the best SINR scheme and best channel availability scheme, in terms higher successful solution ratio, higher route availability. Our proposed method achieves quite close results to the optimization software MOSEK. The rest of the chapter is organized as follows. We introduce the system model in Section 6.1 and formulate the optimization problem in Section 6.2. In Section 6.3, we introduce the solution by Lagrangian relaxation. Then, we propose a low-complexity heuristic scheme in Section 6.4. In Section 6.5, we use matrix transformation so that optimization software such as MOSEK can be used to solve our problem. In Section 6.6, we evaluate the performance of our proposed scheme. Finally, we draw the conclusions in Section 6.7.

# 6.1 System model and assumptions

In this section, we describe the system model, introduce the channel model, analyze the end-to-end delay, and route availability due to PU's activities.

#### 6.1.1 System model

Suppose an SMU wants to transmit some data through the CogMesh to a user in the Internet as shown in Fig. 1.4. Since the communication bottleneck is CogMesh, we focus on the QoS from the SMR by which the SMU is attached to the secondary mesh gateway (SMG).

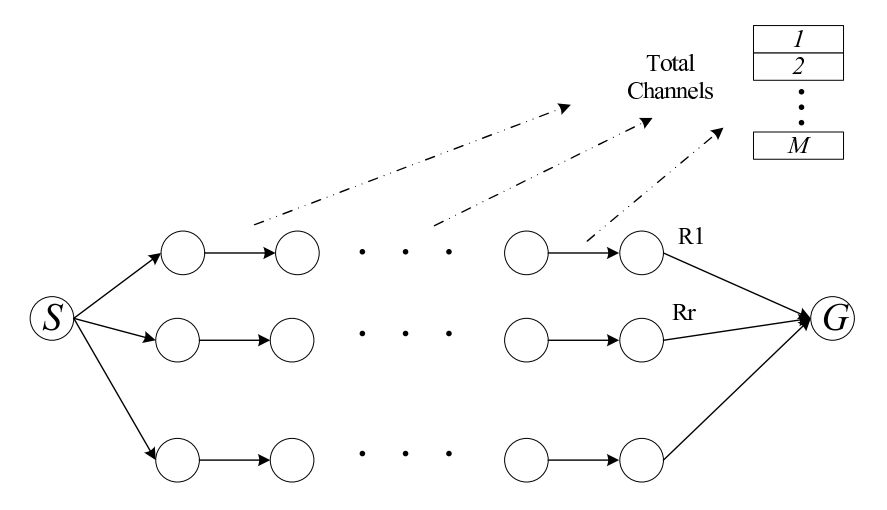


**Figure 6.1:** System model for route and channel selection in cognitive radio mesh networks

Figure 6.1 illustrates the system model, while Table 6.1 lists the main notations used in this chapter. In this model, there are sets of  $\mathcal{R}$  routes from the source SMR S to the gateway SMG G. For each route r ( $r = 1, ..., |\mathcal{R}|$ ), the set of nodes can be denoted as  $\mathcal{N}_r$  while the set of links can be denoted as  $\mathcal{L}_r$  ( $|\mathcal{L}_r| = |\mathcal{N}_r| - 1$ ).

The available spectrum can be characterized in a set of  $\mathcal{M}$  ( $\mathcal{M} \neq \emptyset$ ) channels. For each link l on route r, the available channels form a subset of  $\mathcal{M}$ , which can be denoted as  $\mathcal{M}_{rl}$  ( $\mathcal{M}_{rl} \in \mathcal{M}$ ). At any moment, each channel can be either free or occupied by the primary system. Thus, these  $\mathcal{M}$  channels are not always be available for every link, and the SMRs will stop working on the channel when PUs return. The SMRs will then either wait until the channel becomes free or switch to another free channel. We assume all SMRs and SMG are equipped with two radio transceivers. One is CR which can dynamically choose working channels. The other one is used for the control information exchange, wherein a dedicated narrow spectrum band may be allocated for this purpose.

**Table 6.1:** Table of notations for cognitive radio mesh networks

Symbol	Meaning
r	a route
l	a link
n	an SMR
m	a channel
$\mathcal{R}$	the set of routes
$\mathcal{L}_r$	the set of links for a given route $r \in \mathcal{R}$
$\mathcal{I}_{rl}$	the set of interfered links of $l$
$\mathcal{M}_{rl}$	the set of channels of link $l$ on route $r$
$\mathcal{N}_r$	the set of SMRs on route $r$
L	the packet length
D	the packet end-to-end delay threshold
$B_m$	the spectrum bandwidth of channel $m$
$d_{i,j}$	the distance between SMR $i$ and $j$
$\lambda_{rlm}$	the transmission rate on channel $m$ of link $l$ on route $r$
$x_{rlm}$	the binary indicator of channel $m$ at link $i$ on route $r$
$v_{rlm}$	the channel availability of channel $m$ at link $l$ on route $r$
$\Gamma_k$	the $k$ -th SINR threshold

# 6.1.2 Channel model and adaptive modulation coding

Different channels at the same link may have different channel fading parameters, interference, and spectrum bandwidth, while the same channel may have different channel fading parameters and interference on different links.

We assume that the transmission power is fixed during the data transmission. Therefore, the received SINR on each link of the CogMesh will be a variable. According to different SINR, the modulation scheme used in this channel can be different. Higher modulation scheme and wider spectrum bandwidth can bring out higher data transmission rate and low transmission latency. We assume that the channel fading is slow fading, which means that the channel quality will not change fast in a certain area. Therefore, each channel between two neighbor SMRs has a fixed quality for a holding time.

We consider the time and frequency selective slow fading channels, and use the Finite-State Markov Channel (FSMC) model [112] to represent of the dynamic state of the wireless channel. Assume that all channels have K+1 states. In each state, the received SINR is different. We define  $\Gamma_k$  (k=0,1,...,K) as the lower bound threshold of the state k, where  $0=\Gamma_0<\Gamma_1<...<\Gamma_K<\Gamma_{K+1}=\infty$ . We say link  $e_i$  is in state k, if the SINR is between  $\Gamma_k$  and  $\Gamma_{k+1}$ .

AMC technique is used in our system model to adaptively change the modulation scheme according to the quality of the channel. Where, channel's quality can be estimated by the SINR measured on the receiving node. Different modulation schemes can bring out different data transmission rate.

For a K+1 state wireless channel with the bandwidth of  $B_0$ , we can employ K types of modulation schemes. For any modulation scheme k (k = 1, ..., K), the data transmission rate is  $\lambda_k$ , while the SINR threshold is  $\Gamma_k$ . Without loss of generality, let the sequence of  $\Gamma_1$  to  $\Gamma_K$  be of increasing order. Therefore, the data rate function can be defined as follows in equation (6.1).

$$f(\xi, B_0) = \begin{cases} 0 & \text{if } \xi < \Gamma_1 \\ \lambda_1 & \text{if } \Gamma_1 \le \xi < \Gamma_2 \\ \lambda_2 & \text{if } \Gamma_2 \le \xi < \Gamma_3 \\ \dots & \dots \\ \vdots & \dots \\ \lambda_k & \text{if } \xi \ge \Gamma_k \end{cases}$$

$$(6.1)$$

According to Shannon's channel capacity formula, the maximum data transmission rate is in directly proportional to the bandwidth. For any channel m with bandwidth  $B_m$  at any link l on route r, the data rate can be achieved as follows.

$$\lambda_{rlm} = \frac{B_m}{B_0} f(\xi_{rlm}, B_0) \tag{6.2}$$

We employ a binary variable  $x_{rlm}$   $(x_{rlm} \in \{0,1\}, \forall r \in \mathcal{R}; \forall l \in \mathcal{L}_r; \forall m \in \mathcal{M}_{rl})$  to indicate whether channel m is selected for the link l on route r or not. If  $x_{rlm}$  is equal to 1, channel m is selected for the link l on route r, 0

otherwise. Therefore, the transmission data rate for link l on route r, can be described as follows.

$$\lambda_{rl} = \sum_{m \in \mathcal{M}_{rl}} \lambda_{rlm} x_{rlm}, \quad \forall r \in \mathcal{R}; \forall l \in \mathcal{L}_r$$
 (6.3)

# 6.1.3 Interference-avoid channel selection for adjacent links

We assume the antenna equipped at each SMR is half-duplex, which means it can either transmit or receive data, but not both at the same time. The 1-hop neighbors can work in the same link, since they will not transmit data at the same time. But there exist other links which are in the interference range of the link. For example, suppose link  $l_i$  and  $l_j$  work on the same channel, we call link  $l_i$  is interfered by  $l_j$  if SMR i + 1 is in the interference range of SMR j (as shown in Fig. 6.2).

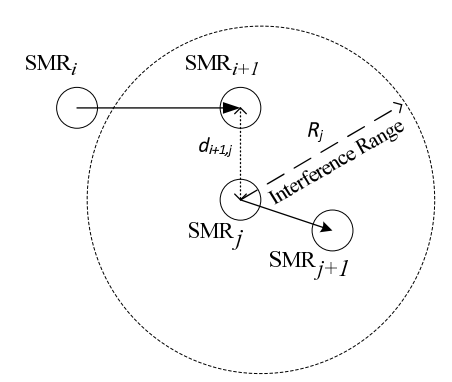


**Figure 6.2:** An illustration of interfered links

Suppose the distance between i+1 and j is  $d_{i+1,j}$ , the interference range of j is  $R_j$ . Thus, if  $d_{i+1,j} \leq R_j$ , node i+1 is in the interference area of j. Following the scheduling method in [94], we do not allow the interference links work on the same channel at the same time. Specially, we can assign different channels for link  $l_i$  and  $l_j$ .

## 6.1.4 End to end delay

We focus on the delay caused inside CogMesh, without considering the delay from the source SMU to its nearby source SMR, and the delay from SMG to the user in the Internet. The average end to end delay for route r consists of the queueing and transmission delay  $D_{r,t}$  on each link along the route, and

#### QoS-aware Spectrum Access for Cognitive Radio Mesh Networks

channel switching delay  $D_{r,s}$  at each intermediate SMRs. Thus, the end to end delay is as follows.

$$D_r = D_{r,t} + D_{r,s} (6.4)$$

Subsequently, we give the expressions of  $D_{r,t}$  and  $D_{r,s}$ .

#### Queueing and transmission delay

Suppose the average queue length (number of packets buffered) is  $Q_{rl}$  for link l on route r, and the average delay for for a packet to deliver on channel m at link l on route r is  $D_{rlm}$ .

$$D_{r,t} = \sum_{l \in \mathcal{L}_r} (Q_{rl} + 1) \sum_{m \in \mathcal{M}_{rl}} D_{rlm}$$

$$\tag{6.5}$$

In [91], the authors presented a closed form for the queueing and transmission delay for wireless mesh networks using 802.11 distributed coordination function (DCF) MAC protocol, considering inter-flow and intra-flow interference. According to [91], the average queueing and transmission delay in wireless mesh networks can be expressed as follows.

$$D_{rlm} = \frac{L}{\lambda_{rlm}} \left[ \frac{1 - \alpha_{rlm}^{N_{rlm}}}{1 - \alpha_{rlm}} \right] + B_{rlm}$$
 (6.6)

where, for any channel m at link l on route r,  $N_{rlm}$  is the maximum number of retransmissions,  $\alpha_{rlm}$  is the transmission failure probability, and assume it is stable during the retransmissions of the packet [91], and  $B_{rlm}$  is the back off delay.

$$B_{rlm} = \left(\frac{W_{min}[1 - (2\alpha_{rlm})^{N_{rlm}+1}]}{2(1 - 2\alpha_{rlm})} - \frac{1 - \alpha_{rlm}^{N_{rlm}}}{2(1 - \alpha_{rlm})}\right)$$
(6.7)

where  $W_{min}$  is the minimal contention window.

#### Channel switching delay

Channel switching delay caused at intermediate SMRs where the upstream link and downstream link work on different channels. Let  $D_{s0}$  denote the switching delay at one SMR from one channel to another. For example, in IEEE standard 802.11-2007, the switching delay is defined as  $224\mu s$  [113].

Assume each SMR can finish receiving all buffered packets before it starts forwarding to its next SMR. Thus, channel switching only happens at most once for a given SMR during a packet travels on the route. Then, the total

switching delay accumulated by all the SMRs on the route r to SMG can be calculated as follows.

$$D_{r,s} = \sum_{l \in \mathcal{L}_r} D_{s,l}$$

$$= D_{s0} \sum_{j=i+1; i,j \in \mathcal{L}_r} \sum_{m \in \mathcal{M}} \frac{|x_{rim} - x_{rjm}|}{2}.$$
(6.8)

where  $D_{s,l}$  denotes the switching delay on the SMR where link l is the incoming link.

#### 6.1.5 Route availability

We consider the route availability in the CogMesh from the source SMR to the SMG. In CogMesh, routes become unavailable mostly in the case when SMRs are working on channels where PUs return. We employ *channel availability* to distinguish the difference of PUs' activities on different channels. The channel availability of channel m at link l on route r can be defined as follows.

$$v_{rlm} = \frac{E(T_{rlm}^I)}{E(T_{rlm}^I) + E(T_{rlm}^B)}, \quad \forall l \in \mathcal{L}_r, m \in \mathcal{M}.$$
 (6.9)

where  $T^I_{rlm}$  and  $T^B_{rlm}$  represent the idle and busy time of primary user on channel m at link l on route r, respectively. Higher channel availability also indicates lower transmission error and packet loss rate.  $E(T^I_{rlm})$  and  $E(T^B_{rlm})$  represent the mean value of idle and busy time, respectively. The channel availability is measured periodically, and will update accordingly.

Assume each link can only work on one channel. Let  $v_r$  denote the end to end route availability from SMR to the SMG on route r, we can obtain

$$v_r = \prod_{l \in \mathcal{L}_r} \left( \sum_{m \in \mathcal{M}_{rl}} v_{rlm} x_{rlm} \right) \tag{6.10}$$

where  $x_{rlm}$  is a 0-1 binary variable, which indicates the channel selection strategy for channel m at link l on route r. Since we assume only one channel is used for a given link, we have

$$\sum_{m \in \mathcal{M}_{rl}} x_{rlm} = 1, \quad \forall l \in \mathcal{L}_r; r \in \mathcal{R}$$

#### 6.2 Problem formulation

In this section, we formulate the optimization problem to maximize route availability while considering the end-to-end delay and interference constraints between neighbouring links.

#### 6.2.1 Formulation of route and channel selection

For any route r ( $r \in \mathcal{R}$ ), we formulate a channel selection problem to maximize route availability while guaranteeing the end-to-end delay and interference constraints. We assume that any link l ( $l \in \mathcal{L}_r$ ) has at least one channel that can be used. The problem we study is how does every link choose an optimal channel for data transmission. This decision process may happen in the following cases. 1), When the source SMR wants to start a new session of data transmission. 2), When any SMR has to stop transmission on a channel because of PUs' return. 3), When the channel quality varies and affect the end-to-end delay. Hence, the problem is formulated as follows:

P1

maximize 
$$v_r$$
 (6.11)

subject to:

$$D_r \le D \tag{6.12}$$

$$\sum_{m \in \mathcal{M}_{rl}} x_{rlm} = 1, \quad \forall l \in \mathcal{L}_r$$
 (6.13)

$$\sum_{i \in \mathcal{I}_{rl}} x_{rim} + x_{rlm} \le 1, \quad \forall l \in \mathcal{L}_r; m \in \mathcal{M}_{rl};$$
(6.14)

$$x_{rlm} \in \{0, 1\}, \quad \forall l \in \mathcal{L}_r; m \in \mathcal{M}_{rl}.$$
 (6.15)

where D is the required delay threshold. Constraint (6.12) represents the end-to-end delay can not exceed the threshold D. Constraint (6.13) indicates that each link should work on one and only one data channel. Constraint (6.14) means the link in interference range area can not work on the same channel. The solution is to find out every  $x_{rlm}$  ( $\forall l \in \mathcal{L}_r, m \in \mathcal{M}_{rl}$ ), so that all the constraints are satisfied and the objective function  $v_r$  is maximized. Since  $v_r$  is nonlinear function to  $x_{rlm}$ , the formulated problem is a nonlinear integer problem.

After we select channels for all possible routes, we would finally select one route with the maximum route availability with PUs, while the end-to-end delay is guaranteed.

$$r^* = \arg\max_{r \in \mathcal{R}} v_r \tag{6.16}$$

We can also use the above metric to select multiple routes as backup routes.

Note, the channel and route selection scheme should update periodically according to periodical measure results of availability on each channel as well as the channel quality.

#### 6.2.2 Problem transformation

The formulated nonlinear problem can be transformed into linear by the following methods.

#### Transform the nonlinear objective function into linear form

Using the monotonously increased function ln, we can transform the objective function from  $\prod$  to  $\sum$ . The deduction is as follows.

In consequence, we can reformulate the objective function (6.11) in P1 as follows:

maximize 
$$\sum_{l \in \mathcal{L}_r} \sum_{m \in \mathcal{M}_{rl}} v_{rlm} x_{rlm}$$
 (6.17)

#### Transform the nonlinear constraint into linear form

Substituting (6.4) and (6.5) into (6.12), we have

$$\sum_{l \in \mathcal{L}_r} (Q_{r,l} + 1) \sum_{m \in \mathcal{M}_{rl}} D_{rlm} x_{rlm} + D_{r,s} \le D$$

$$(6.18)$$

For the channel switching delay  $D_{r,s}$  along the route r, we consider the worst case where each adjacent link works in different channels. Therefore,

$$D_{r,s} = D_{s0}(|\mathcal{L}_r| - 1) \tag{6.19}$$

which is a constant for the variable  $x_{rlm}$ . The benefit of this worst case consideration can result in a more reliable solution for channel selection. The reason is as follows: channels may change during the flow transmission, the number of switching channels may vary. If we can guarantee the worst case channel switching delay, it is believed that our solution is feasible for all the cases.

Substituting (6.19) into (6.18), we have

$$\sum_{l \in \mathcal{L}_r} (Q_{rl} + 1) \sum_{m \in \mathcal{M}_{rl}} D_{rlm} x_{rlm} \le D - D_{s0}(|\mathcal{L}_r| - 1)$$
 (6.20)

Moreover, we introduce positive variable  $w_{rlm}$  to denote the coefficient in the modified objective function and constraint function as follows.

$$w_{rlm} = \frac{(Q_{rl} + 1)D_{rlm}}{D - D_{s0}(|\mathcal{L}_r| - 1)}, \quad \forall l \in \mathcal{L}_r; m \in \mathcal{M}_{rl}$$

$$(6.21)$$

For any channel m in link l on route r, the analog meaning of  $v_{rlm}$  is the value (profit), while the meaning of  $w_{rlm}$  is the weight (cost). Therefore, the nonlinear constraint (6.12) changes into a linear constraint. Thus, the original non-linear problem can be reformulated as the following linear programming problem. The re-transformed problem can be defined as follows.

P2

Maximize 
$$\sum_{l \in \mathcal{L}_n} \sum_{m \in \mathcal{M}_{nl}} v_{rlm} x_{rlm}$$
 (6.22)

Subject to:

$$\sum_{l \in \mathcal{L}_r} \sum_{m \in \mathcal{M}_{rl}} w_{rlm} x_{rlm} \le 1 \tag{6.23}$$

$$\sum_{m \in \mathcal{M}_{rl}} x_{rlm} = 1, \quad \forall l \in \mathcal{L}_r \tag{6.24}$$

$$\sum_{i \in \mathcal{I}_{rl}} x_{rim} + x_{rlm} \le 1, \quad \forall l \in \mathcal{L}_r; m \in \mathcal{M}_{rl}$$
(6.25)

$$x_{rlm} \in \{0, 1\}, \quad \forall l \in \mathcal{L}_r; m \in \mathcal{M}_{rl}.$$
 (6.26)

This is a 0-1 integer linear problem, which is in general NP-complete [114]. Moreover, without constraint (6.25), this problem can be viewed as an instance of Multiple-Choice Knapsack Problem, where we have  $|\mathcal{L}_r|$  mutually disjoint classes (links) of items (channels) to be packed into a knapsack of capacity 1. Each item m ( $m \in \mathcal{M}_{rl}$ ) has a profit  $v_{rlm}$  and a cost  $w_{rlm}$ . The problem is to choose exactly one item from each class such that the total profit is maximized without exceeding the capacity. In addition, the item in interfered classes should be varied from each other.

# 6.3 Solutions from Lagrangian relaxations

By introducing the Lagrangian multipliers p ( $p \ge 0$ ), we can get the Lagrangian as follows

$$L_{1}(p) = \sum_{l \in \mathcal{L}_{r}} \sum_{m \in \mathcal{M}_{rl}} v_{rlm} x_{rlm} + p \left( 1 - \sum_{l \in \mathcal{L}_{r}} \sum_{m \in \mathcal{M}_{rl}} w_{rlm} x_{rlm} \right)$$

$$= \sum_{l \in \mathcal{L}_{r}} \sum_{m \in \mathcal{M}_{rl}} \beta_{rlm} x_{rlm} + p$$
(6.27)

where

$$\beta_{rlm} = v_{rlm} - pw_{rlm} \tag{6.28}$$

In this chapter, we call  $\beta_{rlm}$  the Lagrangian price. The Lagrangian relaxed problem is

P3

$$Z_{L_1}(p) = \max L_1(p) \tag{6.29}$$

s.t. (6.24), (6.25), and (6.26).

All feasible solutions to P2 are also feasible solutions to P3. Given an optimal solution set of  $\{x_{rlm}^*\}$  for P2, we have

$$Z_{L_1}(p) = \sum_{l \in \mathcal{L}_r} \sum_{m \in \mathcal{M}_{rl}} v_{rlm} x_{rlm}^* + p \left( 1 - \sum_{l \in \mathcal{L}_r} \sum_{m \in \mathcal{M}_{rl}} w_{rlm} x_{rlm}^* \right)$$

$$\geq \sum_{l \in \mathcal{L}_r} \sum_{m \in \mathcal{M}_{rl}} v_{rlm} x_{rlm}^*$$

$$= Z$$

$$(6.30)$$

#### QoS-aware Spectrum Access for Cognitive Radio Mesh Networks

Therefore,  $Z_{L_1}(p)$  is an upper bound for Z. This bound can be derived by choosing the channel with the maximum Lagrangian price  $\beta_{rlm}$  in each link, and by checking the constraint (6.25). The corresponding solution is  $x_{rlm} = 1$  for  $m = \arg \max_{m \in \mathcal{M}_{rl}} \beta_{rlm}$  and 0 otherwise. The tightest bound can be found by solving the Lagrangian dual problem.

$$Z_{LD} = \min_{p \ge 0} Z_{L_1}(p) \tag{6.31}$$

The Lagrangian dual problem  $Z_{LD}$  yields the minimum upper bound from all Lagrangian relaxations. It can be stated as a linear programming problem to find an optimal vector of multipliers p.

For the Lagrangian multiplier v, we can use a subgradient method to update it as follows.

$$p_{k+1} = \left[ p_k + t_k \left( 1 - \sum_{l \in \mathcal{L}_r} \sum_{m \in \mathcal{M}_{rl}} w_{rlm} x_{rlm}^* \right) \right]^+$$
 (6.32)

where  $x_{rl^*m}$  is an optimal solution to P3 and  $t_k$  is a positive scalar step size, which can be set as follows according to [115],

$$t_{k} = \frac{\Delta_{k}(Z^{*} - Z_{L_{1}}(p_{k-1}))}{\left\|1 - \sum_{l \in \mathcal{L}_{r}} \sum_{m \in \mathcal{M}_{rl}} w_{rlm} x_{rlm}^{*}\right\|^{2}}$$
(6.33)

where  $\Delta_k$  is a positive scalar satisfying  $\Delta_k \in (0,2]$ .  $Z^*$  is a upper bound on  $Z_{L_1}$ . Since any feasible solution of P2 serves as an upper bound on P2, and can also used as the upper bound of  $Z_{L_1}$ .  $\Delta_k$  is often determined by setting  $\Delta_0 = 2$  and halving  $\Delta_k$  whenever  $Z_{L_1}(p)$  has failed to decrease in some fixed number of iterations.  $p_0 = 0$ .

For each link l, the channel selection procedure can work in a sequential and cooperative way. It can also be extended to simultaneous and independent ways by different interference avoidance schemes.

In our strategy, the link with maximum  $\beta_{rlm}$  will be selected to use channel m, any other link l' in the interfered range will remove its channel m, and delete the  $\beta_{rl'm}$  accordingly. Subsequently, we follow this process until all the links allocate a channel without interfering with each other. The detailed algorithm is shown in Algorithm 9.

Let  $M_r$  denote the sum of number of channels for all links on route r.

$$\hat{M}_r = \sum_{l \in \mathcal{L}_r} |\mathcal{M}_{rl}|$$

**Algorithm 9** Channel selection scheme for route r with Lagrangian Methods Input:  $\{\mathcal{L}_r\}, \{\mathcal{M}_{rl}\}, \{v_{rlm}\}, \{w_{rlm}\}.$ Output:  $\{x_{iim}\}$ . 1: Initialize  $k = 0, \Delta_0 = 2 p_0 = 0$ 2: Calculate the upper bound  $Z^*$ while Not Converged do Update p according to (6.32). 4: while  $\mathcal{L}_r \neq \emptyset$  do 5: for each link  $l \in \mathcal{L}_r$  do 6: for each available channel m do7: 8:  $\beta_{rlm} \leftarrow v_{rlm} - pw_{rlm}$  $\triangleright$  According to (6.28) 9: end for Find the maximum  $\beta_{rlm}$  on each link l. 10: 11: end for Find the link  $l^*$  and channel  $m^*$  with maximum  $\beta_{rlm}$  over all links. 12:  $\triangleright$  Assign channel  $m^*$  for link  $l^*$ 13: Remove channel  $m^*$  for the interfering links 14:  $\mathcal{L}_r \leftarrow \mathcal{L}_r - l^*$ 15: end while 16: Get the value of  $Z_{L_1}(p)$ 17: 18: Update  $t_k$  according to (6.33).

Assume it can be terminated in  $N_I$  iterations. In each iterative, it spends  $O(\hat{M}_r)$  to get an optimal solution. Therefore, the total time complexity is  $O(N_I \hat{M}_r)$ .

19: end while

This is the solution for the Lagrangian dual problem P3. There may be a duality gap between P3 and P2. Therefore, to obtain the optimal solution for P2, we need to combine the Lagrangian methods with other techniques, such as branch-and-bound, and dynamic programming. For example, the Lagrangian methods can be used to calculate the lower bound for each branching in branch-and-bound method.

# 6.4 Low-complexity heuristic channel selection schemes

In this section, we propose a heuristic channel selection scheme for a given route r, and then choose the route with maximum route availability. We also introduce two alternative channel selection schemes in the end of this section.

#### 6.4.1 Proposed channel selection scheme

For any link l in route r, we sort the channels according to increasing weights  $w_{rlm}$ , and derive  $\mathcal{M}_{rl}^*$ . Therefore, the index of channels in  $\mathcal{M}_{rl}^*$  is different from that in  $\mathcal{M}_{rl}$ . We then construct an instance of knapsack by setting

$$\tilde{v}_{rlm} = v_{rlm} - v_{rl,m-1}, \forall l \in \mathcal{L}_r, m = 2, 3, ..., |\mathcal{M}_{rl}^*|.$$

and

$$\tilde{w}_{rlm} = w_{rlm} - w_{rl,m-1}, \forall l \in \mathcal{L}_r, m = 2, 3, ..., |\mathcal{M}_{rl}^*|.$$

and the residual capacity is

$$\bar{c} = 1 - \sum_{l \in \mathcal{L}_r} w_{rl1}$$

If  $\bar{c}$  is less than 0 at this step, it indicates there is no solution, because  $w_{rl1}$  is already the minimal weight from every link l.

If  $\bar{c}$  is non-negative, we need to check the interference constraints. The method is to see if any two interfering links use the same channel. We need to replace the channels by interfering links and check  $\bar{c}$  again. After we get rid of the interference constraints and  $\bar{c}$  is still non-negative, we sort all the link-channel pair according to decreasing incremental efficiencies defined as follows.

$$\tilde{\eta}_{rlm} = \frac{\tilde{v}_{rlm}}{\tilde{w}_{rlm}} \tag{6.34}$$

We then fill the knapsack up to capacity  $\bar{c}$  according to the order of the link-channel pair sorting in terms of incremental efficiencies  $\tilde{\eta}_{rlm}$ . Capacity constraint and interference constraints are checked before adding a link-channel pair. After adding a link-channel pair, the channel  $m^*$  used in this link  $l^*$  is marked as inactive from any interfering links  $\mathcal{I}_{rl^*}$ , and the previous channel m' from the same link  $l^*$  in the knapsack is taken out, which means  $x_{rl^*m'}=0$ , and channel m' in interfering links  $\mathcal{I}_{rl^*}$  is marked as active. The residual capacity  $\bar{c}$  updates as follows.

$$\bar{c} = \bar{c} - \tilde{w}_{rlm}$$

Following this approach until either the capacity constraint is broken or no different channels can be assigned for interfering links. The channel selection for all links on route r is then finished. The details of this scheme is shown in Algorithm 10. The time complexity is  $O(\hat{M}_r)$ 

#### 6.4.2 Alternative channel selection schemes

In order to demonstrate the performance of our proposed channel selection scheme, we introduce the following two channel selection schemes.

**Algorithm 10** Proposed heuristic channel selection algorithm for a given route r in CogMesh

```
Input: r, \mathcal{L}_r, \mathcal{M}_{rl}.
Output: \{x_{ijc}\}.
 1: Initialization: \bar{c} \leftarrow 1
 2: Calculate w_{rlm}, v_{rlm}, \mu_{rlm} for all route link and channels.
 3: for l \in \mathcal{L}_r do
 4:
          Remove the channels where w_{rlm} > 1.
 5:
          Sort the channels according to increasing w_{rlm} and derive \mathcal{M}_{rl}^*.
          for i = 2; i \le |\mathcal{M}_{rl}^*|; i + + do
 6:
 7:
              \tilde{v}_{rli} \leftarrow v_{rli} - v_{rl,i-1}
              \tilde{w}_{rli} \leftarrow w_{rli} - w_{rl,i-1}
 8:
          end for
 9:
          \bar{c} \leftarrow \bar{c} - w_{rl1}
10:
11: end for
12: if \bar{c} < 0 then
          Return;
                                                                   \triangleright No solution in this case.
13:
14: end if
15: Sort the link-channel pairs according to decreasing incremental efficien-
     cies \tilde{\eta} according to (6.34).
16: while Interfering links use the same channel do
          Adjust channels for interfering links, update \bar{c}
18: end while
19: if \bar{c} < 0 then
          Return;
                                                                   \triangleright No solution in this case.
20:
21: end if
22: while 1 do
          while Interfering links use the same channel do
23:
              Reselect another link-pair \{l^*, m^*\}.
24:
25:
          end while
         \bar{c} \leftarrow \bar{c} - \tilde{w}_{rl*1}
26:
         if \bar{c} < 0 then
27:
              Return;
                                                                  \triangleright Has solution in this case.
28:
29:
          else
              Record the old channel index m' for link l^* in the knapsack.
30:
              Mark channel m' for all the interfering links as active.
31:
32:
              x_{rl^*m'} \leftarrow 0
              Mark channel m^* for all the interfering links as inactive.
33:
              x_{rl^*m^*} \leftarrow 1
34:
              \{l^*, m^*\} \leftarrow \arg\max_{l \in \mathcal{L}_r, m \in \mathcal{M}_{rl}^*}
                                                            ▷ Get the index of link-channel
35:
     pair with the maximal \tilde{\eta}
         end if
36:
                                                 123
37: end while
```

#### Channel selection with best SINR

In this method, every node selects the channel with maximum SINR which can achieve highest data transmission rate, without considering the channel availability. The similar scheme was used in [90] to verify their proposed scheme.

In our scenario, we describe the scheme with best SINR as follows. For each route r, the link  $l^*$  with maximum SINR among all other links select its channel  $m^*$  first. The interfering links will remove  $m^*$  from their channel table. Follow this procedure, until every link selects a channel. We repeat it for all other routes. Finally, the route  $r^*$  with maximum sum of channel availability will be selected. In the later performance evaluation, we denote this scheme as best-SINR for short.

#### Channel selection with best availability

In this method, every node selects the channel with maximum channel availability, without considering SINR and other factors. For each route r, the link  $l^*$  with maximum channel availability  $v_{rlm}$  is selected to use the channel  $m^*$ . The interfering links will remove  $m^*$ . Follow this procedure until every link selects a channel. We repeat it for all other routes. Finally, the route  $r^*$  with maximum sum of channel availability will be selected. In the later performance evaluation, we denote this scheme as best-availability for short.

# 6.5 Matrix transformation for problem solving by optimization software

Matrix form is used in calculation the optimal solution using optimization tools such as MOSEK [37] and CPLEX [98].

For any given route r,  $\mathbf{V}_{1 \times \hat{M}_r}$  denotes the profit matrix for all links and channels, while  $\mathbf{W}_{1 \times \hat{M}_r}$  denotes the cost matrix for all links and channels. Let  $\mathbf{H}_{\hat{M}_r \times \hat{M}_r}$  denote the interference matrix for all channels on all links on route r.

$$\mathbf{X}_{\hat{M}_r \times 1} = \begin{pmatrix} (x_{r11}, x_{r12}, ..., x_{r1|\mathcal{M}_{r1}|})^T, \\ (x_{r21}, x_{r22}, ..., x_{r2|\mathcal{M}_{r2}|})^T, \\ \vdots \\ (x_{r|\mathcal{L}_r|1}, x_{r|\mathcal{L}_r|2}, ..., x_{r|\mathcal{L}_r||\mathcal{M}_{r|\mathcal{L}_r|}|})^T \end{pmatrix}$$

$$\mathbf{G}_{|\mathcal{L}_r| \times \hat{M}_r} = \begin{pmatrix} (1, 1, ..., 1)_{1 \times |M_{r1}|} & (0, 0, ..., 0)_{1 \times |\mathcal{M}_{r2}|} & \cdots & (0, 0, ..., 0)_{1 \times |\mathcal{M}_{r|\mathcal{L}_r|}|} \\ (0, 0, ..., 0)_{1 \times |\mathcal{M}_{r1}|} & (1, 1, ..., 1)_{1 \times |\mathcal{M}_{r2}|} & \cdots & (0, 0, ..., 0)_{1 \times |\mathcal{M}_{r|\mathcal{L}_r|}|} \\ \vdots & \vdots & \ddots & \vdots \\ (0, 0, ..., 0)_{1 \times |\mathcal{M}_{r1}|} & (0, 0, ..., 0)_{1 \times |\mathcal{M}_{r2}|} & \cdots & (1, 1, ..., 1)_{1 \times |\mathcal{M}_{r|\mathcal{L}_r|}|} \end{pmatrix}$$

We introduce **A** to denote the joint matrix of  $\mathbf{W}_{1 \times \hat{M}_r}$  and  $\mathbf{H}_{\hat{M}_r \times \hat{M}_r}$ 

$$\mathbf{A}_{(\hat{M}_r+1) imes\hat{M}_r} = egin{pmatrix} \mathbf{H}_{\hat{M}_r imes\hat{M}_r} \ \mathbf{W}_{1 imes\hat{M}_r} \end{pmatrix}$$

maximize 
$$\mathbf{V}_{1 \times \hat{M}_r} \mathbf{X}_{\hat{M}_r \times 1}$$
  
subject to  $\mathbf{A}_{(\hat{M}_r+1) \times \hat{M}_r} \mathbf{X}_{\hat{M}_r \times 1} \leq 1$   
 $\mathbf{G}_{|\mathcal{L}_r| \times \hat{M}_r} \mathbf{X}_{\hat{M}_r \times 1} = \mathbf{1}_{|\mathcal{L}_r| \times 1}$   
 $\mathbf{x} \in \{0, 1\}$  (6.35)

In the following simulation study, we use MOSEK to get the optimal solution for the above problem.

# 6.6 Simulation results and analysis

We have implemented a CogMesh simulator on MATLAB platform. We consider a grid topology similar to the topology used in [91], where SMRs are uniformly placed. The interference range of any SMR is one hop.

Detailed simulation parameters are shown in Table 6.2. The number of available routes is 10. For each route, the number of hops changes from 2 to 10. For each link, the number of available channels changes from 2 to 10. We follow the AMC table in [90], where there are four modes shown in Table 6.3. Each channel on every link selects a data rate from  $\{11, 5.5, 2, 1\}$  Mbps according to the quality of that channel. We assume the traffic follows the constant bit rate with the packet size of 512 bytes. The maximum number of retransmissions  $K_{rlm}$  is randomly generated in [1, 5]. The slot time is  $20\mu s$ , while the minimum contention window size  $W_{min}$  is 0.2ms which is 10 slots. The channel availability  $v_{rlm}$  is randomly generated in [0.5,1]. For any given number of routes, hops, and channels, we randomly generated the parameters for 200 times.

To verify and compare the performance of our proposed scheme with best-SINR scheme, best-availability scheme, and optimal solution from MOSEK, we introduce the following definition of *successful solution ratio*.

Symbol Value Symbol Value  $B_0$ 10 MHz[0.5, 1] $v_{rlm}$  $T_{s0}$ 0.224ms $N_{rlm}$ [1, 5] $\overline{512}$  Bytes D40msL $W_{min}$ 0.2ms[0, 0.5] $\alpha$ 

**Table 6.2:** Simulation parameters for CogMesh

Table 6.3: AMC code rate and SINR table for CogMesh

[1, 10]

Data rate (Mbps)	11	5.5	2	1
SINR (dB)	$[8,+\infty)$	[6, 8)	[4, 6)	[0, 4)

Successful solution ratio Assume the total number of seeds for the simulation is  $N_{seed}^{max}$ . In each seed, there are  $|\mathcal{R}|$  different routes. We call a seed has a valid solution, if there is at least one solution from its  $|\mathcal{R}|$  different routes. Let  $N_{seed}^{valid}$  denote the sum of seeds with valid solution. The successful solution ratio is the ratio between  $N_{seed}^{valid}$  and  $N_{seed}^{max}$ .

successful solution ratio := 
$$\frac{N_{seed}^{valid}}{N_{seed}^{max}}$$
 (6.36)

In our simulation,  $N_{seed}^{max}$  is equal to 200, and  $|\mathcal{R}|$  is equal to 10. A higher successful solution ratio indicates a better channel selection scheme. In addition, we also present the results of route availability from all different channel selection schemes. Route availability is set to 0 for those seeds which can not get valid solutions. We calculate and compare the average route availability from all 200 seeds for all schemes.

## 6.6.1 Successful solution ratio

 $Q_l$ 

The successful solution ratio for all schemes are shown in Fig. 6.3 (3D visualization) and Fig. 6.4. Both figures show that best-availability scheme has the lowest successful solution ratio when the number of hops is more than 6. The reason is the best-availability scheme selects the channel with maximal channel availability for each link without considering the delay constraints. The solutions from best-availability scheme have higher chance to break the

delay constraints and result in invalid solutions. Our proposed scheme has similar successful solution ratio with best-SINR scheme, since both scheme take the delay constraints into account.

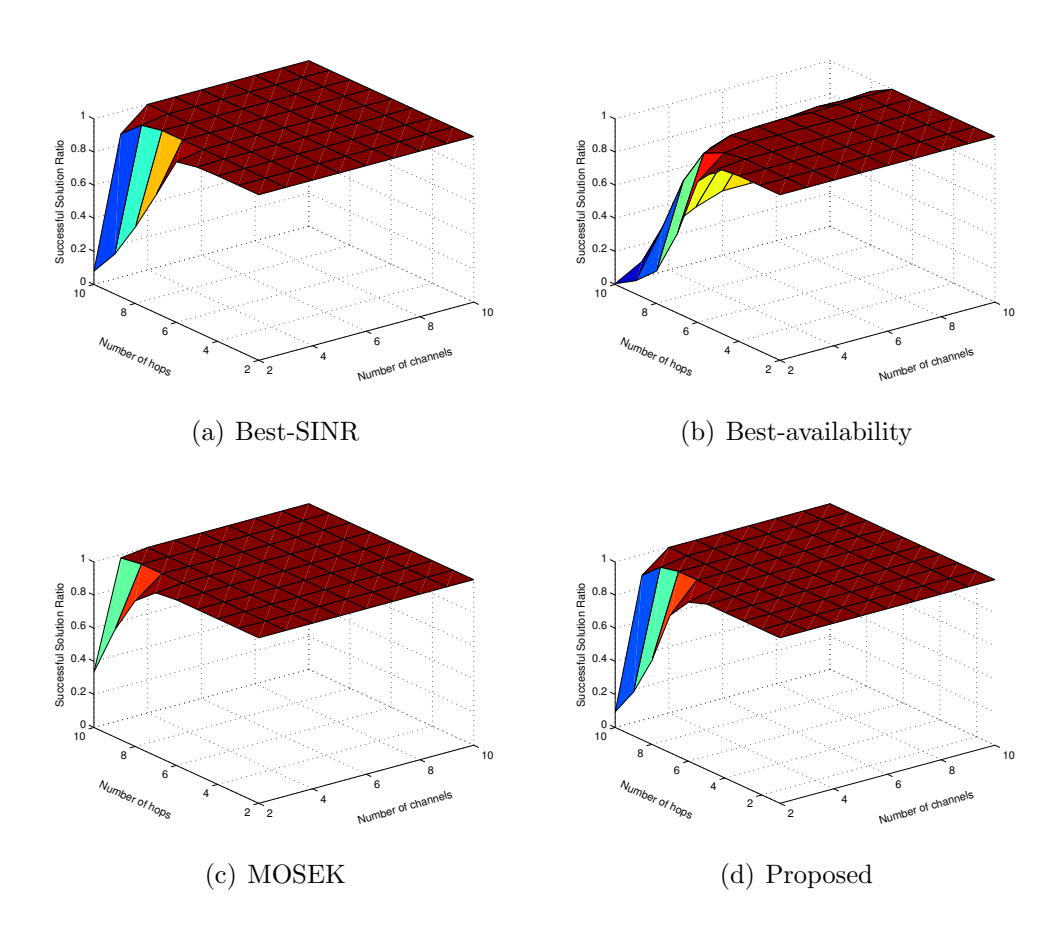


**Figure 6.3:** Successful solution ratio from different channel selection schemes (3D visualization)

Figure 6.4 shows that when there are 2 or 3 channels, our proposed scheme and best-SINR scheme achieve a bit lower successful solution ratio than the optimal solution from MOSEK. For both our proposed scheme and best-SINR scheme, the successful solution ratio starts dropping from 6 hops when there are only 2 channels, while it starts dropping from 9 hops when there are 3 channels. From the optimal solution, it starts dropping from 7 hops instead of 6 hops when there are 2 channels, and it starts dropping from 10 hops instead of 9 hops when there are 3 channels. When there are more than 3 channels, our proposed scheme and best-SINR scheme always have the same 100% successful solution ratio as the optimal solution from MOSEK.

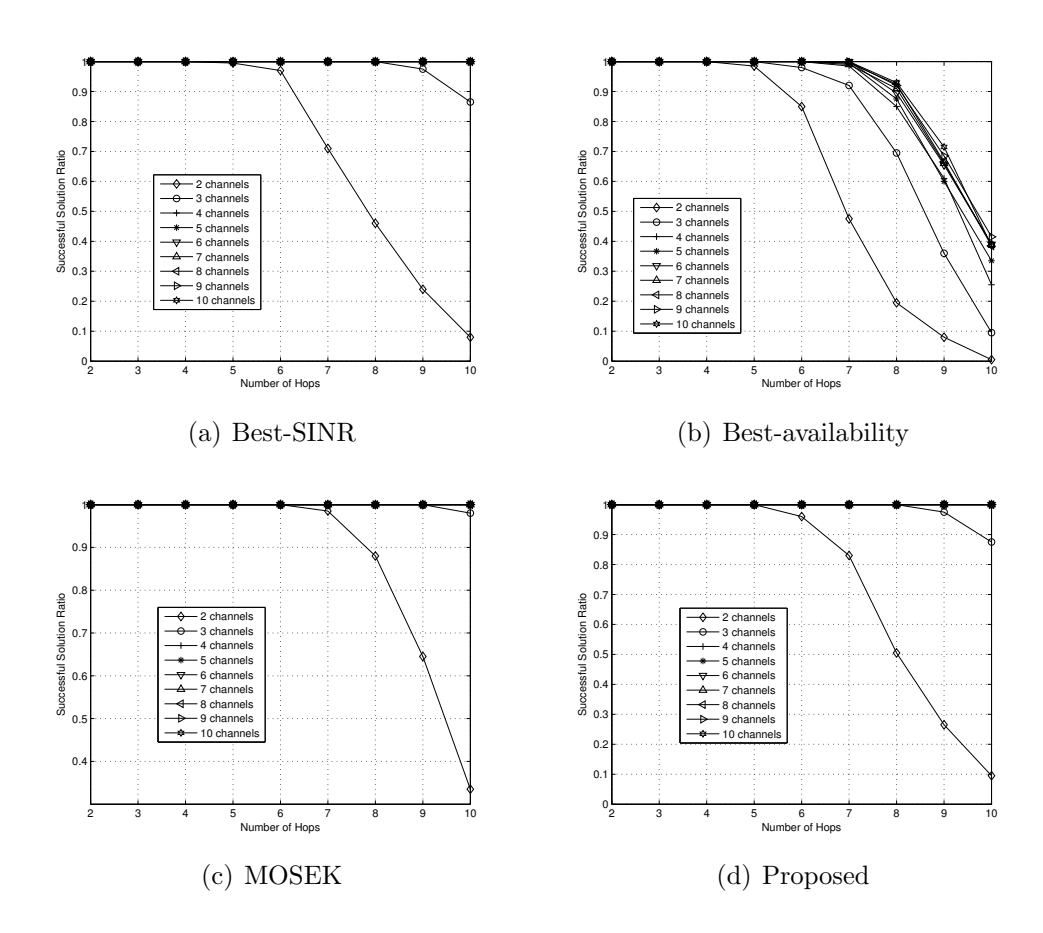


Figure 6.4: Successful solution ratio from different channel selection schemes

## 6.6.2 Route availability

The route availability for all schemes are shown in Fig. 6.5 (3D visualization) and Fig. 6.6. Both figures show that best-SINR scheme has the lowest route availability in all the cases. The reason is the best-SINR scheme selects the channel with maximal channel SINR for each link without considering the channel availability. The solutions from best-SINR scheme have higher chance to select channels with lower channel availability and result in lower route availability solutions.

From Fig. 6.5, we can see the route availability got from our proposed scheme has the closest pattern of the optimal solution from MOSEK comparing with the route availability from other two schemes.

From Fig. 6.6, we can see our proposed scheme achieves a bit lower route availability than the best-availability when there are less than 6 hops. However, the route availability got by the best-availability scheme drops faster

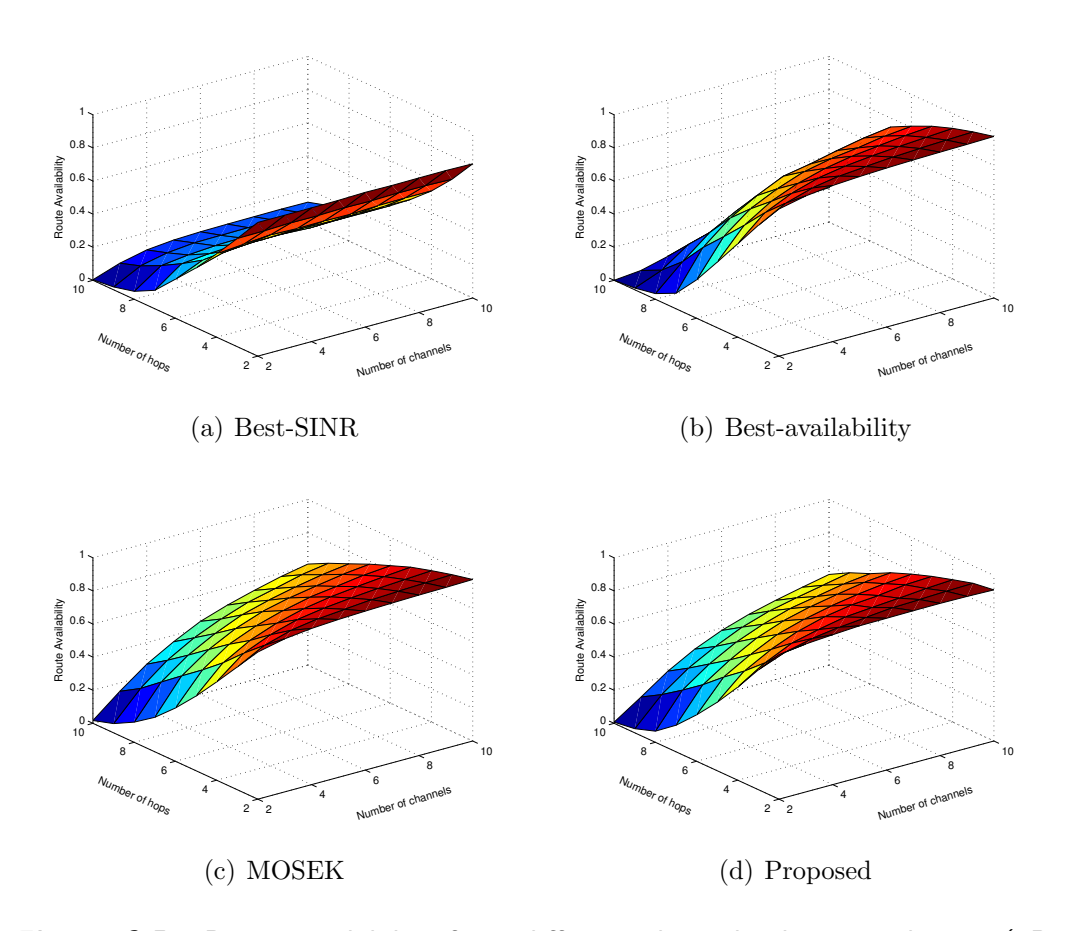


**Figure 6.5:** Route availability from different channel selection schemes (3D visualization)

than that got by our proposed scheme when the number of hops keeps increasing from 6 to 10. Our proposed scheme outperforms the best-availability scheme in case of longer hops (larger than 6). Moreover, the route availability achieved by our proposed scheme is closest to the optimal solution from MOSEK among all other three schemes in long hop cases.

## 6.7 Conclusion

In this chapter, we have investigated the real-time communication problem in CogMesh. We have formulated this problem of maximization the route availability, while guaranteeing the end-to-end delay from SMR to the gateway. We transformed the original non-liner integer programming problem to a linear integer programming problem. Then we modeled it as a vari-

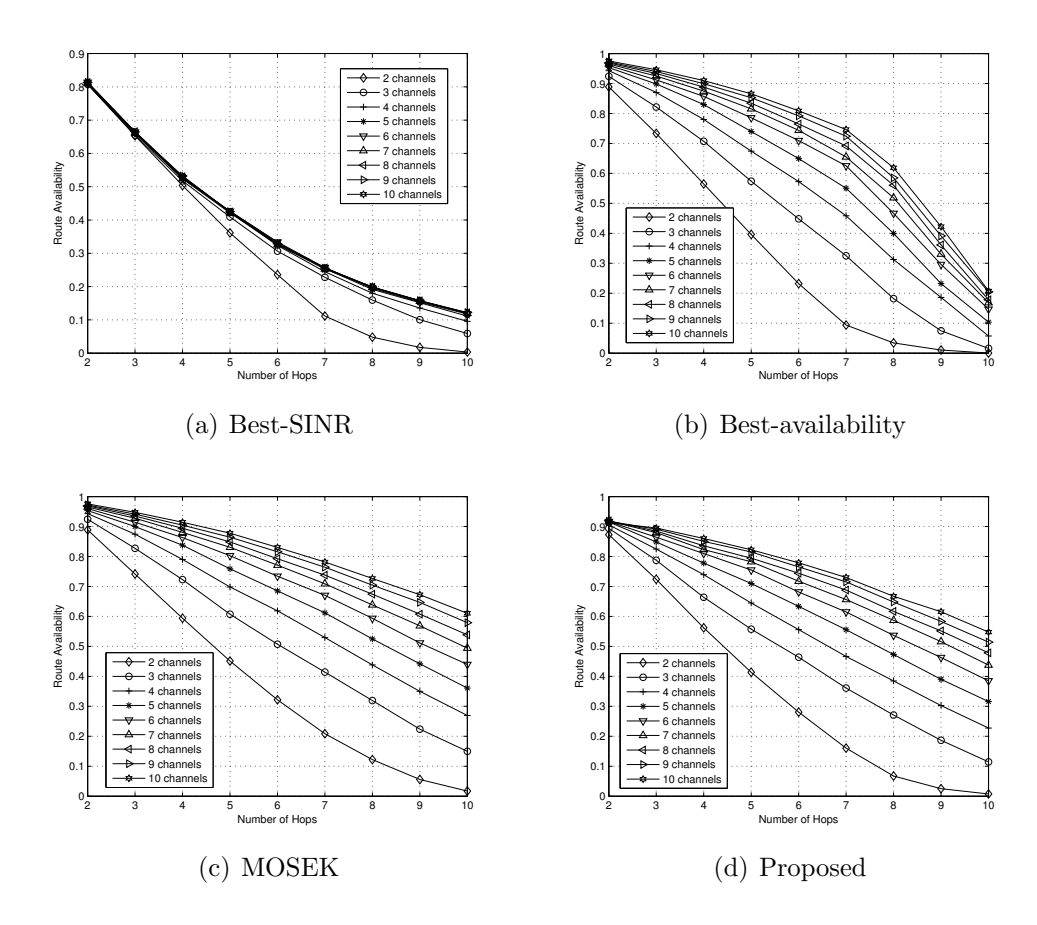


Figure 6.6: Route availability from different channel selection schemes

ant of the multiple-choice knapsack problem, and proposed a low-complexity heuristic algorithm to solve it. Simulation results showed that our proposed scheme achieved quite close successful solution ratio and route availability to the results from MOSEK, and outperformed the channel selection schemes based on best SINR and best channel availability schemes in terms of higher successful solution ratio and better route availability in most cases.

# Chapter 7

## Conclusion and Future Work

Throughout this thesis, we have studied the resource optimization problems in CogCell, CogFem, and CogMesh. Our contributions include the problem modeling, formulation, and solutions. Our work sheds a light on the future deployment of cognitive radio technology into cellular networks, femtocell networks, and mesh networks. In this chapter, we will draw our conclusions on both research scenarios and methods, and present the future work.

## 7.1 Conclusion

#### 7.1.1 On research scenarios

### Cognitive radio cellular networks

Firstly, we have addressed the admission and power control problem in one-channel CogCell. The objective is to maximize the secondary revenue to the operator, while guaranteeing the interference constraints on primary receivers. In addition, the QoS level in terms of data rate is satisfied for admitted SUs. In our earlier study, we proposed a joint admission and power control scheme using minimal revenue efficiency removal algorithm called JAPC-MKP to address the operator problem. In our later study, we further improved JAPC-MRER by reformulation and remodeling. The admission and power control problem is reformulated and remodeled as a MKP. Then, we propose a novel admission and power control scheme called JAPC-MKP which is heuristic with low complexity. Finally, simulation results show that our proposed JAPC-MKP can approach the optimal results from the optimization software MOSEK [37], and greatly outperform the previous fixed power scale JAPC-MRER schemes.

Secondly, we have studied the multi-channel CogCell scenario, where

channel allocation strategies need to consider in addition to admission and power control. We have the same objective as the one-channel CogCell case. But we have more resource in terms of number of channels. We formulate the joint channel allocation, admission and power control problem as a MINLP problem which is NP-hard in general. Then, we modeled it as a MMKP, and proposed a heuristic method to solve it. Our solution is quite close to MOSEK from the simulation results.

### Cognitive radio femtocell networks

In the scenario of CogFem, we have studied the spectrum sharing problem to maximize the total capacity of femtocell networks. We employed mixed primal and dual decomposition methods to solve the spectrum sharing problem. We also studied the robust optimization considering the worst case due to FUs' random movements. According to the solution of the decomposed problem, we proposed a joint channel allocation and power control scheme. Simulation results showed our proposed channel allocation scheme achieved much higher capacity and lower user blocking rate than traditional coloring method. Our proposed dynamic power control scheme can converge very fast. Using the fixed power control scheme together with our proposed channel allocation scheme achieves only 2% less capacity than the dynamic power control scheme.

#### Cognitive radio mesh networks

In the scenario of CogMesh, we have investigated the real-time communication problem. We formulated this problem of maximization the route availability, while guaranteeing the end-to-end delay from SMR to the gateway. We transformed the original non-liner integer programming problem to a linear integer programming problem. Then we modeled it as a variant of MCKP. Based on the MCKP modeling, we proposed a heuristic method to solve this problem. Simulation results showed that our proposed scheme achieved quite close successful solution ratio and route availability to the results from MOSEK, and outperformed the channel selection schemes based on best SINR and best channel availability schemes in terms of higher successful solution ratio and better route availability in most cases.

## 7.1.2 Comparison

### Overlay vs underlay spectrum sharing modes

Basically, the spectrum utilization efficiency is higher in the underlay spectrum sharing mode than that in the overlay spectrum sharing mode, because SUs in the underlay spectrum sharing mode can use the spectrum even PUs exist. The problem to solve in the underlay spectrum sharing mode is to carefully control the interference to primary receivers, so that the interference is not harmful to primary receivers, such as our study in CogCell. On the other hand, channel allocation strategy is very important in the overlay spectrum sharing mode. Where we need to take channel availability into account to design a most reliable route in CogMesh.

#### One-hop vs Multi-hop scenarios

In one-hop scenarios, we have two scenarios: CogCell and CogFem.

In CogCell, we need to consider the interference from SUs to primary receivers in the underlay spectrum sharing mode. In CogFem, we need to consider the interference between secondary femtocell base stations.

In multi-hop scenarios, the interference between neighbouring links in interference range should take into account. The end-to-end performance is more important than one hop performance in multi-hop scenarios.

### One-channel vs Multiple-channel scenarios

In one-channel scenarios, optimal power and admission control can achieve optimal revenue to secondary base station operators, while in multiple-channel scenarios, channel allocation strategies dominates power and admission control.

#### 7.1.3 On research methods

We have done our research by problem modeling and formulations. Then we design algorithms according to the solution of the optimization problem, and use our simulator based on MATLAB to verify the performance of our proposed algorithms. We also compare our solutions to optimization software MOSEK.

We have learnt from Chapter 3 that a proper problem modeling and formulation dominates the algorithm design and final performance. It is very important for problem solving and algorithm design. According to our earlier problem formulation, we proposed a joint admission and power control

Scenarios	Objective	Constraints	Modeling	Solutions
One-Channel	Secondary	Date rate, Inter-	MKP	Heuristic algo-
CogCell	revenue	ference, power	MIKI	rithm
Multi- Channel CogCell	Secondary revenue	Date rate, Interference, power	MMKP	Heuristic algorithm
CogFem	Sum of capacity	SINR, power	MINLP	primal and dual decomposition
CogMesh	Route availability	Delay, interference, power	Variant MCKP	Heuristic algorithm

Table 7.1: Summary of different scenarios

scheme using minimal revenue efficiency removal algorithm called JAPC-MKP to address the operator problem. We further improve JAPC-MRER by reformulation and remodeling our problem as a MKP. According to the solution of the reformulated problem, we proposed a novel admission and power control scheme called JAPC-MKP which is heuristic with low complexity. Simulation results show that our proposed JAPC-MKP can approach the optimal results from the optimization software MOSEK, and greatly outperform the previous fixed power scale JAPC-MRER schemes.

We summarize our methods as follows: Modeling and Formulation -> Re-Formulation -> Problem re-modeling to a kind of well studied problems (such as knapsack problems) -> design algorithms based on solutions to well studied problems (such as knapsack problems).

## 7.2 Future work

In future, there are several directions in the research of resource optimization in cognitive radio networks.

• Efficient way to get information of primary receivers

The information of primary receivers includes the geo-locations and interference threshold is quite important in resource optimization in cognitive radio networks. In [116], the authors introduced a primary receiver detection method by exploiting the local oscillator leakage power emitted by the RF front end of primary receivers.

In practice, this kind of information may be done by dedicated primary receiver detection server, cooperated with lots of sensors. Those

#### 7.2 Future work

information can be stored and the operator can use it while doing optimization. And this information should be updated regularly.

### • Extension to more objective functions

The objective we studied in this thesis includes secondary revenue, capacity, and route availability. In the future, we want to extend our studies into more objective functions, e.g., fairness.

#### • Demonstration on testbeds

So far we have verified our algorithms and schemes by simulations. In the future, it will be more helpful to implement our algorithms on testbeds. The testbed platforms can be GNU Radio [117] with USRP [118], WARP [119], and ASRP2 [120].

# **Bibliography**

- [1] "United States radio spectrum frequency allocations chart as of 2003." [Online]. Available: http://www.ntia.doc.gov/osmhome/allochrt.pdf
- [2] S. Haykin, "Cognitive radio: brain-empowered wireless communications," *IEEE Journal on Selected Areas in Communications*, vol. 23, no. 2, pp. 201 220, feb. 2005.
- [3] (2010) Fcc. [Online]. Available: http://www.fcc.gov/
- [4] (2010) Ecc. [Online]. Available: http://www.ero.dk/ECC1/
- [5] (2010) The norwegian post and telecommunications authority (npt). [Online]. Available: http://http://www.npt.no/
- [6] (2010) Ofcom. [Online]. Available: http://www.ofcom.org.uk/
- [7] (2008) TeliaSonera to build 4G next generationmobile network. http://www.teliasonera.com/News-and-Archive/Press-releases/2008/TeliaSonera-to-build-4G-next-generation-mobile-network/.
- [8] (2010) TeliaSonera has won a 4G license in Denmark. http://www.teliasonera.com/News-and-Archive/Press-releases/2010/TeliaSonera-has-won-a-4G-license-in-Denmark/.
- [9] (2009) Sonera wins 4G frequencies in the Finnish auction. http://www.teliasonera.com/News-and-Archive/Press-releases/2009/Sonera-wins-4G-frequencies-in-the-Finnish-auction/.
- [10] Federal Communications Commission Spectrum Policy Task Force. (2002, November) FCC Report of the Spectrum Efficiency Working Group. http://www.fcc.gov/sptf/files/SEWGFinalReport\_1.pdf.

- [11] Shared Spectrum Company, "Spectrum reports," http://www.sharedspectrum.com/papers/spectrum-reports/, January 2011.
- [12] M. A. McHenry and D. McCloskey, "Spectrum occupancy measurements: Chicago, illinois, november 16-18, 2005," Shared Spectrum Company, Tech. Rep., 2005.
- [13] T. Erpek, M. Lofquist, and K. Patton, "Spectrum occupancy measurements: Loring commerce centre, limestone, maine, september 18-20, 2007," Shared Spectrum Company, Tech. Rep., 2007.
- [14] S. S. Company, "Spectrum occupancy measurements: Chicago, illinois, september 1-5, 2009," Tech. Rep.
- [15] (2003) Cognitive Radio Technologies Proceeding (CRTP) ET Docket No. 03-108. http://www.fcc.gov/oet/cognitiveradio/.
- [16] (2004) ET Docket No. 04-186. http://www.fcc.gov/oet/projects/tvbanddevice/.
- [17] "IEEE 802.22/D1.0 Draft Standard for Wireless Regional Area Networks Part 22: Cognitive Wireless RAN Medium Access Control (MAC) and Physical Layer (PHY) Specifications: Policies and Procedures for Operation in the TV Bands," *IEEE Draft Standard* 802.22, April 2008.
- [18] J. Mitola and G. Maguire, "Cognitive radio: making software radios more personal," *IEEE Personal Communications*, vol. 6, no. 4, pp. 13–18, 1999.
- [19] I. F. Akyildiz, W.-Y. Lee, M. C. Vuran, and S. Mohanty, "Next generation/dynamic spectrum access/cognitive radio wireless networks: a survey," *Computer Networks*, vol. 50, no. 13, pp. 2127–2159, 2006.
- [20] (2009) TeliaSonera first in the world with 4G services. http://www.teliasonera.com/News-and-Archive/Press-releases/2009/TeliaSonera-first-in-the-world-with-4G-services/.
- [21] M. Ahmed, "Call admission control in wireless networks: a comprehensive survey," *Communications Surveys & Tutorials, IEEE*, vol. 7, no. 1, pp. 49–68, First Qtr. 2005.
- [22] M. Chiang, P. Hande, T. Lan, and C. W. Tan, Power Control in Wireless Cellular Networks Power Control in Wireless Cellular Networks. now Publishers Inc., May 2008.

- [23] (2007)Presentaions by ABI Research, Picochip, Airvana, IP.access, Gartner, Telefonica Espana, the 2nd Interna-Conference on Home Access Points and Femtocells. tional http://www.avrenevents.com/dallasfemto2007/purchase\_presentations.htm.
- [24] S. Higgins, C. Mah, and T. Anderson. (2009) Cisco medical-grade network (mgn) 2.0 wireless architectures. [Online]. Available: http://www.cisco.com/en/US/docs/solutions/Verticals/Healthcare/MGN\_wireless\_adg.pdf
- [25] V. Chandrasekhar, J. Andrews, and A. Gatherer, "Femtocell networks: a survey," *IEEE Communications Magazine*, vol. 46, no. 9, pp. 59–67, September 2008.
- [26] H. Claussen, L. T. W. Ho, and L. G. Samuel, "An overview of the femtocell concept," Bell Lab. Tech. J., vol. 13, no. 1, pp. 221–245, 2008.
- [27] C. Peng, H. Zheng, and B. Y. Zhao, "Utilization and fairness in spectrum assignment for opportunistic spectrum access," *Mobile Networks and Applications*, vol. 11, no. 4, pp. 555–576, 2006.
- [28] Y. Zhang, J. Luo, and H. Hu, Wireless Mesh Networking: Architectures, Protocols and Standards (Wireless Networks and Mobile Computing). Auerbach Publications, December 2006.
- [29] B. H. Walke, S. Mangold, and L. Berlemann, IEEE 802 Wireless Systems: Protocols, Multi-Hop Mesh/Relaying, Performance and Spectrum Coexistence. Wiley, January 2007.
- [30] K. R. Chowdhury and I. F. Akyildiz, "Cognitive wireless mesh networks with dynamic spectrum access," *IEEE Journal on Selected Areas in Communications*, vol. 26, no. 1, pp. 168–181, 2008. [Online]. Available: http://dx.doi.org/10.1109/JSAC.2008.080115
- [31] T. Chen, H. Zhang, G. Maggio, and I. Chlamtac, "Topology management in cogmesh: A cluster-based cognitive radio mesh network," in *IEEE International Conference on Communications (ICC '07)*, June 2007, pp. 6516–6521.
- [32] R. C. Pereira, R. D. Souza, and M. E. Pellenz, "Overlay cognitive radio in wireless mesh networks," 2008. [Online]. Available: http://www.citebase.org/abstract?id=oai:arXiv.org:0805.3643

- [33] T. Weiss and F. Jondral, "Spectrum pooling: an innovative strategy for the enhancement of spectrum efficiency," *Communications Magazine*, *IEEE*, vol. 42, no. 3, pp. S8–14, Mar 2004.
- [34] D. Tse and P. Viswanath, Fundamentals of Wireless Communication. Cambridge University Press, June 2005.
- [35] G. Dodig-Crnkovic, "Scientific methods in computer science," in Conference for the Promotion of Research in IT at New Universities and at University Colleges in Sweden, April 2002. [Online]. Available: http://www.mrtc.mdh.se/index.php?choice=publications&id=0446
- [36] (2009) MATLAB. http://www.mathworks.com/products/matlab/.
- [37] "The mosek optimization software." [Online]. Available: http://www.mosek.com/
- [38] J. Xiang, Y. Zhang, and T. Skeie, "Joint admission and power control for cognitive radio cellular networks," 11th IEEE Singapore International Conference on Communication Systems (ICCS 2008), pp. 1519–1523, Nov. 2008.
- [39] L. Zhang, Y.-C. Liang, and Y. Xin, "Joint Admission Control and Power Allocation for Cognitive Radio Networks," Acoustics, Speech and Signal Processing, 2007. ICASSP 2007. IEEE International Conference on, vol. 3, pp. III-673-III-676, 15-20 April 2007.
- [40] J. Xiang, Y. Zhang, and T. Skeie, "Admission and power control for cognitive radio cellular networks: A multidimensional knapsack solution," CogART 2010, Nov. 2010.
- [41] "Cognitive Radio Technologies Proceeding (CRTP) ET Docket No. 03-108." [Online]. Available: http://transition.fcc.gov/oet/cognitiveradio/
- [42] F. F. Digham, M.-S. Alouini, and M. K. Simon, "On the energy detection of unknown signals over fading channels," *Communications, IEEE Transactions on*, vol. 55, no. 1, pp. 21–24, Jan. 2007.
- [43] P. Sutton, K. Nolan, and L. Doyle, "Cyclostationary signatures in practical cognitive radio applications," *Selected Areas in Communications*, *IEEE Journal on*, vol. 26, no. 1, pp. 13–24, Jan. 2008.
- [44] Y. Youn, H. Jeon, H. Jung, and H. Lee, "Discrete wavelet packet transform based energy detector for cognitive radios," *Vehicular Technology*

- Conference, 2007. VTC2007-Spring. IEEE 65th, pp. 2641–2645, 22-25 April 2007.
- [45] A. Ghasemi and E. Sousa, "Collaborative spectrum sensing for opportunistic access in fading environments," New Frontiers in Dynamic Spectrum Access Networks, 2005. DySPAN 2005. 2005 First IEEE International Symposium on, pp. 131–136, 8-11 Nov. 2005.
- [46] M. Gandetto and C. Regazzoni, "Spectrum sensing: A distributed approach for cognitive terminals," *Selected Areas in Communications*, *IEEE Journal on*, vol. 25, no. 3, pp. 546–557, April 2007.
- [47] P. A. K. Acharya, S. Singh, and H. Zheng, "Reliable open spectrum communications through proactive spectrum access," in *TAPAS '06:* Proceedings of the first international workshop on Technology and policy for accessing spectrum. New York, NY, USA: ACM, 2006, p. 5.
- [48] Q. Zhao, L. Tong, A. Swami, and Y. Chen, "Decentralized cognitive mac for opportunistic spectrum access in ad hoc networks: A pomdp framework," *Selected Areas in Communications, IEEE Journal on*, vol. 25, no. 3, pp. 589–600, April 2007.
- [49] S. Geirhofer, L. Tong, and B. Sadler, "Cognitive radios for dynamic spectrum access dynamic spectrum access in the time domain: Modeling and exploiting white space," *Communications Magazine*, *IEEE*, vol. 45, no. 5, pp. 66–72, May 2007.
- [50] K. Chowdhury and I. Akyildiz, "Cognitive wireless mesh networks with dynamic spectrum access," *Selected Areas in Communications, IEEE Journal on*, vol. 26, no. 1, pp. 168–181, Jan. 2008.
- [51] Q. Zhao, S. Geirhofer, L. Tong, and B. Sadler, "Opportunistic spectrum access via periodic channel sensing," Signal Processing, IEEE Transactions on [see also Acoustics, Speech, and Signal Processing, IEEE Transactions on], vol. 56, no. 2, pp. 785–796, Feb. 2008.
- [52] A. E. Leu, M. McHenry, and B. L. Mark, "Modeling and analysis of interference in listen-before-talk spectrum access schemes," *Int. J. Netw. Manag.*, vol. 16, no. 2, pp. 131–147, 2006.
- [53] M. Sharma, A. Sahoo, and K. D. Nayak, "Channel selection under interference temperature model in multi-hop cognitive mesh networks," The 2nd IEEE International Symposium on New Frontiers in Dynamic

- Spectrum Access Networks, 2007 (DySPAN 2007), pp. 133–136, 17-20 April 2007.
- [54] J. Bater, H.-P. Tan, K. N. Brown, and L. Doyle, "Modelling interference temperature constraints for spectrum access in cognitive radio networks," *Communications*, 2007. ICC '07. IEEE International Conference on, pp. 6493–6498, 24-28 June 2007.
- [55] D. Xu, E. Jung, and X. Liu, "Optimal bandwidth selection in multichannel cognitive radio networks: How much is too much?" in *The* 3rd IEEE Symposium on New Frontiers in Dynamic Spectrum Access Networks (DySPAN 2008), Oct. 2008, pp. 1–11.
- [56] P. Fuxjager, D. Valerio, and F. Ricciato, "The myth of non-overlapping channels: interference measurements in ieee 802.11," in *The 4th Annual Conference on Wireless on Demand Network Systems and Services (WONS '07)*, Jan. 2007, pp. 1–8.
- [57] A. Mishra, V. Shrivastava, S. Banerjee, and W. Arbaugh, "Partially overlapped channels not considered harmful," ACM SIGMETRICS Performance Evaluation Review, vol. 34, no. 1, pp. 63–74, 2006.
- [58] "IEEE Standard for Local and metropolitan area networks Part 16: Air Interface for Broadband Wireless Access Systems," *IEEE Std 802.16-2009 (Revision of IEEE Std 802.16-2004)*, pp. C1–2004, 29 2009.
- [59] H. Su and X. Zhang, "Cross-Layer Based Opportunistic MAC Protocols for QoS Provisionings Over Cognitive Radio Wireless Networks," *IEEE Journal on Selected Areas in Communications*, vol. 26, no. 1, pp. 118–129, Jan. 2008.
- [60] D. Djonin, Q. Zhao, and V. Krishnamurthy, "Optimality and complexity of opportunistic spectrum access: A truncated markov decision process formulation," in *IEEE International Conference on Communications 2007 (ICC '07)*, June 2007, pp. 5787–5792.
- [61] Q. Zhao, L. Tong, and A. Swami, "A Cross-Layer Approach to Cognitive MAC for Spectrum Agility," in Conference Record of the Thirty-Ninth Asilomar Conference on Signals, Systems and Computers (ACSSC '05), 28 2005-Nov. 1 2005, pp. 200-204.
- [62] H. Su and X. Zhang, "Cognitive Radio Based Multi-Channel MAC Protocols for Wireless Ad Hoc Networks," in *IEEE Global Telecommunications Conference 2007 (GLOBECOM '07)*, Nov. 2007, pp. 4857–4861.

- [63] H. Kim and K. Shin, "Efficient Discovery of Spectrum Opportunities with MAC-Layer Sensing in Cognitive Radio Networks," *IEEE Transactions on Mobile Computing*, vol. 7, no. 5, pp. 533–545, May 2008.
- [64] M. Ma and D. Tsang, "Impact of channel heterogeneity on spectrum sharing in cognitive radio networks," *IEEE International Conference on Communications 2008 (ICC '08)*, pp. 2377–2382, May 2008.
- [65] Y. Kondareddy, P. Agrawal, and K. Sivalingam, "Cognitive radio network setup without a common control channel," *IEEE Military Communications Conference*, 2008 (MILCOM 2008), pp. 1–6, Nov. 2008.
- [66] P. Pawelczak, R. Venkatesha Prasad, L. Xia, and I. Niemegeers, "Cognitive radio emergency networks requirements and design," The 1st IEEE International Symposium on New Frontiers in Dynamic Spectrum Access Networks, 2005 (DySPAN 2005), pp. 601–606, Nov. 2005.
- [67] V. Brik, E. Rozner, S. Banerjee, and P. Bahl, "Dsap: a protocol for coordinated spectrum access," in *The 1st IEEE International Symposium on New Frontiers in Dynamic Spectrum Access Networks (DySPAN 2005)*, Nov. 2005, pp. 611–614.
- [68] A. Chia-Chun Hsu, D. Weit, and C.-C. Kuo, "A Cognitive MAC Protocol Using Statistical Channel Allocation for Wireless Ad-Hoc Networks," in *IEEE Wireless Communications and Networking Conference (WCNC 2007)*, March 2007, pp. 105–110.
- [69] J. Jia, Q. Zhang, and X. Shen, "HC-MAC: A Hardware-Constrained Cognitive MAC for Efficient Spectrum Management," *IEEE Journal on Selected Areas in Communications*, vol. 26, no. 1, pp. 106–117, Jan. 2008.
- [70] Q. Zhao, L. Tong, A. Swami, and Y. Chen, "Decentralized cognitive MAC for opportunistic spectrum access in ad hoc networks: A POMDP framework," *IEEE Journal on Selected Areas in Communications*, vol. 25, no. 3, pp. 589–600, April 2007.
- [71] B. Hamdaoui and K. Shin, "OS-MAC: An Efficient MAC Protocol for Spectrum-Agile Wireless Networks," *IEEE Transactions on Mobile Computing*, vol. 7, no. 8, pp. 915–930, Aug. 2008.
- [72] K. Bian and J.-M. Park, "MAC-Layer Misbehaviors in Multi-Hop Cognitive Radio Networks," 2006 US Korea Conference on Science, Technology, and Entrepreneurship (UKC2006), Aug. 2006.

- [73] C. Cordeiro and K. Challapali, "C-MAC: A Cognitive MAC Protocol for Multi-Channel Wireless Networks," in *The 2nd IEEE International Symposium on New Frontiers in Dynamic Spectrum Access Networks* 2007 (DySPAN 2007), April 2007, pp. 147–157.
- [74] Y. Xing, C. N. Mathur, M. Haleem, R. Chandramouli, and K. Subbalakshmi, "Dynamic spectrum access with qos and interference temperature constraints," *IEEE Transactions on Mobile Computing*, vol. 6, no. 4, pp. 423–433, April 2007.
- [75] L. Zhang, Y.-C. Liang, and Y. Xin, "Joint admission control and power allocation for cognitive radio networks," *IEEE International Conference* on Acoustics, Speech and Signal Processing (ICASSP 2007), vol. 3, pp. III-673-III-676, 15-20 April 2007.
- [76] J. Xiang, Y. Zhang, and T. Skeie, "Joint admission and power control for cognitive radio cellular networks," The 11th IEEE International Conference on Communication Systems (ICCS 2008), pp. 1519–1523, Nov. 2008.
- [77] L. Zhang, Y.-C. Liang, and Y. Xin, "Joint beamforming and power allocation for multiple access channels in cognitive radio networks," *IEEE Journal on Selected Areas in Communications*, vol. 26, no. 1, pp. 38–51, Jan. 2008.
- [78] J. Xiang, Y. Zhang, T. Skeie, and J. He, "Qos aware admission and power control for cognitive radio cellular networks," *Wiley Wireless Communications and Mobile Computing*, vol. 9, no. 11, pp. 1520–1531, 2009.
- [79] D. Kim, L. Le, and E. Hossain, "Joint rate and power allocation for cognitive radios in dynamic spectrum access environment," *IEEE Transactions on Wireless Communications*, vol. 7, no. 12, pp. 5517–5527, December 2008.
- [80] Y. Zhu, Z. Sun, W. Wang, T. Peng, and W. Wang, "Joint power and rate control considering fairness for cognitive radio network," in *IEEE Wireless Communications and Networking Conference (WCNC 2009)*., April 2009, pp. 1–6.
- [81] L. B. Le and E. Hossain, "Resource allocation for spectrum underlay in cognitive radio networks," *IEEE Transactions on Wireless Communications*, vol. 7, no. 12, pp. 5306–5315, December 2008.

- [82] P. Cheng, Z. Zhang, H.-H. Chen, and P. Qiu, "Optimal distributed joint frequency, rate and power allocation in cognitive ofdma systems," *IET Communications*, vol. 2, no. 6, pp. 815–826, July 2008.
- [83] W. Wang, W. Wang, Q. Lu, and T. Peng, "An uplink resource allocation scheme for ofdma-based cognitive radio networks," *International Journal of Communication Systems*, vol. 22, no. 5, pp. 603–623, 2009.
- [84] H.-Y. Gu, C.-Y. Yang, and B. Fong, "Low-complexity centralized joint power and admission control in cognitive radio networks," *IEEE Com*munication Letters, vol. 13, no. 6, pp. 420–422, 2009.
- [85] D. Lopez-Perez, A. Valcarce, G. De La Roche, E. Liu, and J. Zhang, "Access methods to wimax femtocells: A downlink system-level case study," in 11th IEEE Singapore International Conference on Communication Systems (ICCS 2008), Nov. 2008, pp. 1657–1662.
- [86] A. Valcarce, G. D. L. Roche, álpar Jüttner, D. López-Pérez, and J. Zhang, "Applying fdtd to the coverage prediction of wimax femtocells," EURASIP Journal on Wireless Communications and Networking, pp. 555–576, 2009.
- [87] D. Lopez-Perez, G. de la Roche, A. Valcarce, A. Juttner, and J. Zhang, "Interference avoidance and dynamic frequency planning for wimax femtocells networks," in 11th IEEE Singapore International Conference on Communication Systems (ICCS 2008), Nov. 2008, pp. 1579–1584.
- [88] K. Sundaresan and S. Rangarajan, "Efficient resource management in ofdma femto cells," in *MobiHoc '09: Proceedings of the tenth ACM international symposium on Mobile ad hoc networking and computing*. New York, NY, USA: ACM, 2009, pp. 33–42.
- [89] P. Dutta, S. Jaiswal, D. Panigrahi, and R. Rastogi, "A new channel assignment mechanism for rural wireless mesh networks," in *IEEE IN-FOCOM 2008*, April 2008, pp. 2261–2269.
- [90] D. Niyato and E. Hossain, "Cognitive radio for next-generation wireless networks: an approach to opportunistic channel selection in ieee 802.11-based wireless mesh," *IEEE Wireless Communications*, vol. 16, no. 1, pp. 46–54, February 2009.
- [91] H. Li, Y. Cheng, C. Zhou, and W. Zhuang, "Minimizing end-to-end delay: A novel routing metric for multi-radio wireless mesh networks," in *IEEE INFOCOM 2009*, April 2009, pp. 46–54.

- [92] H. N. Pham, J. Xiang, Y. Zhang, and T. Skeie, "Qos-aware channel selection in cognitive radio networks: A game-theoretic approach," in *IEEE Global Telecommunications Conference (GLOBECOM 2008)*, Nov. 30 Dec. 4 2008, pp. 1–7.
- [93] M. H. Rehmani, A. C. Viana, H. Khalife, and S. Fdida, "Adaptive and occupancy-based channel selection for unreliable cognitive radio networks," in *Rencontres Francophones sur les Aspects Algorithmiques des Telecommunications (ALGOTEL) 2009*, Juni 2009.
- [94] Y. Hou, Y. Shi, and H. Sherali, "Optimal spectrum sharing for multi-hop software defined radio networks," in *IEEE INFOCOM 2007*, May 2007, pp. 1–9.
- [95] Y. Song, Y. Fang, and Y. Zhang, "Stochastic channel selection in cognitive radio networks," in *Global Telecommunications Conference*, 2007. *GLOBECOM '07. IEEE*, Nov. 2007, pp. 4878–4882.
- [96] P. N. Anggraeni, N. H. Mahmood, J. Berthod, N. Chaussonniere, L. My, and H. Yomo, "Dynamic channel selection for cognitive radios with heterogenous primary bands," Wireless Personal Communications, vol. 45, no. 3, pp. 369–384, 2008.
- [97] J. Matousek and B. Gärtner, *Understanding and Using Linear Programming*. Springer, November 2006.
- [98] (2010) ILOG CPLEX. [Online]. Available: http://www-01.ibm.com/software/integration/optimization/cplex-optimizer/
- [99] H. Kellerer, U. Pferschy, and D. Pisinger, *Knapsack Problems*. Springer, Berlin, Germany, 2004.
- [100] W. Shih, "A branch and bound method for the multiconstraint zero-one knapsack problem," *Journal of the Operational Research Society*, vol. 30, no. 4, pp. 369–378, Apr., 1979.
- [101] P. C. Gilmore and R. E. Gomory, "The theory and computation of knapsack functions," *Operations Research*, vol. 14, no. 6, pp. 1045– 1074, Nov. - Dec., 1966.
- [102] H. M. Weingartner and D. N. Ness, "Methods for the solution of the multidimensional 0/1 knapsack problem," *Operations Research*, vol. 15, no. 1, pp. 83–103, Jan. Feb., 1967.

- [103] P. Setoodeh and S. Haykin, "Robust transmit power control for cognitive radio," *Proceedings of the IEEE*, vol. 97, no. 5, pp. 915–939, May 2009.
- [104] C. Stevenson, G. Chouinard, Z. Lei, W. Hu, S. Shellhammer, and W. Caldwell, "IEEE 802.22: The first cognitive radio wireless regional area network standard," *IEEE Communications Magazine*, vol. 47, no. 1, pp. 130–138, January 2009.
- [105] T. Yucek and H. Arslan, "A survey of spectrum sensing algorithms for cognitive radio applications," *IEEE Communications Surveys Tutorials*, vol. 11, no. 1, pp. 116 –130, first 2009.
- [106] "Guidelines for evaluation of radio transmission technologies for imt-2000," RECOMMENDATION ITU-R M.1225, 1997.
- [107] "Digital mobile radio towards future generation systems cost 231 final report," COST Action 231, 1999.
- [108] D. Palomar and M. Chiang, "A tutorial on decomposition methods for network utility maximization," *Selected Areas in Communications*, *IEEE Journal on*, vol. 24, no. 8, pp. 1439 –1451, aug. 2006.
- [109] —, "Alternative distributed algorithms for network utility maximization: Framework and applications," *IEEE Transactions on Automatic Control*, vol. 52, no. 12, pp. 2254 –2269, dec. 2007.
- [110] S. Boyd and L. Vandenberghe, *Convex Optimization*. Cambridge University Press, March 2004.
- [111] J. Xiang, Y. Zhang, and T. Skeie, "Dynamic spectrum sharing in cognitive radio femtocell networks," *Lecture Notes of the Institute for Computer Sciences, Social Informatics and Telecommunications Engineering*, vol. 52, no. 12, pp. 164 178, dec. 2010.
- [112] H. S. Wang and N. Moayeri, "Finite-state markov channel-a useful model for radio communication channels," *Vehicular Technology, IEEE Transactions on*, vol. 44, no. 1, pp. 163–171, Feb 1995.
- [113] "IEEE Standard for Information technology-Telecommunications and information exchange between systems-Local and metropolitan area networks-Specific requirements Part 11: Wireless LAN Medium Access Control (MAC) and Physical Layer (PHY) Specifications," *IEEE Std 802.11-2007 (Revision of IEEE Std 802.11-1999)*, pp. C1–1184, 12 2007.

- [114] D. P. Bertsekas, Network Optimization: Continuous and Discrete Models. Athena Scientific, May 2008.
- [115] —, Nonlinear Programming. Athena Scientific, September 1999.
- [116] B. Wild, "Detecting primary receivers for cognitive radio applications," in *in Proc. of the First IEEE Symposium on New Frontiers in Dynamic Spectrum Access Networks*, 2005, pp. 124–130.
- [117] "GNU Radio." [Online]. Available: http://www.gnuradio.org/
- [118] "USRP by Ettus Research LLC." [Online]. Available: http://www.ettus.com/
- [119] "Rice University WARP Project." [Online]. Available: http://warp.rice.edu
- [120] "Agile SDR Solutions." [Online]. Available: http://www.agile-sdr-solutions.com/

# Appendix A

## Publication list

Most of the material in this work has previously been published in the proceedings of various international conferences and journals. Here we provide a list of publications during this thesis work.

## **Book Chapters**

- 1. Jie Xiang and Yan Zhang, "Medium Access Control Protocols for Cognitive Radio Networks," in *Cognitive Radio Networks: Architectures, Protocols and Standards*, edited by Y. Zhang, J. Zheng, H.H. Chen, CRC Press, USA, 2010.
- 2. Jianhua He, Jie Xiang, Zuoyin Tang and Yan Zhang, "Dynamic and Fair Spectrum Access for Autonomous Communications," in *Autonomic Computing and Networking*, edited by M. Denko, Laurence T. Yang and Y. Zhang, Springer, USA, 2009.
- 3. Jianhua He, Xiaoming Fu, Jie Xiang, Yan Zhang and Zuoyin Tang, "Routing and Scheduling for WiMAX Mesh Networks," in *WiMAX Network Planning and Optimization*, edited by Y. Zhang, CRC Press, USA, 2009.

#### Journal Articles

- 1. Jie Xiang, Yan Zhang, Tor Skeie, and Lang Xie. "Downlink Spectrum Sharing for Cognitive Radio Femtocell Networks," *IEEE Systems Journal*, special issue on Broadband Access Networks, 4(4):524-534, 2010.
- 2. Jie Xiang, Yan Zhang and Tor Skeie. "Medium Access Control Protocols in Cognitive Radio Networks," Wireless Communications and Mo-

- bile Computing, Wiley, special issue on Recent Advances in Wireless Communications and Networks, 10(1):31-49, 2010.
- 3. Jie Xiang, Yan Zhang, Tor Skeie, and Jianhua He. "QoS Aware Admission and Power Control for Cognitive Radio Cellular Networks," Wireless Communications and Mobile Computing, Wiley, special issue on Cognitive Radio and Advanced Spectrum Management, 9(11):1520-1531, 2009.
- 4. Supeng Leng, Yan Zhang, Hsiao-Hwa Chen, Jie Xiang, and Mohsen Guizani. "Power-fixed and Power-aware MAC Protocols for Multi-hop Wireless Networks with Large Interference Area," *IEEE Transactions on Vehicular Technology*, 58(6):2966-2976, July 2009.

## Conference Proceedings

- Jie Xiang, Yan Zhang, and Tor Skeie, "Admission and Power Control for Cognitive Radio Cellular Networks: A Multidimensional Knapsack Solution," In Proc. of CogART 2010.
- 2. Lang Xie, Poul E. Heegaard, Yan Zhang, and Jie Xiang. "Reliable Channel Selection and Routing for Real-time Services over Cognitive Radio Mesh Networks," In Proc. of Qshine 2010.
- 3. Sabita Maharjan, Jie Xiang, Yan Zhang and Stein Gjessing, "Delay Reduction for Real Time Services in IEEE 802.22 Wireless Regional Area Network," In Proc. of the 21st Annual IEEE International Symposium on Personal, Indoor and Mobile Radio Communications (PIMRC), September 26 29, 2010, Istanbul Turkey.
- 4. Lang Xie, Jin Zhang and Jie Xiang, "Cognitive Networking for Wireless Mesh Networks using Swarm Intelligence," In Proc. of the 6th IEEE International Conference on Wireless Communications, Networking and Mobile Computing (WiCOM 2010), September 23 25, 2010, Chengdu, China.
- 5. Lang Xie, Poul E. Heegaard, Jin Zhang, Jie Xiang, "System State aware Admission Control scheme for IEEE 802.16 WiMAX-based healthcare system," In Proc. of the 6th International Wireless Communications and Mobile Computing Conference (IWCMC 2010), June 28 July 2, 2010, Caen, France.

- 6. Jie Xiang, Yan Zhang and Tor Skeie. "Dynamic Spectrum Sharing in Cognitive Radio Femtocell Networks," In Proc. of the 4th International Conference on Access Networks (ACCESSNETS 2009), Nov. 1 3, 2009, Hongkong, China. (Invited Paper)
- 7. Qin Xin and Jie Xiang. "Joint QoS-aware Admission Control, Channel Assignment, and Power Allocation for Cognitive Radio Cellular Networks," In Proc. of the 6th IEEE International Conference on Mobile Ad-hoc and Sensor Systems (MASS 2009), pp. 294-303, Oct. 12 15, 2009, Macau, China.
- 8. Lang Xie, Jie Xiang, Yan Zhang and Jin Zhang. "Joint Bandwidth Reservation and Admission Control in IEEE 802.16e based Networks," In Proc. of the 2009 IEEE International Conference on Communications (ICC 2009), pp. 1-6, June 14 18, 2009, Dresden, Germany.
- 9. Qin Xin, Yan Zhang and Jie Xiang. "Minimum-Latency Gossiping in Multi-hop Wireless Mesh Networks," In Proc. of the 2009 IEEE International Conference on Communications (ICC 2009), pp.1-5, June 14 18, 2009, Dresden, Germany.
- Yan Zhang, Jie Xiang, Qin Xin and Geir Egil Øien. "Optimal Sensing Cooperation for Spectrum Sharing in Cognitive Radio Networks," Accepted by European Wireless 2009 (EW 2009), May 17 - 20, 2009, Aalborg, Denmark.
- Hai Ngoc Pham, Jie Xiang, Yan Zhang and Tor Skeie. "QoS-Aware Channel Selection in Cognitive Radio Networks: A Game-Theoretic Approach," In Proc. of the 2008 IEEE Global Communications Conference (GLOBECOM 2008), Nov. 30 Dec. 3, 2008, New Orleans, LA, USA.
- 12. Jie Xiang, Yan Zhang and Tor Skeie. "Joint Admission and Power Control for Cognitive Radio Cellular Networks," In Proc. of the 11th IEEE International Conference on Communication Systems 2008 (ICCS 2008), pp.1519-1523, Nov. 19 21, 2008, Guangzhou, China. (Invited Paper)
- 13. Lang Xie and Jie Xiang. "A Novel Bandwidth Degradation Scheme for Admission Control in IEEE 802.16e Networks," In Proc. of the 4th IEEE International Conference on Wireless Communications, Networking and Mobile Computing (WiCOM 2008), pp.1-4, Oct. 12-14, 2008, Dalian, China.

- 14. Lang Xie, Jie Xiang and Yan Zhang. "Revenue-based Admission Control for Cognitive Radio Cellular Systems". Presented in the 2008 International Workshop on Cognitive Networks and Communications (COGCOM 2008), In Proc. of the 2008 International Conference on Communications and Networking in China (ChinaCom 2008), pp.1200-1204, Aug. 25-27, 2008, Hangzhou, China.
- 15. Qin Xin, Yan Zhang and Jie Xiang. "Optimal Spectrum Scheduling in Cognitive Wireless Mesh Networks", In Proc. of the 2008 International Wireless Communications and Mobile Computing Conference (IWCMC 2008), pp.724-728, Aug. 6-8, 2008, Crete Island, Greece.
- 16. Yan Zhang and Jie Xiang. "A New Adaptive Energy Management Scheme in IEEE 802.16e Mobile WiMAX," In Proc. of the 2007 Norwegian Informatics Conference (NIK 2007), pp. 111-114, Nov. 19-21, 2007, Oslo, Norway.

# Appendix B

# Acronym List

AMC	Adaptive Modulation Coding. 8, 112
AWGN	Additive White Gaussian Noise. 92

BS Base Station. 21, 22, 27, 28, 30-32, 36, 39, 57,

59

CCC Common Control Channel. 20, 21

CDMA Code Division Multiple Access. 23, 24, 62, 88 CogCell Cognitive Radio Cellular Networks. 4, 5, 9,

10, 22, 23, 27, 28, 30, 31, 37, 55, 60–62, 65,

131 - 133

CogFem Cognitive Radio Femtocell Networks. 5, 6, 9,

11, 21, 22, 87, 88, 91, 93, 94, 97, 99, 101, 103,

106, 107, 131–133

CogMesh Cognitive Radio Mesh Networks. 7–9, 12, 22,

25, 109, 110, 112, 113, 115, 125, 128, 131–133

CR Cognitive Radio. 3–5, 7, 11, 16, 18, 20, 23–25,

107

CSI Channel State Information. 99

DoS Denial-of-Service. 20
DSL Digital Subscriber Line. 5

DTR Data Transmission Rate. 29–31, 36, 55, 60, 76

ECC Electronic Communications Committee. 1

FBS Femtocell Base Station. 5, 88–100, 102, 103,

106, 107

FCC Federal Communications Commission. 1, 2

FSMC Finite-State Markov Channel. 112

FU Femtocell User. 5, 11, 100

ISM Industrial, Scientific and Medical. 1, 2

JAPC-MKP Joint Admission and Power Control with Mul-

tidimensional Knapsack Problem modeling.

27, 53, 55, 57–61, 75, 131, 134

JAPC-MRER Joint Admission and Power Control scheme

using a Minimal Revenue Efficiency Removal algorithm.  $10,\ 27,\ 32,\ 36-40,\ 42,\ 55,\ 57-60,$ 

131, 134

JAPC-MSRA Joint Admission and Power Control scheme

using a Minimal SINR Removal Algorithm.

10, 27, 32, 34, 36–40, 42, 55, 57–60

JAPC-Rand Joint Admission and Power Control scheme

using a Random removal algorithm. 10, 27,

32, 35–40, 60

MCKP Multiple-Choice Knapsack Problem. 12, 132,

133

MINLP Mixed Integer Non-linear Programming. 65,

94, 107, 132, 133

MKP Multidimentional Knapsack Problem. 10, 61,

69, 70, 84, 131, 133, 134

MMKP Multidimentional Multiple Knapsack Prob-

lem. 11, 61, 67, 69, 84, 132, 133

MRS Maximization of Revenue from SUs. 64

NPT The Norwegian Post and Telecommunications

Authority. 1

OFDM Orthogonal Frequency-Division Multiplexing.

18

OFDMA Orthogonal Frequency-Division Multiple Ac-

cess. 24, 62, 88

## Appendix B Acronym List

POMDP	Partially observable Markov Decision Processe. 17
PR	Primary Receiver. 4, 5, 10, 28–30
PT	Primary Transmitter. 28, 29
PU	Primary User. 3–5, 7, 8, 16–25, 27–29, 31–33, 36–40, 42, 55, 57, 58, 60–65, 75, 76, 111, 115, 117
QoS	Quality of Service. 5, 10, 17, 21, 22, 27–31, 60, 109, 110, 131
SIMO-MAC	Single Input Multiple Output Multiple Access Channel. 23, 24
SINR	Signal to Interference and Noise Ratio. 10, 12, 19, 23, 30–32, 34, 36, 38, 40, 42, 55, 56, 59–61, 75, 92, 109, 112, 124, 133
SMG	Secondary Mesh Gateway. 7, 110, 111, 115
SMR	Secondary Mesh Router. 7, 109–115, 128, 132
SMU	Secondary Mesh User. 7, 8, 110
SU	Secondary User. 3–5, 8, 10, 11, 16–25, 27–40, 45, 46, 53, 55–65, 75, 76, 78, 85
WLAN	Wireless Local Area Network. 1
WPAN	Wireless Personal Area Network. 1
WRAN	Wireless Regional Area Network. 2